The Impact of Fiber-Reinforced Polymer Constructions on Risk Level onboard Large Passenger Ships

Anders Lynnér
Josip Novacic

Department of Fire Safety Engineering
Lund University, Sweden

Brandteknik
Lunds tekniska högskola
Lunds universitet

Report 5480, Lund 2014

The Impact of Fiber-Reinforced Polymer Constructions on Risk Level onboard Large Passenger Ships

Anders Lynnér
Josip Novacic

Lund 2014

Titel
Fiberförstärkta plastkonstruktioners inverkan på risknivå ombord på stora passagerarfartyg

Title
The Impact of Fiber-Reinforced Polymer Constructions on Risk Level onboard Large Passenger Ships

Authors
Anders Lynnér
Josip Novacic

Report 5480
ISSN: 1402-3504
ISRN: LUTVDG/TVBB--5480--SE

Number of pages: 102
Illustrations: By authors

Keywords
Lightweight materials, fiber-reinforced polymer, FRP, fire safety, evacuation, ship, fire dynamics simulator, FDS, critical conditions, corridor, cabin, risk.

Sökord
Lättviktsmaterial, brandsäkerhet, utrymning, fartyg, kritiska förhållanden, FDS, FRP, korridor, kabin, risk.

Abstract
The main objective of this project was to determine how a FRP composite structure performs compared to a steel structure in regard to fire safety and risk level during an evacuation. More specifically the objective was to study how the differences in the thermal properties influence the smoke layer height, visibility and the temperature of the gases in the early stages of a fire. This was done by performing several FDS simulations and analyzing the results from these. In order to evaluate the difference in risk level, the time until critical conditions occurred was compared between the FRP and steel cases. The results showed small differences in time until critical conditions for the smoke layer height and visibility while the temperatures also showed only slight differences near the fire but larger differences further away and as time went by. This led to the conclusions that there is a difference in risk level based on the reasoning that time until critical conditions further away also matter. However, additional research is needed in order to determine if the difference is significant or not.

Brandteknik
Lunds tekniska högskola
Lunds universitet
Box 118
221 00 Lund

http://www.brand.lth.se

Telefon: 046 - 222 73 60

Department of Fire Safety Engineering
Faculty of Engineering
Lund University
P.O. Box 118
SE-221 00 Lund
Sweden

http://www.brand.lth.se

Telephone: +46 46 222 73 60

Sammanfattning

Användning av lättviktsmaterial inom den marina sektorn är ett forskningsområde som har blivit alltmer intressant sedan hållbar utveckling blivit en allt viktigare fråga. Genom användning av lättare konstruktionsmaterial såsom kompositmaterial av fiberförstärkt plast (FRP) kan den totala vikten signifikant reduceras vilket leder till ett minskat behov av drivmedel. Således kan man uppnå både ekonomiska vinster och minskad miljöpåverkan. Dock finns det några praktiska problem med att använda kompositmaterial av FRP på större passagerar-fartyg. Dessa hinder utgörs i huvudsak av den befintliga regleringen och brandriskerna som kan uppkomma vid användning av sådana material. Det finns också en stark tradition av att använda stålkonstruktioner på fartyg och faktumet att FRP är brännbart, till skillnad från stål, gör att det krävs en större mängd brandisolering för att FRP ska uppnå samma funktionskrav som stål.

Målet med detta projekt var att undersöka om den ökade mängden isolering som används i FRP fallet har några effekter på risken under utrymningsförloppet. Detta gjordes genom att jämföra hur en kompositkonstruktion av FRP påverkar utrymningsförhållandena jämfört med en stål-konstruktion. För att uppnå detta mål togs två specifika frågeställningar fram:

- Hur påverkar en brand-isolerad kompositkonstruktion av FRP brandgaslagerhöjd, siktbarhet och brandgasernas temperatur i det tidiga brandförloppet?
- Bidrar den tillagda isoleringen till en högre risknivå under tiden då utrymning sker?

Riskanalysen utgick från resultat framtagna från FDS-simuleringar som gjordes för en specifik geometri. Denna geometri var enkel och representerade en öppen korridor med passagerarkabiner på varje sida i en överbyggnad på ett passagerar-fartyg. Överbyggnadens bärande delar konstruerades i två olika byggnadsmaterial – FRP och stål.

I riskanalysen ingick fyra olika brandscenarion. Dessa var följande:

- Geometrin utgörs av kompositkonstruktion av FRP och sprinkler aktiverar.
- Geometrin utgörs av stål och sprinkler aktiverar.
- Geometrin utgörs av kompositkonstruktion av FRP och sprinkler aktiverar **inte**.
- Geometrin utgörs av stål och sprinkler aktiverar **inte**.

Temperaturer, siktbarhet och brandgaslagerhöjd studerades för varje simulering och kriterier för dessa variabler användes för att bestämma tiden till kritiska förhållande för varje scenario. Kritiska förhållande antogs uppstå när det uppstår kritiska förhållande utanför de till brandrummet intilliggande kabinerna. Detta innebär således att kritiska förhållanden antogs uppstå när förhållandena påverkar utrymningen för människor i de intilliggande kabinerna. Resultaten visades bland annat i diagram som visade hur stor del av korridoren som hade kritiska förhållanden för olika tider. Resultaten påvisade små skillnader i tid till kritiska förhållanden för brandgaslagerhöjden och siktbarheten. För temperaturerna påvisades bara små skillnader i tid till kritiska förhållanden nära branden, men större skillnader längre bort från branden och desto längre tiden gick. Detta ledde till slutsatsen att det finns en skillnad i risknivå vilket baseras på att även kritiska förhållanden längre bort från branden också inverkar på utrymningssäkerheten. Dock krävs det ytterligare forskning för att bestämma om dessa skillnader är signifikanta eller ej.

Känslighetsanalyser som gjordes på parametrar i indata visade att den viktigaste parametern för skillnad i risknivå mellan fallen med FRP och stål är tillväxthastigheten, vilken också ligger till grund för metoden i hur den ökade brandisoleringen modellerades för i FDS för FRP-fallet.

Summary

The use of lightweight materials in the maritime sector is a field of research that is of great interest since sustainability has become a more important issue. With use of lighter construction materials, such as fiber-reinforced polymer (FRP) composites, the total weight of a ship can be significantly reduced, potentially resulting in fuel savings. This will benefit financial profits as well as the environment. There are however some practical problems with the implementation of FRP composite structures on larger passenger ships, mainly in regard to fire safety risks and the current legislation. This complicates the transition from the use of steel which is traditionally the material of choice. The fact that FRP is combustible, unlike steel, demands the use of additional thermal insulation.

The aim of this project was to identify if the added insulation used in the FRP case has any effects on the risks regarding fire safety during an evacuation. This was done by comparing the performance of a FRP composite structure with that of a steel structure. To fulfill this objective two specific research questions were formulated and answered:

- How does an insulated FRP composite structure influence the smoke layer height, visibility and gas temperature in the early stages of a fire?
- Does the added insulation result in a higher risk level during evacuation time frame?

The risk analysis consisted of analysis from results of conducted FDS simulations for a specific geometry representing an accommodation area in a passenger ship superstructure. The decks and bulkheads of this superstructure were constructed using two different building materials, FRP composite and steel. More precisely the model represented a corridor with passenger cabins on both sides, the fire was assumed to start in one of these cabins where the door had been left open.

Four different scenarios were part of the risk analysis. The scenarios were as follows:

1. A FRP composite structure is used and sprinkler activation takes place.
2. A steel structure is used and sprinkler activation takes place.
3. A FRP composite structure is used and **no** sprinkler activation takes place.
4. A steel structure is used and **no** sprinkler activation takes place.

The temperatures, visibilities and smoke layer heights were studied for each simulation and criteria for these variables were used to determine the time until critical conditions for each scenario. Critical conditions were assumed to occur when people in the cabins adjacent to the fire room could be exposed to critical conditions. The results were, among other ways, presented in charts which for different times show a fraction that represents the amount of corridor area where critical conditions have occurred. The results showed small differences in time until critical conditions for the smoke layer height and visibility while the temperatures also showed only slight differences near the fire but larger differences further away and as time went by. This led to the conclusions that there is a difference in risk level based on the reasoning that time until critical conditions further away also matter. However, additional research is needed in order to determine if the difference is significant or not.

Sensitivity analyses of input parameters were also performed and showed that the most important parameter for the differences in risk level between the FRP and steel case is the fire growth rate, which also is a founding parameter in the methodology used for modeling the additional thermal insulation in the FRP case.

Acknowledgements

We, the authors of this report, would like to show our gratitude to the people who have been of great help during the concluding part of our education and the realization of this master thesis.

***Thank you**;*

Bjarne Husted, our main supervisor, at the Department of Fire Safety Engineering, Lund University. You have helped us not only with the very technical headaches that a project based on FDS simulations involve, but also by giving us continuous feedback on the work during long meetings.

Dan Lauridsen, our external supervisor at DBI, but also **Carsten Møller** and **Claus Langhoff.** You have given us a background of the issues regarding lightweight materials in the maritime sector and pointed us in the right direction when formulating the scope of this project.

Sebastian Sivam Wada, close friend and same year student. You have been of great help in getting the LUNARC cluster to work our way. We hope to be able to repay the favor when it is time for your up-and-coming master thesis!

Henrik Hassel, Program Director for the Master's program in Risk Management and Safety Engineering. You have been of great assistance in helping us integrate the risk aspect in this project through discussion and in providing us with useful literature.

Lund, November 2014.

Anders Lynnér

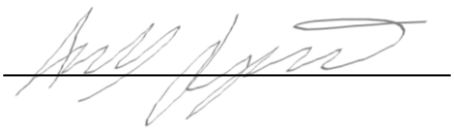

Josip Novacic

Abbreviations

BIV	-	Föreningen för brandteknisk ingenjörsvetenskap (Swedish SFPE chapter)
FDS	-	Fire dynamics simulator
FRD	-	fire-resistant divisions
FRM	-	fire-restrictive materials
FRP	-	fiber-reinforced polymer
FTP Code	-	International Code for the Application of Fire Test Procedures
HRR	-	Heat Release Rate
HSC Code	-	High-Speed Craft Code
IMO	-	International Maritime Organization
ISO	-	International Standards Organization
LASS	-	Lightweight Applications at Sea
LUNARC	-	Lund University NIC Application Research Center
MSC	-	Maritime Safety Committee
NIC	-	Numeric Intensive Computation
PVC	-	Polyvinyl chloride
RoPax	-	Roll-on/roll-off passenger vessel
SFPE	-	Society of Fire Protection Engineers
SOLAS	-	International Convention for the Safety of Life at Sea
SP	-	Technical Research Institute of Sweden

Table of contents

1 Introduction

In the maritime sector steel has out of tradition become the material of choice when constructing large ships. From a fire safety and risk perspective this is beneficial since steel is a non-combustible material. However with increasing world population and decreasing energy resources the demands on the transport sector has become more severe concerning sustainability and effectiveness. This has led to increasing research and development of lightweight constructions where materials such as fiber-reinforced polymer (FRP) are used. The problem is that the materials used in these structures are not approved by the International Convention for the Safety of Life at Sea (SOLAS convention), which is published by International Maritime Organization (IMO) and is considered to be the main international standard for ship construction.

1.1 Background

For more than a decade parts of the maritime sector have been interested in research concerning whether or not it is possible to use lightweight materials on ships in order to make them lighter and thereby more environmentally friendly. Of course the possibility of more cost effective solutions has also been a motive that has led to the involvement and economic investments of actors. A project that deals with this was requested by VINNOVA which is a Swedish government-owned agency funding innovation and sustainable development. The project has made it evident that there is an interest in the development and that the field could have a promising future (Hertzberg et al., 2009). In total 29 different actors, both organizations within the maritime sector as well as research institutes have joined and contributed to this project group which formed in 2004 under the name Lightweight Applications at Sea, LASS. This group has developed into a non-profit organization working for acquiring and spreading knowledge about lightweight materials in the maritime sector. The organization aims to increase funding of research by formulating common issues that actors in the maritime sector have regarding lightweight materials. The group also strives for international cooperation within the research area (S-LÄSS, 2014).

There are however some obstacles other than the technical ones that have to be tackled in order to begin using lightweight materials. First of all, the maritime sector is conservative, and in order for new techniques to be used, they all have to be thoroughly tested, which in the traditional way is best done by long-time usage. Secondly, the regulation that governs ship construction is today decided by every specific flag state as well as by international organizations such as IMO. Most regulations are based on SOLAS convention which is the prescriptive code for ship construction that IMO has developed. Recently, the code was changed and this has made it possible to use constructions in other materials than just steel or non-combustible materials as long as they can be shown to be just as safe as the conventional structures. This is where the next problem is encountered; there are no specific reference points, like acceptance criteria for safe evacuation used in the building codes on land, that make it possible to use analytical design methods instead of prescriptive rules. Thus, a new design has to be proven equal to steel regarding fire safety which calls for methods that compare the new design to the prescriptive rules (Hertzberg et al., 2009).

The LASS project has shown that, in some applications, it may be possible to use FRP. During the project an FRP composite structure was tested according to standards for testing maritime materials. The material tested consisted of two laminates of fiber-reinforced polymer with a core of PVC foam. The problem with this material is that it is combustible and that it can soften at temperatures as low as 100°C. To overcome this issue the researchers used fire insulation and the LASS group showed that

the material can endure a full scale furnace fire test for 60 minutes. This is the same fire test that materials must pass to comply with the perspective requirements and it can thus be argued that the FRP composite fulfills the requirements regarding insulation and integrity even if the materials used are combustible (Hertzberg et al., 2009).

1.1.1 Alternative fire safety designs

The previously mentioned fire safety regulation that concerns alternative designs is SOLAS II-2/17. The regulation states that any designs that deviate from the prescriptive requirements must fulfill the functional requirements in order to make sure that the fire safety objectives of SOLAS are met. There are five fire safety objectives and eight functional requirements listed in SOLAS II-2/2. The fire safety objectives cited from SOLAS are as follows (IMO, 2004):

“

- *Prevent the occurrence of fire and explosion*
- *Reduce the risk to life caused by fire*
- *Reduce the risk of damage caused by fire to the ship, its cargo and the environment*
- *Contain, control and suppress fire and explosion in the compartment of origin*
- *Provide adequate and readily accessible means of escape for passengers and crew*

”

These objectives are very general and leave much room for different interpretations and solutions. However the functional requirements, listed below, give slightly more detailed information on what is needed to fulfill the objectives (IMO, 2004).

“

- *Division the ship into main vertical and horizontal zones by thermal and structural boundaries*
- *Separation of accommodation spaces from reminder of the ship by thermal and structural boundaries*
- *Restricted use of combustible materials*
- *Detection of any fire in the zone of origin*
- *Containment and extinction of any fire in the space of origin*
- *Protection of means of escape and access for fire fighting*
- *Ready availability of fire-extinguishing appliances*
- *Minimization of possibility of ignition of flammable cargo vapor*

”

As mentioned above these requirements are also quite non-specific, this can have both positive and negative implications from a design perspective. The lack of concrete criteria in form of quantitative limits can result in more liberty for the designers but in the end it makes it harder to show that the functional requirements have been met.

The first step that needs to be taken when moving towards approval of an alternative design is, according to SOLAS II-2/17, to perform an engineering analysis. The analysis must as minimum include the elements listed in the regulation and the objective of this engineering analysis is to show

that the functional requirements are met. Some of the components that must be included are identification of which of the perspective requirements that the ship will fail to comply with, identification of fire hazards of the concerned space and a technical demonstration that shows compliance with the functional requirements. This engineering analysis is then evaluated by the responsible government body of the particular ships flag state and if it is deemed acceptable it is approved for use (IMO, 2004).

1.2 Aim and objectives

The aim of the project is to identify some of the possible risks, in regard to fire safety, that are introduced when converting from a structure made of steel to the use of FRP onboard large passenger ships. This is an important concern that must be dealt with when moving towards approving and enabling the use of FRP in the maritime sector. The desire is to assess if the existing level of safety for the passengers can be maintained during an evacuation despite the added insulating capabilities of the FRP construction. The term risk is in this project defined as the combination of the probability and the consequences of a certain scenario.

More specifically the objective is to study how the differences in the thermal properties influence the smoke layer height, visibility and the temperature of the gases in the early stages of a fire. This is done in order to compare the risk of using a FRP composite superstructure relative to the more traditional steel superstructure. Further the project aims to determine if the effects of the added insulation is a factor that should be considered when making the risk level comparison.

1.3 Research questions

In order to achieve the objective the following research questions will be answered.

General

- How does the insulated FRP composite structure perform compared to the steel structure in regard to fire safety and risk during an evacuation?

Specific

- How does an insulated FRP composite structure influence the smoke layer height, visibility and gas temperature in the early stages of a fire?

- Does the added insulation result in a higher risk level during evacuation time frame?

1.4 Delimitations

The aim is not to investigate a total conversion from steel to FRP but rather the superstructure exclusively. Hence, the material used in the structures that form the hull, engine rooms and similar spaces is steel.

The aim is not to simulate the evacuation process since this does not change depending on the building material. Rather the focus lies on the fire development in the early stages that are significant for assuring the safety of people during evacuation. Because of this the geometry used in this work is fairly simple and represents a corridor with cabins on both sides.

Since it has been shown that the FRP construction can maintain integrity and temperature requirements for 60 minutes, given it has sufficient fire insulation (Hertzberg et al., 2009), the production of toxins generated from the FRP will not be studied. This will have an effect only in the later stages of the fire and therefore does not pose a threat to the people evacuating. The same

reasoning applies to a possible collapse of the construction during evacuation, since it is sufficiently protected by the thermal insulation and has been shown to maintain its load bearing capacity for 60 minutes (Hertzberg et al., 2009).

2 Methodology

The approach that was used to compare the risk level between the FRP and steel case was based on risk assessment which is a part of the risk management process, shown in Figure 2.1. The first step in this process is establishing the context including goals, strategies and different prerequisites for the whole risk management process. The second step is the risk assessment, where the identification of hazards combined with an estimation of probabilities makes up the analysis and hence lays out the options for the risk treatment. The risk treatment is the process of choosing actions to reduce or remove the risks. Risk management is an iterative process which requires constant evaluation and monitoring (ISO 31000, 2009).

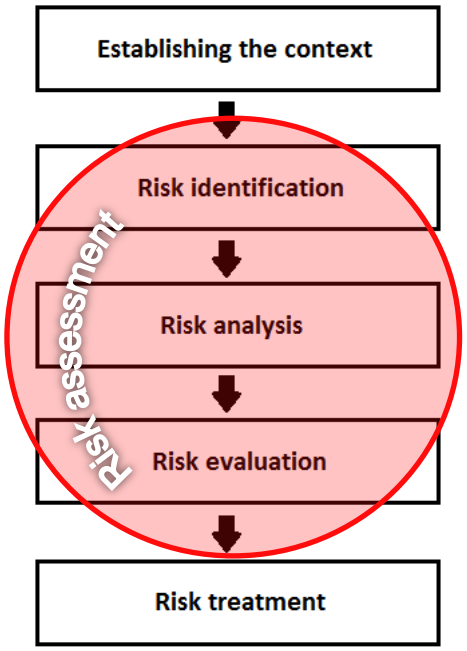

Figure 2.1. Simplified version of the risk management process.

In this project the main focus is put on the risk assessment part, marked with the red box. Further, in this specific case where the aim is to compare the risk level of a steel structure and a FRP composite structure, the emphasis is put on determining the consequence part of the risk. This is explained by the fact that the difference in boundary structure materials will influence the fire development and have an impact on the time until critical conditions occur. The difference in building materials does however not influence the probability of a fire occurring and does not affect the evacuation time since the geometry and the furnishing remains unchanged. Therefore there has been little or no regard taken to the estimation of probabilities, instead most focus is put on comparing consequences of different scenarios.

To gain understanding about the risks that may be introduced when using FRP on ships a literature study was performed. The literature that was read consisted of previous research which addresses issues and gives suggestions on possible solutions to certain problem areas towards implementing lightweight materials in the maritime sector. The issues are as mentioned before in 1.1, that a lightweight construction such as a FRP composite structure is made up of combustible materials and soften at lower temperatures than the conventional steel construction. Since this is dealt with by using a larger amount of fire insulation, thus leading to higher gas temperatures and quicker fire growths, the added insulation could have a negative effect on the risk level in regard to human safety during evacuation.

The risk analysis in general is the way of gaining input for evaluation of risks and identification of the most favorable actions or strategies. It should involve a mapping of risk sources, an estimation of their consequences and an establishment of the probabilities for these consequences. These combinations of probabilities and consequences must be in line with the risk criteria which are stated by the project. There should also be an expressed confidence of the stated risk level, which can be done by for example uncertainty analysis (ISO 31000, 2009). In this project the risk analysis was based on a relative comparison of the different consequences that emerge from having two choices of construction – the lightweight construction and the traditional steel construction. Since the probabilities of different fire scenarios are not dependent on the construction materials it is, as previously mentioned, not interesting to evaluate or weigh in the probabilities in the risk assessment.

Hence the focus was instead put on comparing the consequences of the scenarios by preforming fire dynamics simulator (FDS) simulations and studying the results. This was done by simulating the scenarios in two different setups, one representing the use of a FRP composite structure and the other representing a steel structure, a more thorough description of the FDS setup is given in chapter 5. The geometry that was used represented a corridor with cabins on both sides and was identical in both the FRP and steel case but the building materials that made up the structure varied for the floor-, ceiling- and outer wall structure. When comparing the two cases the most critical difference that was specified in FDS was however the different design fires that were used. Because of the expected effects of the added thermal insulation the design fire that was used in the steel case had a slower growth rate compared to the fire used in the FRP case. This was done by studying results and drawing conclusions from experiments made in previous research, carried out by Back (2012). Conclusions from the previous research are presented in 4.2 and the method used to reduce the fire growth rate is described further in 5.4.

The variable that was used to quantify the risk in order to be able to perform for the risk comparison in this project was the time until critical conditions for safe evacuation occurs. The criteria for when critical conditions occur were from the Swedish building regulations, as stated in BFS 2013:12 (Boverket, 2013). The reason for using these criteria is that there are no such criteria specified for ship construction. In addition the purpose of the criteria is to enable safe evacuation and since they apply for analytical design methods used for land based constructions they should be applicable for safe evacuation in maritime environments as well. For a view of the mentioned criteria see Table 2.1.

In order for the evacuation to be considered safe, criterion 1 or 2 and criteria 3-5 must be fulfilled (Boverket, 2013).

Table 2.1. Translated to English from BFS 2013:12 (Boverket, 2013).

Level of critical impact in the analysis of evacuation safety	
Criterion	**Level**
1. The smoke layer height above the floor	Minimum of 1.6 + (room height (m) x 0.1)
2. Visibility, 2.0 m above the floor	10.0 m in spaces >100 m^2
	5.0 m in spaces ≤100 m^2 The criterion can also apply to situations where queuing occurs at an early stage, at the place where the queue arises.
3. Thermal radiation / heat dose	Maximum of 2.5 kW/m^2 or a short-lived radiation at a maximum of 10 kW/m^2 combined with a maximum of 60 kJ/m^2 in addition to the energy from a radiation level of 1 kW/m^2
4. Temperature	Maximum of 80 ° C
5. Toxicity, 2.0 m above the floor	Carbon monoxide concentration (CO)<2000 ppm Carbon dioxide concentration (CO_2) <5% Oxygen concentration (O_2)>15%

Of the five given criteria the focus was put on the three criteria that apply for smoke layer height, visibility and temperature. The radiation criterion would be of interest but since the radiation model in

FDS requires a larger amount of simulation time in order to make good predictions this variable is not measured. Production of toxic species was also not measured as previously mentioned in 1.4.

The measurements for visibility and temperatures were made at a height of 2 m above the floor, along the centerline of the corridor. The reason for measuring the times until critical conditions in the corridor is that it is the only escape route from a cabin. Looking at the critical conditions inside the cabins would only be relevant for the case when people are still inside the cabin at the time of critical conditions within the cabin, which is highly unlikely. The reason for measuring the temperature at the height of 2 m is that this is what is proposed by BIV- the official Swedish chapter of the Society of Fire Protection Engineers (2013).

There were four different scenarios that were part of the risk analysis. The scenarios were as follows:

1. A FRP composite structure is used and sprinkler activation takes place.
2. A steel structure is used and sprinkler activation takes place.
3. A FRP composite structure is used and **no** sprinkler activation takes place.
4. A steel structure is used and **no** sprinkler activation takes place.

Since FDS cannot account for the effects that the boundaries have on the HRR, the difference in HRR between the steel and the FRP case was taken into account by, as previously mentioned choosing a lower fire growth rate in the steel case. This method is further described in 5.4.

The results from the scenario analysis were extracted with FDS2ASCII from temperature and visibility slice files in the corridor. The values were time averaged over 10 seconds where the intervals between the measured times were 10 seconds and 20 seconds where the intervals between the measured times were 50 seconds. The averaging over time was done in order to get smoother lines and make sure no extreme values were chosen. The values were extracted from the centerline of the corridor at 2 m above the floor.

The results are shown in two different types of diagrams (see examples of these in Figure 2.2):

1. With visibility and temperatures on the y-axis and the corridor length on the x-axis. The different curves within each diagram, represents a step in time. Critical conditions are also presented in these diagrams as horizontal lines.
2. With a time on the x-axis and a fraction that expresses the amount of corridor area where critical condition have occurred on the y-axis.

Looking at the type 1 diagrams it is possible to see that critical conditions have occurred in the center of the corridor for different times. For every time step, i.e. every curve, it is possible

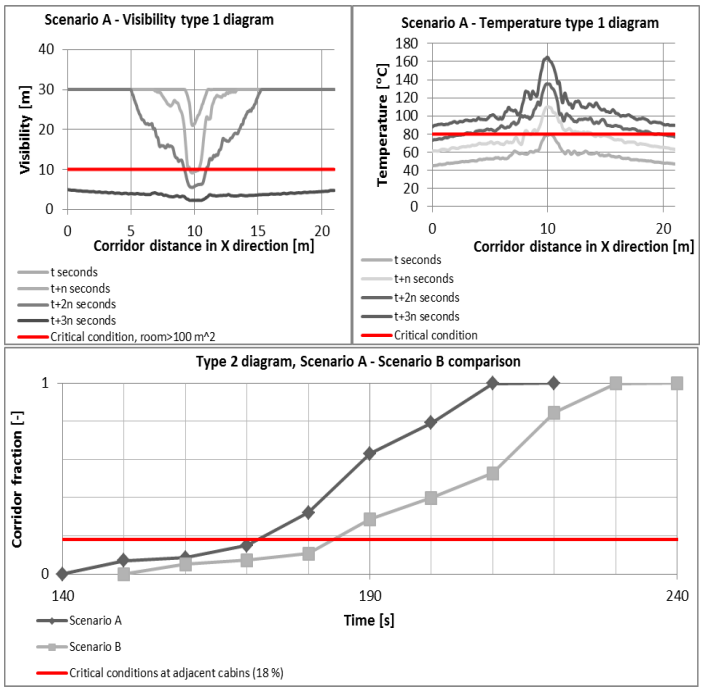

Figure 2.2. Examples of result diagrams.

to see that a larger part of the corridor is under critical conditions. For the time t+3n there are critical conditions over the whole length of the corridor. Consequently, these diagrams shows time until critical conditions, without a specification of how big fraction of the corridor that is regarded as acceptable regarding occurrence of critical conditions.

In the type 2 diagram, it is possible to see the variation in time until critical conditions occur in a given fraction of the corridor. For an example when the whole corridor is under critical conditions (fraction = 1) the difference in time for scenario A and B is ~20 seconds. The red line indicates the threshold where an unacceptable fraction of the corridor is exposed to critical conditions. This fraction was specified to 0.18, which represents an area that stretches over the nearest adjacent cabin doors. This fraction was chosen since it is the point where evacuation becomes unsafe for people in other cabins than the fire cabin (in which people are not expected to be present during the fire anyway). For an explanation, see Figure 2.3.

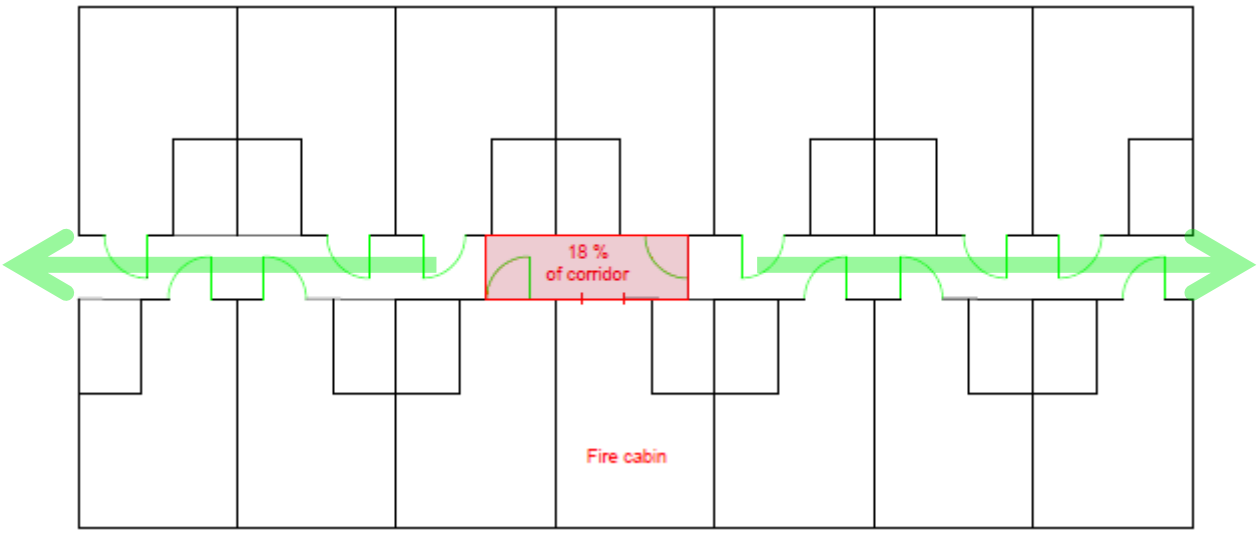

Figure 2.3. Threshold for acceptable fraction of corridor for occurrences of critical conditions and possible escape routes.

The program Smokeview was used for determining the smoke layer height. The soot mass fraction was captured and rendered in 2D pictures with a view of the whole corridor at the time when the visibility criterion became critical in the 18% fraction. This time was chosen since the purpose was to decide which of the parameters that was decisive when determining the time until critical conditions. This is because the requirement states that only one of the two criteria must be fulfilled in order to maintain safe evacuation conditions. Also pictures from the later stages showing the stabilized smoke layer height have been extracted from smokeview.

In order to evaluate uncertainties, a sensitivity analysis was carried out. The results from these simulations were taken from output data from devices and pictures rendered from slice files.

The first two parts of the sensitivity analysis consisted of simulations that had the purpose of making sure an appropriate model was chosen. Firstly two different FDS versions were compared and secondly the results from three different grid sizes were analyzed to make sure that the end results produced from the simulations would be of good quality. However, the main part of the sensitivity analysis focused on the parameter that has a direct effect on the relative difference in time until critical conditions for the steel and the FRP case. This parameter is the fire growth rate. Hence, new

simulations were performed where the growth rate was varied to see how this influenced the investigated variables.

A parameter that does by an equal amount influence the output in both simulation cases would not be of interest, since it does not change the relative difference in risk level in the comparison between the steel and the FRP case. For example, if the soot yield of the fuel is increased by the same amount in both cases the visibility will decrease by the same relative amount in both simulations. To prove this point simulation where the soot yield was increased were included in the sensitivity analysis.

To summarize the parameters investigated in the sensitivity analysis were:

- Choice of FDS version.
- Grid size.
- Soot yield of the fire.
- Difference in fire growth rate between the steel and FRP case.

With the results from the simulations, conclusions were drawn on whether the level of risk for a FRP structure is acceptable relative to the steel structure during the early stages of a fire when people are expected to be evacuating.

3 Theory

This chapter will provide a technical background for this project. Starting with a background in basic fire dynamics and then going through different design method for sprinklered fires.

3.1 Basic fire dynamics

The development of an enclosure fire can be described in different ways, Karlsson and Quintiere (2000) divide it into the following phases:

- ignition
- growth
- flashover
- fully developed fire
- decay

The ignition, which can be either piloted or spontaneous, is the start of the combustion process and the heat production or in plain words the fire. Following the ignition the fire enters the growth phase where the heat release rate increases. Several parameters influence how fast the fire grows for example the fuel properties, the amount of available oxygen and the surroundings. The next possible phase that can be achieved is flashover where the fire swiftly spreads to all combustible materials and the compartment is engulfed in flames. This causes an intense rise in the heat release rate and is followed by the fully developed fire phase were the peak heat release rate is reached. The fully developed fire will continue to burn and the high heat release rate will be maintained until there is an insufficient amount of either oxygen or fuel. Once the amount of available oxygen is too low or most of the fuel has been consumed the fire will start to decay. During the decay phase the heat release rate gradually declines as the oxygen and fuel levels diminish (Karlsson & Quintiere, 2000). The development of the fire is also shown in Figure 3.1, the figure has been slightly altered to illustrate the heat release rate of the fire instead of the temperature in the compartment on the vertical axis.

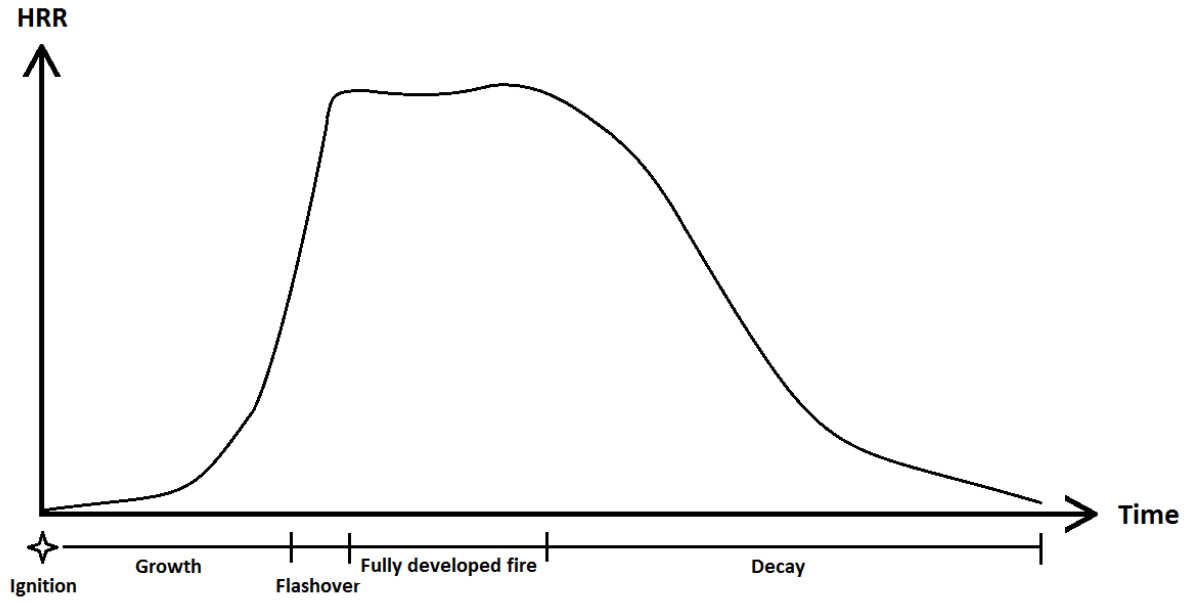

Figure 3.1. Description of a possible fire development for an enclosure fire.

Since flashover is of such a significant event it is also common to simply divide the fire into two stages depending on whether or not flashover has occurred. In this way a fire can be described as a pre-flashover fire or a post-flashover fire. From a human safety perspective the pre-flashover stage of the fire is of most importance since it is during this time that people will be evacuating in the majority of cases (Karlsson & Quintiere, 2000). It is highly unlikely that someone who has not evacuated a compartment before flashover will survive and the risk of the fire spreading to neighboring compartments will also greatly increase once flashover has occurred. Because of this it is important to investigate if a fire can reach the flashover stage but also how long the time until flashover will be since this can give a first indication on whether people will have time to evacuate (Drysdale, 2011).

As earlier mentioned there are different parameters that influence the development of a fire. Some of these are tied to the fuel properties, the placement of the fuel and the ignition source while others depend on the enclosure properties such as the geometry and the thermal properties of the enclosure boundaries (Karlsson & Quintiere, 2000). It is not difficult to grasp the fact that some types of fuels give more intense fires and that the size and position of the fire source will greatly impact the early fire growth since these factors affect the fire directly. The enclosure properties should however not be overlooked. Even if these parameters may not have the same direct influence on the fire development they will most certainly play an important role. For example ceiling height and the insulation capabilities of the boundaries determine the level of radiation that is reflected towards the fuel bed and thus influences the mass loss rate that is proportional to the heat release rate (Drysdale, 2011). In the following chapter the effects of the enclosure boundaries will be more thoroughly described. The effects of the geometrical properties will not be specified in this report since it does not relevant for this specific case.

3.1.1 The influence of the enclosure boundaries

One of the factors that can influence the fire growth and the time to flashover is as mentioned above the thermal properties of the boundary materials. More specifically these properties are thermal conductivity (k), density (ρ) and specific heat (c) which together form a property called thermal inertia ($k\rho c$). Insulating materials like mineral wool that are intended to conserve heat or protect the structure from high temperatures have a low thermal inertia and will therefore act like an obstacle that limits the amount of heat entering the structure. This results in higher gas temperatures within the enclosure since more of the energy is retained inside the fire compartment (Karlsson & Quintiere, 2000). As previously mentioned this will cause the heat release rate to increase faster as well because of the greater mass loss rate of fuel that arises due to the thermal radiation from the hotter smoke layer and boundary surfaces. It is important to realize that it is mainly the innermost layer of the boundaries, namely the inner surface material that significantly affects the temperature and heat release rate increase. Since it is closest to the fire it will be directly exposed to the heat flux unlike the inner materials. In most practical cases insulation material is covered by some kind of surface material for example gypsum- or fiber boards which have a higher thermal inertia than the insulation and the effects of added insulation on fire growth is therefore limited. Added insulation can however still give some effects and tends to contribute to a more severe fire once it is fully developed since the thermal conduction through the boundaries is limited and thus the temperature in the compartment will be higher (Drysdale, 2011).

3.2 Sprinklers

In SOLAS II-2/10.6.1 it is clearly stated that passenger ships that carry more than 36 passengers must be protected with an automatic sprinkler system in all spaces, except for those spaces where the fire

risk is low or where water may damage more than it helps. The latter is e.g. spaces such as control stations with water-sensitive equipment (IMO, 2004).

To fulfill the SOLAS requirements for sprinkler systems, the guidelines from Resolution A.800(19) developed by IMO (1995) must be followed, i.e. the sprinklers should be water mist sprinklers, have fast response characteristics and activate at temperatures ranging from 57 to 79°C (IMO, 1995).

3.2.1 Influence on fire

Sprinkler activation influences the fire scenario in several ways. Firstly, the heat release rate will be reduced by the sprinkler. Secondly, the conditions regarding temperatures, gas flow and toxicity within the compartment will change not only because of the change in heat release rate, but also because of the turbulence induced by the evaporating water. When the sprinkler activates the fire either gets extinguished or becomes controlled by the sprinkler. The amount of toxic gases, heat and soot produced depends on the fuel and the heat release rate of the fire, and thereby can be reduced by an effective sprinkler. Sprinkler tests have shown that using sprinklers is a way of decreasing the heat release rate on the fire before critical conditions for human safety has been reached, with a reliability of 90-95 %. However, it does not mean that the fire does not produce a lot of gases even if it is controlled by a sprinkler. There is a production of gases ongoing when the sprinkler is active; yet, it has been shown that the temperature and toxicity of the gases are so low that they do not pose a threat to people in the fire compartment. In smaller compartments, such as cabins, the gases become mixed when sprinkler is active, meaning that it is not possible to distinguish a stratified gas layers within the enclosure (Nystedt, 2011).

Depending on whether or not the fire is extinguished or controlled, the heat release rate will be influenced in different ways. These different ways can be accounted for when choosing the design fire and these design fire methods will be described in the following design methods. What also affects the impact the sprinkler has on the fire is how well it hits the flames and how great the fire has become before the sprinkler activates (Nystedt, 2011).

3.2.2 Sprinklered design fire

To choose a design fire that represents a given fire scenario, the HRR of the unsprinklered design fire must first be established. Subsequently, the unsprinklered design fire has to be modified so that it represents the sprinklered case of the fire. There are several ways to do this. Some of them are described below.

1. Tests have shown that fires that have a lower HRR than 5 MW when sprinkler activates become extinguished (Nystedt, 2011). A 5 MW fire is considered the maximum that can occur in smaller enclosures such as offices or apartments. Seeing that sprinklers are highly effective in smaller fire enclosures, it is conservative to assume that:
   - The HRR of the sprinklered fire is constant for one minute after sprinkler activates
   - After that the HRR of the fire decreases linearly during one minute to one third of the HRR that was reached at the time of activation.
   - Then the HRR remains constant at one third during the remaining course of the fire (Nystedt, 2011). See Figure 3.2 for visualization of the method.
2. The HRR can be assumed to remain at the level where it was when the sprinkler activated throughout the duration of the fire. This is a traditional but rather conservative approach since it builds on the assumption that the sprinkler can only control the fire and not extinguish it (Staffansson, 2010). If the fire is larger and has a HRR $\geq$ 5 MW when the sprinkler activates, Nystedt (2011) proposes the use this approach. See Figure 3.2 for visualization of the method.

3. Madrzykowski & Vettori (1992) developed an empirical equation for sprinkler fire suppression, which is the next method described. By multiplying the HRR at sprinkler activation with a reduction factor, $e^{-0.0023(t-t_{activation})}$, it is possible to take into account the suppression effect from the sprinkler. The formula for $\dot{Q}$, heat release rate, would be: $\dot{Q}_{supression}(t) = \dot{Q}_{activation} e^{-0.0023(t-t_{activation})}$, and should be calculated for an appropriate amount of time steps in order to represent an acceptable HRR curve. This is an empirical equation that builds on observations of sprinklered and unsprinklered full scale fire tests of unshielded fuels that can be expected to find in an office fire. The algorithm is applicable when using sprinklers with a spray density of at least 0.07 mm/s(4.20 mm/min), in light hazard occupancies (Madrzykowski & Vettori, 1992). See Figure 3.3 for visualization of the method.
4. The next method was brought forth by Evans (1993) and builds on the previous empirical equation. However, the formula has been modified so that it includes the influence that the water density has on the fire suppression. The resulting formula is: $\dot{Q}_{supression}(t) = \dot{Q}_{activation} e^{[-(t-t_{activation})/(3.0(\dot{w}")^{-1.85})]}$, where $\dot{w}"$ is the water density in mm/s. Evans (1993) claims the algorithm to be a conservative estimation of the suppression, because it does not take into account the effects the sprinkler has on the convection driven by the fire. The data used were mainly from experiments from Madrzykowski & Vettori (1992), with sprinkler spray densities higher than 0.07 mm/s, and therefore has the same limitations as the previous empirical formula (Evans, 1993). See Figure 3.3 for visualization of the method.

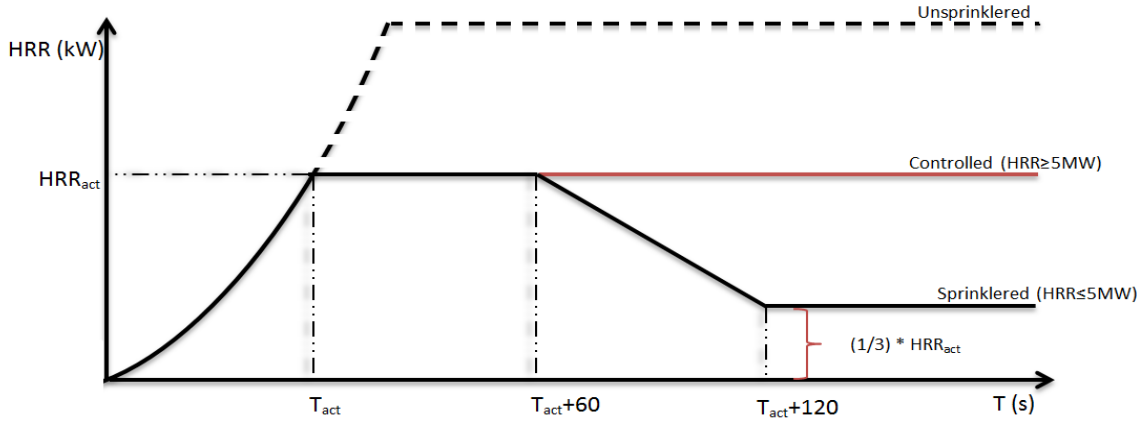

Figure 3.2. Visualization of methods 1 and 2 for choosing of sprinklered design fire.

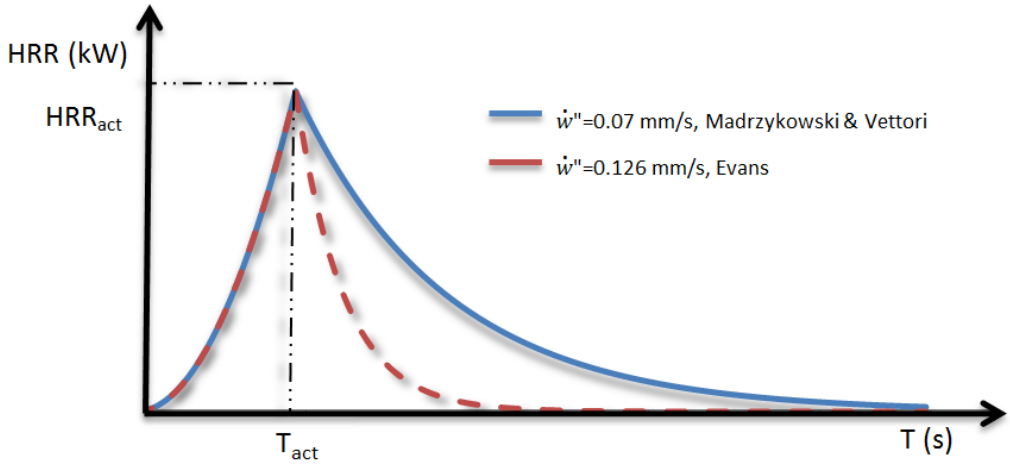

Figure 3.3. Visualization of methods 3 and 4 for choosing of sprinklered design fire.

4 Previous research

In this chapter previous research that is relevant to the project is presented and the most important content is summarized. The chapter is the result of the literature study that was performed in the early stages of the project and much of the information has been gathered from the LASS project.

4.1 Use of lightweight materials

The LASS project has as previously mentioned provided important knowledge on how to implement the use of lightweight materials on different kinds of ships. Besides the technical and mechanical design difficulties that are presented when converting to new construction materials there is also a problem with regard to fire safety design. Social and economic factors also play a part in making the transition more difficult because of the strong tradition of using steel structures and the higher initial building costs that the new materials entail. The LASS project can be seen as a large step in the right direction in regard to overcoming these problems. This is achieved by demonstrating that full scale structures can work in practice and suggesting possible ways to satisfy the present demand for fire safety. LASS also proves that lightweight constructions can be favorable from an economic standpoint if the costs for the entire lifecycle of the ship are analyzed (Hertzberg et al., 2009).

Two separate lightweight materials were used in LASS, aluminum and a FRP composite (consisting of a lightweight core made of PVC foam with a FRP laminate on each side). One of the four ships that were studied was a 188 m long RoPax vessel where the objective was to replace the existing steel superstructure with a FRP composite superstructure. The knowledge and information gained in this part of the LASS project will be of great importance when analyzing potential fire safety risks with connection to the use of FRP composites (Hertzberg et al., 2009).

The single largest difficulty with using a FRP composite material is the fact that it is combustible whereas the traditional material, steel, is not. Another issue is that the FRP composite can lose its structural strength at about 100°C due to the softening of the interface between the core material and the laminate. More temperature resistant composites that soften at 150-200°C are available but these consist of polymers that are more expensive and core materials that often have mechanical disadvantages. The temperatures are in any case low compared to the softening temperature of steel which is 400-500°C. These issues can however be solved by using additional thermal insulation in order to protect the FRP composite structure from high temperatures (Hertzberg et al., 2009).

4.2 Effects of increased thermal insulation

Research conducted by Rodríguez Panagiotopoulos (2014) regarding the use of FRP onboard a large passenger ship showed that added thermal insulation used to protect the FRP greatly improves the fire safety performance compared to an unprotected FRP structure. However, it also showed an increase in gas temperatures due to the added insulation. No consideration was taken to how this difference in temperature might affect the heat release rate.

Other previous research on the effects of increased thermal insulation has been done by Back (2012). The study was based on comparisons between large scale experiments, FDS simulations and hand calculations. The large scale experiments consisted of wood crib and heptane pool fires within containers, with and without thermal insulation on the walls and roof. The insulation that was used consisted of 95 mm thick Rockwool sheets. The container used was 5.9x2.35x2.4 m^3, which is a volume representative for a cabin, i.e. around 30 m^3 and had a door opening.

Back (2012) arrived at the conclusions that:

- Maximum gas temperatures within the insulated enclosure were on average 18% higher in the wood crib case and 26 % higher in the heptane fire case compared to the non-insulated cases.
- Slightly higher heat release rates can be expected in the insulated cases, especially when fuels that are sensitive to incident radiation are present.

- The fire growth rate was roughly twice as large in the insulated container compared to the non-insulated one when heptane was used as the fuel.

In the wood crib case the growth rate did not increase significantly but the heat release rate was higher during the entire growth phase for the insulated compartment.

4.3 SOLAS division classes

In SOLAS II-2/3.2 and SOLAS II-2/3.4 fire resistance classifications for construction materials used on ships are defined. These can be divided into three different classes, A-, B- and C-class. The A- and B-class constructions can be divided further into different types of divisions depending on how well they prevent heat transfer. This property is given as a suffix in the form of a number that specifies the time in minutes that the temperature on the backside of the material is within the predefined temperature limits (IMO, 2004).

A-class divisions are typically used in bulkhead and deck constructions. They have to be constructed in steel or equivalent materials and must be able to uphold integrity for one hour during a large scale standard furnace fire test. Further, non-combustible insulation materials must be used so that depending on which suffix the division has the requirements for temperature restrictions are met for the specific division. For an A-class construction e.g. A-60[*] the average temperature on the unexposed side must not increase more than 140°C and the maximum temperature increase at any point must not exceed 180°C. In order to obtain the classification bulkheads and decks are tested according to the FTP Code (International Code for the Application of Fire Test Procedures) to insure that the requirements above are met (IMO, 2004). The test procedure for the testing is specified in IMO resolution A.754(18) (IMO, 1993). In addition to these tests the materials must also pass a test in accordance with ISO 1182 where a material sample is heated to a temperature of 750^{o}C to make sure it is non-combustible (Hertzberg et al., 2009).

B-classifications are used not only for bulkheads and decks but also linings and ceilings. B-class materials must be non-combustible and able to maintain integrity for half an hour during a large scale standard furnace fire test. The insulation should prevent an average temperature increase of 140°C on the unexposed side and a maximum increase of 225°C at any location during the time given by the suffix[†] (IMO, 2004).

C-class structures are used in areas where fire risks are low and have no requirements regarding integrity or insulation but must be constructed in non-combustible materials (IMO, 2004).

A summary of the different classes, their requirements and which divisions exists within each class can be seen in Table 4.1.

[*] There are four different "A" divisions: A-60, A-30, A-15, A-0
[†] There are two different "B" divisions: B-15, B-0.

Table 4.1. Summary of SOLAS class and division requirements.

Classification	Allowed materials	Integrity Requirement	Temperature restriction on backside	Division types
A-class	Steel or equivalent	60 min	Average: 140°C Maximum: 180°C	A-60, A-30, A-15, A-0
B-class	Non-combustible	30 min	Average: 140°C Maximum: 225°C	B-15, B-0
C-class	Non-combustible	-	-	-

4.3.1 The LASS approach

The prescriptive requirements described in the previous chapter are impossible to comply with when using a FRP composite structure since the material is not equivalent to steel and will not pass the non-combustibility test. It is however still possible to build a FRP composite structure in accordance with SOLAS II-2/17 (IMO, 2004). By using this option, that enables the use of alternative designs, any construction materials can be used as long as they comply with the functional requirements described in SOLAS. The approach that was used in LASS to achieve this consisted of showing the constructions fulfillment of the functional requirements of the A-, B- and C class divisions for fire resistance classification. This was done in a rather straight forward way by testing the constructions according to the High-Speed Craft Code (HSC Code) which does not demand the passing of the ISO 1182 non-combustibility test (Hertzberg et al., 2009). Unlike the conventional fire resistance classifications described in SOLAS the HSC Code also enables the use of fire-restrictive materials (FRM), rather than strictly non-combustible ones, and constructions that are fire-resistant divisions (FRD), see HSC 7.2.1. For a construction material to be classified as fire-restricting it must, according to the FTP code, pass the ISO 9705 full-scale corner fire test with some modifications, see HSC 7.2.2 & 7.4.1.3 (Maritime and Coastguard Agency, 2000). These involve changes in measurements of heat release rate and smoke production (Hertzberg et al., 2009). These modifications are specified in resolution MSC.40(64) and further amendments are made in MSC.45(65) as well as in MSC.90(71), see HSC 7.2.2 & 7.4.1.3 (Maritime and Coastguard Agency, 2000).

A construction composed of FRM materials can in the same way as the non-combustible constructions be put through the large-scale furnace fire test to obtain a classification. Since the materials used are not non-combustible the constructions cannot be classed as A- or B-class but instead FRD 30 or FRD 60 (Hertzberg et al., 2009). The FRD 30 constructions must according to HSC 7.4.2.2 maintain integrity for 30 minutes and the FRD 60 for 60 minutes during the furnace test. According to HSC 7.2.1.5 The temperature restriction requirements are the same as for the A-class constructions namely that the average temperature increase, on the unexposed side, is no more than 140^{o}C and the maximum temperature increase at any point no more than 180^{o}C. This applies to both the FRD 30 and the FRD 60 class (Maritime and Coastguard Agency, 2000). However since the laminate can start to separate from the core at 100°, which causes the FRP composite to lose its strength, this is the critical temperature that is used when studying the temperature restriction of the construction (Hertzberg et al., 2009).

For a summary of the different classes and their functional requirements, see Table 4.2.

Table 4.2. Summary of HSC code class requirements.

Classifications	Allowed materials	Integrity Requirement	Temperature restriction on backside
FRD 60	FRM	60 min	Average: 140°C Maximum: 180°C
FRD 30	FRM	30 min	Average: 140°C Maximum: 180°C
FRM	FRM	-	-

The HSC code, as the name suggests, only provides prescriptive requirements for high-speed crafts. However, since it has been adopted by IMO and is part of SOLAS it must therefore comply with the same functional requirements. There are two main criteria that passenger ships have to fulfill in order to be defined as high speed crafts. According to HSC 1.3.4.1 the ship must first and foremost be able to reach a place of refuge within four hours from the course of its travel when cruising at its operational speed. Secondly the ship must be able to travel at a speed that it at least as high as the speed calculated with equation given below:

$$3.7 \cdot \nabla^{0.1667} \text{ [m/s]}$$

Where ∇ is the volume [m^3] of displacement when the hull is submerged up to the design waterline, see HSC 1.4.30 (Maritime and Coastguard Agency, 2000).

To clarify, passenger ships that fulfill the criteria above are thus able to use FRP composite structures in compliance with the perspective requirements of the HSC code. Examples of these types of carriers are high speed catamaran ferries and carriers used by the coast guards. For other large passenger ships that are not classed as high-speed crafts it must be shown that the functional requirements of the SOLAS convention can be met if a FRP composite superstructure is to be used. As previously mentioned, in LASS this is done by arguing that the functional requirements for the FRD and FRM can be seen as equivalent to the A-, B- and C-class constructions. This means that if it can be demonstrated that the FRP composite structure complies with the prescriptive requirements of the HSC code it will also meet the functional requirements of SOLAS (Hertzberg et al., 2009). For a view of the SOLAS and HSC classes that are equivalent regarding functional requirements, see Table 4.3.

Table 4.3. SOLAS – HSC code class equivalency.

Prescriptive requirement (SOLAS convention)	Functional requirement equivalency (HSC code)
A-class	FRD 60
B-class	FRD 30
C-class	FRM

It should be noted that this approach may come across as a solution that automatically enables the use of FRP composite structures but that is not the case. The main reason for this is that there is another important functional requirement in SOLAS that states that the use of combustible materials shall be restricted. This coupled with the strong tradition of using steel constructions that provide a reliable and well-tested solution makes it hard to argue that the same level of fire safety will be achieved when using a FRP composite structure (Hertzberg et al., 2009). Therefore this approach does not by default give authorization to build FRP composite structures without a risk analysis being performed for the specific case.

5 Simulation setup

In this chapter, the setup for the FDS simulations will be presented. Input data for all essential options will be specified, and those options valued to have a smaller significance will be found in 11Appendix A.

In total 14 different simulations were carried out. Four of them make up the scenario analysis. The rest is for sensitivity analysis purposes and their specific deviations from the base scenarios are presented in chapter 6.6.

The geometry that represents the scenarios that was simulated is presented in Figure 5.1. The geometry was however scaled down in the FDS simulations in order to save time, this was done by removing most of the cabins since they would have no influence on the results, see Figure 5.2.

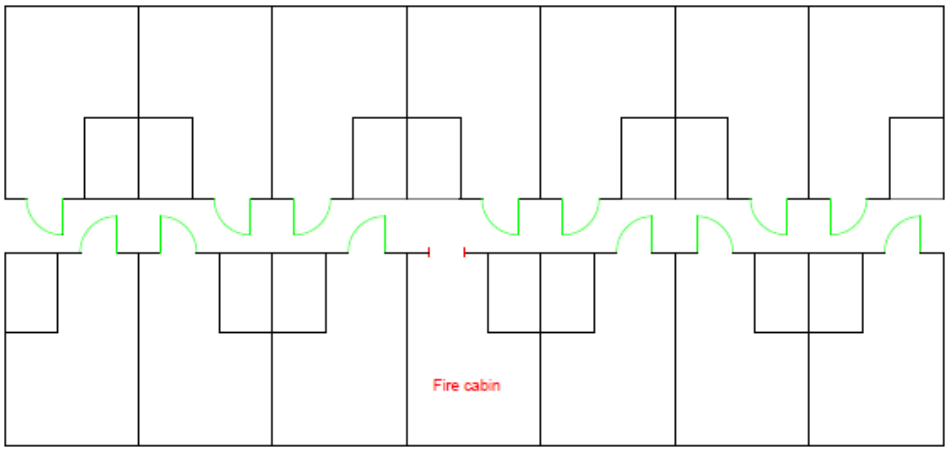

Figure 5.1. Background to simulation geometry.

5.1 Computational domain

In order to decrease the computation time, the computational domain was divided into several smaller meshes, so that they could be run with parallel processing using the MPI function in LUNARC. The number of meshes chosen per FDS computation was eight because there are eight nodes at disposal per node in the LUNARC cluster. The meshes are divided as in Figure 5.2. A detailed description can be found in the bullet list below:

- **The orange** mesh on the first floor contains the fire room, a piece of the room across the corridor and the middle segment of the corridor. Grid size varied between different simulations.
- **The marine blue** mesh is the main part of the room across the corridor from the fire room. Grid size was 0.10 m in all simulations.
- **The yellow** meshes are the main parts of the corridor. Grid size varied between different simulations.
- **The green** meshes are the rooms adjacent to the fire enclosure. Grid size was 0.10 m in all simulations.
- **The purple** mesh is the room above the fire enclosure. Grid size was 0.10 m in all simulations.
- **The small light blue** mesh poses as an air cavity in the outer wall of the fire enclosure. This mesh has very small cells, in order to capture possible convective gas movement due to increased temperature. Grid size was 0.025 m in all simulations

- **The grey meshes** are placed in order to achieve numerical stability in the pressure iterations. They are open to the atmosphere and contain only air. Grid size was 0.2 m in all simulations.

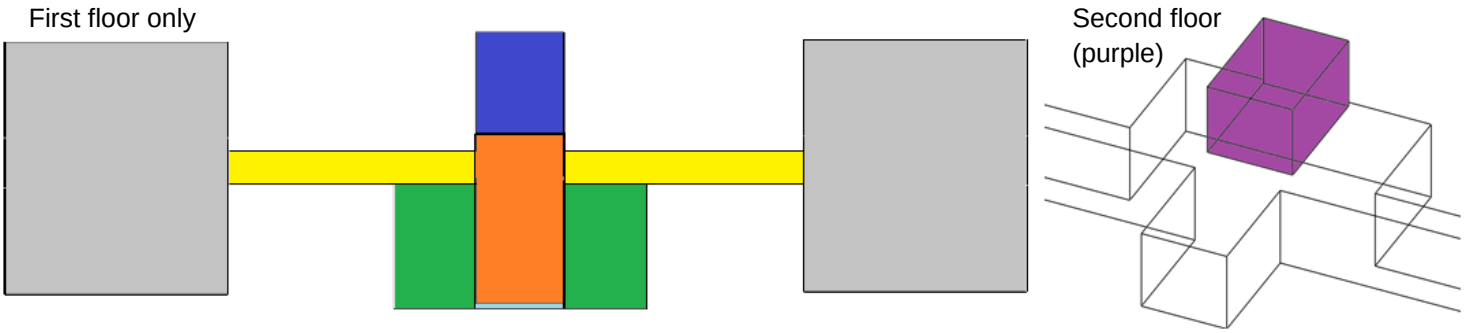

Figure 5.2. The multiple meshes of the computational domain.

5.1.1 Grid size

The grid size for corridor and fire room meshes was 0.1 m for the simulations in the sensitivity analysis. The scenario analysis was simulated with the grid size 0.05 m in these meshes. For more information about the choice of grid sizes, see 7.2.

5.2 Geometry

How the overall geometry and room placement was chosen has been hinted at in the previous sub chapter, where the meshes are described. However, a more thorough description will be presented in this sub chapter.

In order to achieve comparability of results, the choice in building materials and room size have as much as FDS permitted reflected a full scale cabin fire experiment that Arvidson, Axelsson & Hertzberg (2008) conducted.

For a view of the full geometry in 3D, and 2D perspective see Figure 5.3 - Figure 5.6 on pages 22-23. The geometry consisted in total of a corridor and five cabins of which one was the fire compartment. The remaining cabins were specified for the purpose of investigating the heat transport through the inner walls. Consequently, devices were placed in order to measure the temperatures in the adjacent rooms. These are presented in 5.3. The height of the first floor was 2.7 m. An inner ceiling was added at a height of 2.1 m above the floor, between the ceiling and the overhead deck there was consequently a 0.6 m air cavity. The corridor measured 1.2 x 21 x 2 m and the rooms measured 4.3 x 3 x 2.1 m. The fire room also had an air cavity along the short-side wall (assumed to be an outer wall) which was 0.2 m wide, and represented with a mesh entirely on its own, see chapter 5.1. All the doors connecting the cabins to the corridor are assumed to be shut except for the door of the fire cabin. The door chinks were represented with a square element of 0.01 m^{2*}. The two ends of the corridor were specified as open to the outer meshes, resulting in an indirect opening to the atmosphere. An assumption that follows from having the corridor open is that the possibility of any obstructions affecting the smoke filling is neglected. Consequently, the FDS simulations are only applicable for open or very long corridors, and in an early stage of the fire.

5.2.1 Building materials

The building materials of the steel and the FRP case were obviously different. In this sub chapter a specification will be presented on which building materials that was used in the walls, decks and bulkheads. There will be a lot of materials referred to with the line MATL_ID. Most values for these

* This represents a door chink with the width 80 centimeters and the height 1.25 centimeters.

are also given a ramp function that makes the value temperature dependent. See Appendix B for these material data. All surface lines that will be presented in following sub chapters have a corresponding surface line with the command BACKING='EXPOSED' added. The placement of the walls where backing exposed was added is presented in 0. The command was added for those walls where an increase of temperature was expected.

Inner walls and ceiling

According to the LASS project B-class divisions are often used in accommodation areas: "B-class divisions; typically used in cabins or corridors "- (Hertzberg et al., 2009, p.25). However, what can be stated from contents in regulation SOLAS II-2/9.2.2.3 is that the choice of class is more complicated than assuming that all inner walls and ceilings shall be B-class divisions. The class choice of a wall, bulkhead or deck depends on what type of room is above, below or adjacent to the reference room. E.g. if there is an external evacuation route adjacent to a corridor, there should be an A-60 division between. However, between a corridor and an accommodation space with increased fire risk, there should be a B-15 division (IMO, 2004).

The surface line for the inner walls was is specified in FDS as shown below, where "Firemaster" is the insulation material used, material properties can be found in 11Appendix B.

&SURF ID= 'B-class panel', COLOR='BLUE', TRANSPARENCY=0.2,
MATL_ID='Steel','Firemaster','Steel', THICKNESS=0.0007,0.0486,0.0007/

In the large scale cabin test there were PVC surface layering inside the cabin walls (Arvidson et al., 2008), this was however neglected in the geometry in the FDS simulations.

Seeing that the surface was color coded with blue, looking at pictures Figure 5.3 - Figure 5.4, it is possible to recognize which walls that were simulated as B-class panels. The ceiling was specified with a deeper blue, but it received the same surface as the walls, i.e. B-class panel. However, the ceiling in the fire cabin received a yellow color instead. This ceiling was different since it had a function that made it collapse after 420 s the FRP construction simulations and 463 s in the steel construction simulations. The reason for this is that in the large scale cabin fire tests with FRP walls conducted by Arvidson et al. (2008) the roof collapsed after 420 seconds. This happens at a later time in the steel case since the fire is less intense due to the slower growth rate of the fire caused by the lesser isolative properties of the construction. The method used in order to apply the delayed ceiling collapse in the steel cases consisted of making the ceiling collapse at the time where the HRR was equal to the HRR at the time of the collapse in the FRP case.

Decks

This is where the FRP and steel constructions became actualized. The composition of materials in the decks was not symmetrical as it was for the B-class panel. Hence two surface lines were specified in each simulation where backing exposed was used. For the FRP and the steel case this was done as given below where "Laminate" is the FRP-laminate, "DivinycellH80" is the lightweight core and "RockWool" the insulation material. For material properties see 11Appendix B.

&SURF ID= 'FLOOR+CEILING_upwards', COLOR='RED', TRANSPARENCY=0.2,
MATL_ID='Firemaster','Laminate','DivinycellH80','Laminate','RockWool','Aluminium',
THICKNESS=0.1,0.001,0.05,0.001,0.02,0.002/ FRP

&SURF ID= 'FLOOR+CEILING_downwards', COLOR='RED', TRANSPARENCY=0.2,
MATL_ID='Aluminium','RockWool','Laminate','DivinycellH80','Laminate','Firemaster',
THICKNESS=0.002,0.02,0.001,0.05,0.001,0.1/ FRP

&SURF ID='FLOOR+CEILING_upwards_steel', COLOR='RED', TRANSPARENCY=0.2,
MATL_ID='Firemaster','Steel','RockWool','Aluminium', THICKNESS=0.06,0.0045,0.02,0.002/ Steel

&SURF ID= 'FLOOR+CEILING_downwards_steel', COLOR='RED', TRANSPARENCY=0.2,
MATL_ID='Aluminium','RockWool','Steel','Firemaster', THICKNESS=0.002,0.02,0.0045,0.06/ Steel

The parts of the lines marked in grey were what represented the FRP respectively steel parts of the deck constructions. The remaining parts specified the insulation and the floors. Figure 5.3 makes it possible to see that the floor and ceiling i.e. the decks are represented by the pink color which signifies the construction made up of the materials listed in the surface lines above.

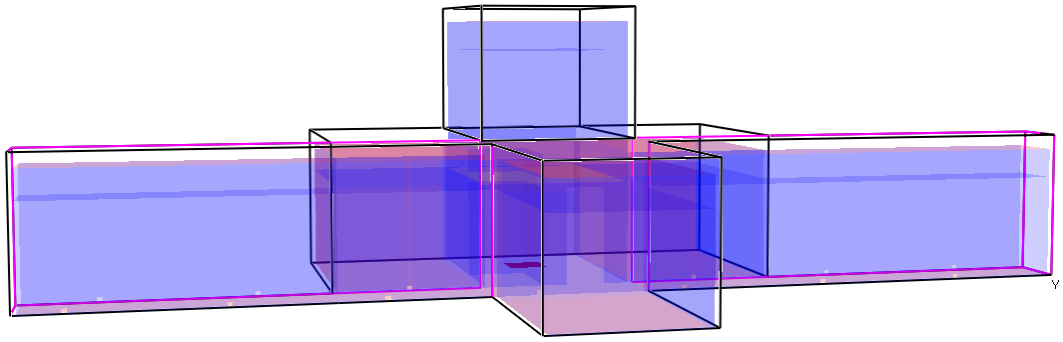

Figure 5.3. Geometry in 3D perspective.

Bulkheads

Only one wall was assumed to be of a bulkhead division, and it was the one that makes up the short side walls of the cabins. The surface lines (two for each case because of asymmetry in material composition) for this wall for the FRP respectively the steel case were specified as follows:

&SURF ID= 'FRP inside', COLOR='RED', TRANSPARENCY=0.2,
MATL_ID='Firemaster','Laminate','DivinycellH80','Laminate',
THICKNESS=0.1,001,0.05,0.001/ FRP

&SURF ID= 'FRP outside', COLOR='RED', TRANSPARENCY=0.2,
MATL_ID='Laminate','DivinycellH80','Laminate','Firemaster',
THICKNESS=0.001,0.05,0.001,0.1/ FRP

&SURF ID='Steel inside', COLOR='RED', TRANSPARENCY=0.2, MATL_ID='Firemaster','Steel',
THICKNESS=0.06,0.0045/ Steel

&SURF ID='Steel outside', COLOR='RED', TRANSPARENCY=0.2, MATL_ID='Steel','Firemaster',
THICKNESS=0.0045,0.06/ Steel

A view of the placement of this bulkhead is shown in Figure 5.4. The bulkhead was colored red, and in front of it was a blue colored wall, which as described previously represents the B-class panel. The space between the bulkhead and the B-class division, i.e. the air cavity, is 0.2 m.

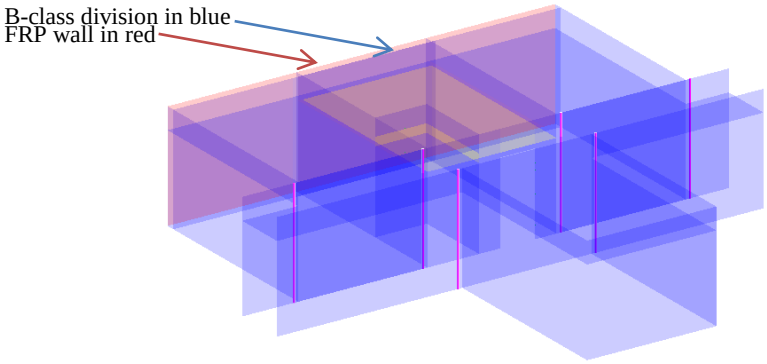

Figure 5.4. Geometry in 3D perspective, with clipped of roof, floor and corridor.

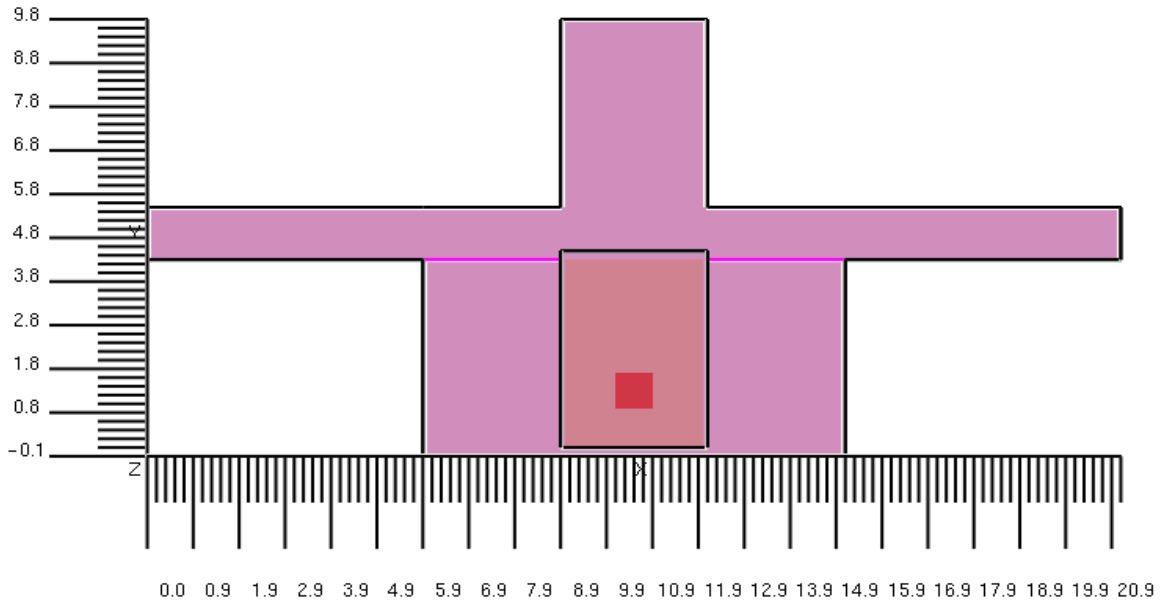

Figure 5.5. Geometry in 2D perspective from above.

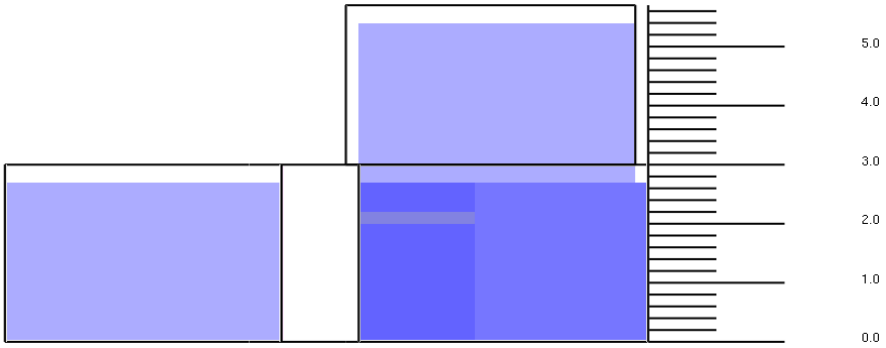

Figure 5.6. Geometry in 2d perspective from side.

5.3 Measurements

The measurements in the FDS simulations were done with slice files and devices for different types of quantities. Placements and other properties of these are presented in this sub chapter.

5.3.1 Devices

The devices that were used were specified to output data for temperatures and velocities. The devices consisted of thermocouples and vector velocity probes with the default properties of FDS. Hence the thermocouples had the specific heat and density of nickel, a bead diameter of 0.001[*] m and an emissivity of 0.85. They were placed in trees with heights similar to how they were placed in the experiments by Arvidson et al. (2008), see Figure 5.7. But a couple extra devices were added to the tree on the second floor, see Figure 5.8.

[*] The thermocouples in the tests by Arvidson et al. (2008) had the diameter 0.0005 m and was of type K.

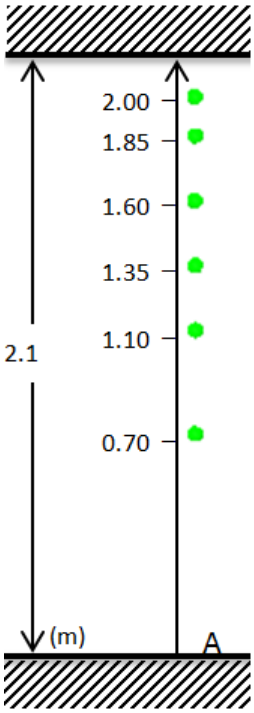

Figure 5.7. Type A device tree, can be found on first floor.

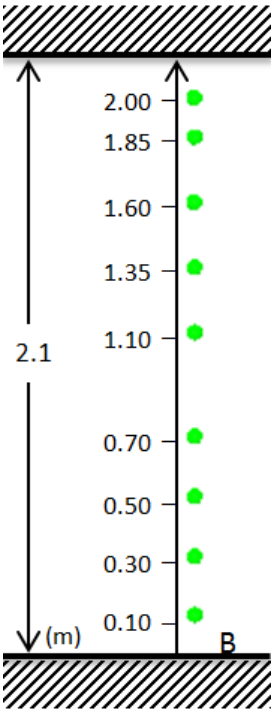

Figure 5.8. Type B device tree, can be found on second floor.

The placements of device trees can be seen in Figure 5.9. The X and Y coordinates of the trees can be seen in Table 5.1.

Table 5.1. Coordinates for device trees. For visualization see Figure 5.9.

		Device tree name											
		A	B	C±	D	E	F	G	H*	I	J	K	L
Coordinates [m]	X	4.9	9.9	19.9	9.9	7.5	8.9	10.5	10.5	12.1	13.5	10.5	11.1
	Y	4.9	4.9	4.9	4.3	2.1	2.1	2.1	2.1	2.1	2.1	1.3	5.5

* Tree was placed on the second floor, and was a type B tree.

± Device at height z=2.0 was mistakenly placed on x=18 instead.

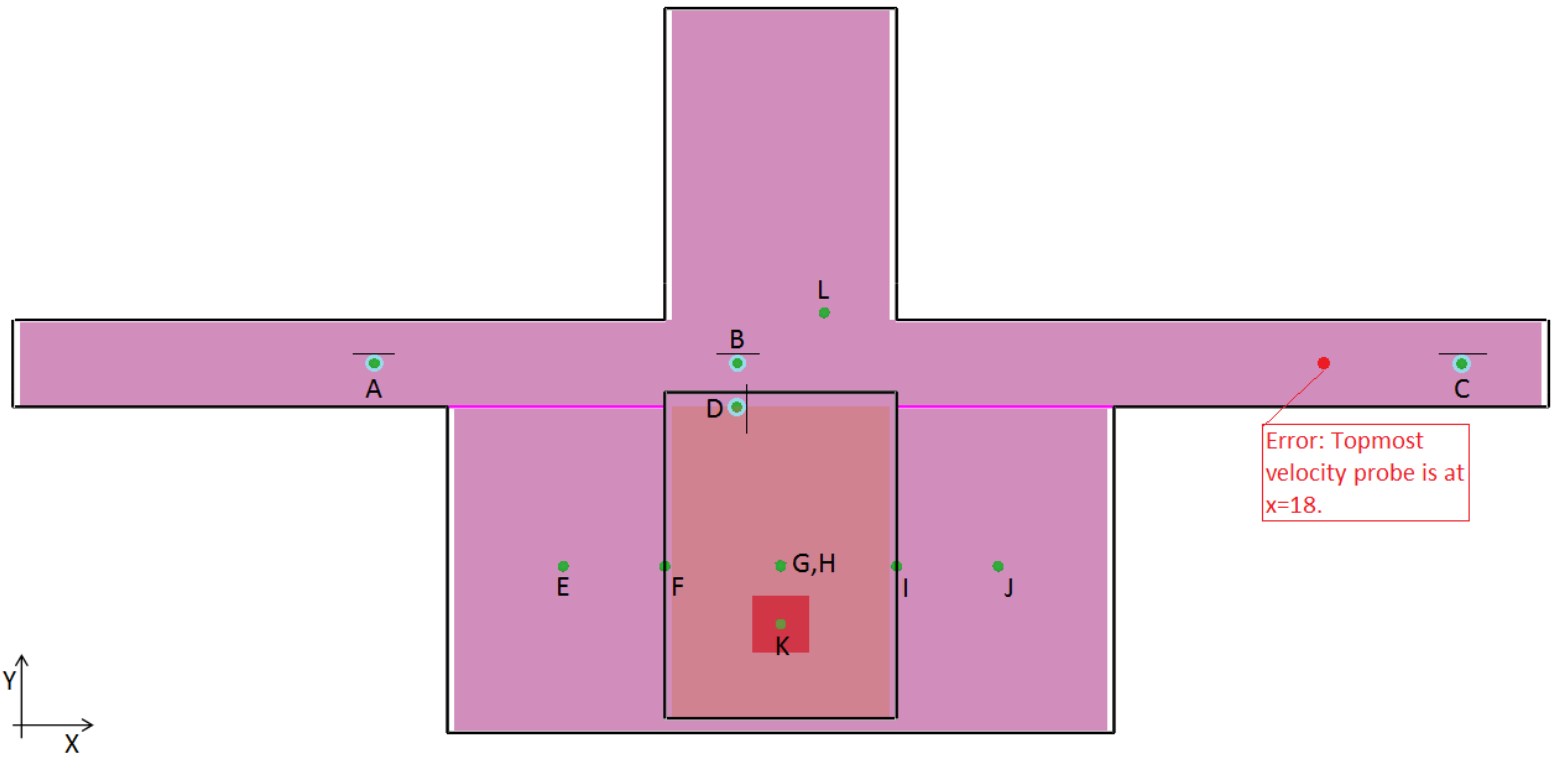

Figure 5.9. Placement of devices. Green is thermocouple, light blue with green is combined thermocouple and velocity probe. The black lines on devices are directions for the vector in which the velocity probes measure flow. For coordinates see Table 5.1.

5.3.2 Slice files

In order to measure outputs for visibility, temperatures and velocities in different planes, a number of slice files were placed.

- Velocity slice files were placed in planes X=10.5, Y_i=-0.1,1.3,4.9.
- Temperature slice files were placed in planes X=10.5, Y_i=-0.1,1.3,4.9, Z=1.81
- Visibility slice file were placed in plane Y=4.9.

The reason for using the temperature slice in Z=1.81 was to make it possible to investigate the temperatures that occur in the critical smoke layer height (1.81 m) which is calculated according to Boverket – the Swedish National Board of Housing, Building and Planning (2013). The temperature slice in y=4.9 was placed for investigation of the critical temperature in the corridor which is 80°C (Boverket, 2013). These values are extracted along the center of the corridor at the height 2 m above floor level which is the height recommended by BIV (2013). The visibility slice in Y=4.9 was placed in order to investigate the critical visibility in the corridor. This visibility should be at least 5 m at the height of 2 m if the floor area is less than 100 m^2. Even though these critical conditions are associated with ordinary buildings they are still interesting to investigate since they have an importance for human safety during evacuation, and should thereby also be applicable in evacuation situations on ships.

5.4 Design fire

The HRR of the FRP case design fire that was used in FDS was based on the HRR that was obtained in the full scale experiment performed by SP (Arvidson et al., 2008). The curve was however slightly modified and fitted to follow an αt^2-curve while still reaching the same peak HRR of 1700 kW, as in the full scale experiment. In order to achieve a more representative fire growth phase the maximum HRR was reached faster in the modified HRR curve compared to the one acquired in the experiment (maximum is reached after 10 min instead of approximately 12 min). This difference does make the scenario more severe but still represents a realistic case and is therefore acceptable since the results will be more conservative.

The experiments that were carried out by Back (2012), see 4.2, were used to estimate the HRR that was used for the steel case design fire. This was done by decreasing the growth rate of the fire used in the FRP case by 17.6% but keeping the same maximum HRR. The reasons for not changing the maximum HRR was that the experiments did not show any great increase of this variable also since the design fire represents a flashover scenario all the fuel will be burning in both cases which will result in similar maximum HRR. The growth rate was however reduced because of the fact that that the HRR was higher throughout the entire growth phase of the wood crib fire, which is the case that best resembles the fire in the passenger cabin because of the fuel type.

When the crib fire in the insulated compartment had reached the maximum HRR of around 800kW the corresponding fire in the non-insulated compartment had only reached a HRR of approximately 650 kW which means that the HRR was almost 20% (18.75%) lower at this time. Therefore the growth rate for the steel case was set so that the HRR of the steel case was 18.75% lower at the time when the maximum HRR was reached in the FRP case. This resulted in the 17,6% lower growth rate when fitted to an αt^2-curve. Like mentioned earlier the steel case design fire still reaches the maximum HRR of 1700kW but at a later time because of the lesser growth rate see Figure 5.11.

The sprinklered design fires were acquired using method number 2 from 3.2.2 and the activation time was calculated using a web implementation of DetactT2 by Molinelli (2012). View of input and output for the FRP and the steel case can be seen in Figure 5.10.

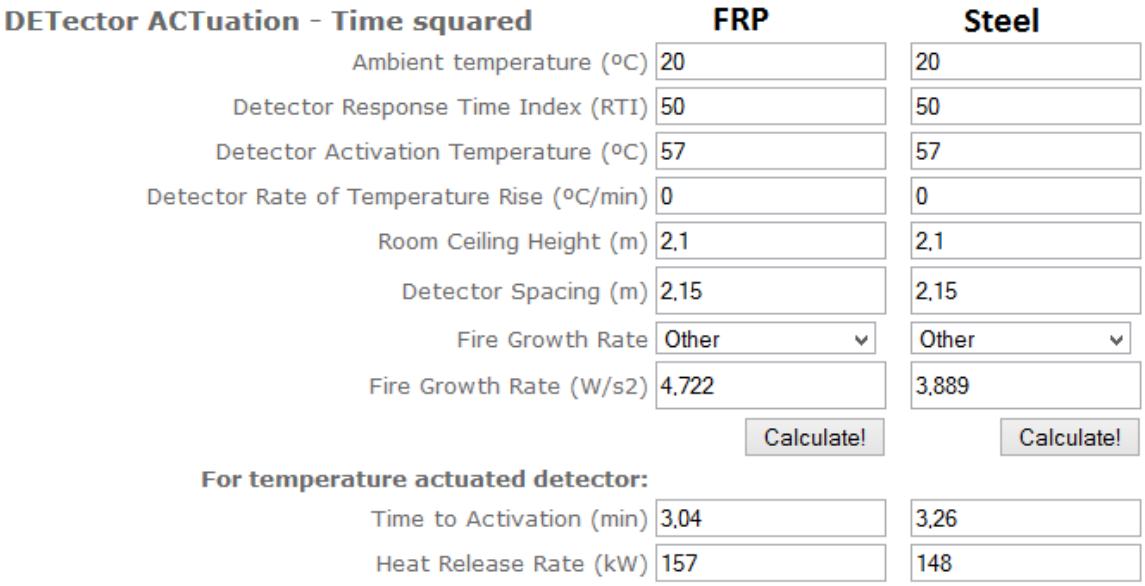

Figure 5.10. Print of input and output of web implementation of DetactT2.

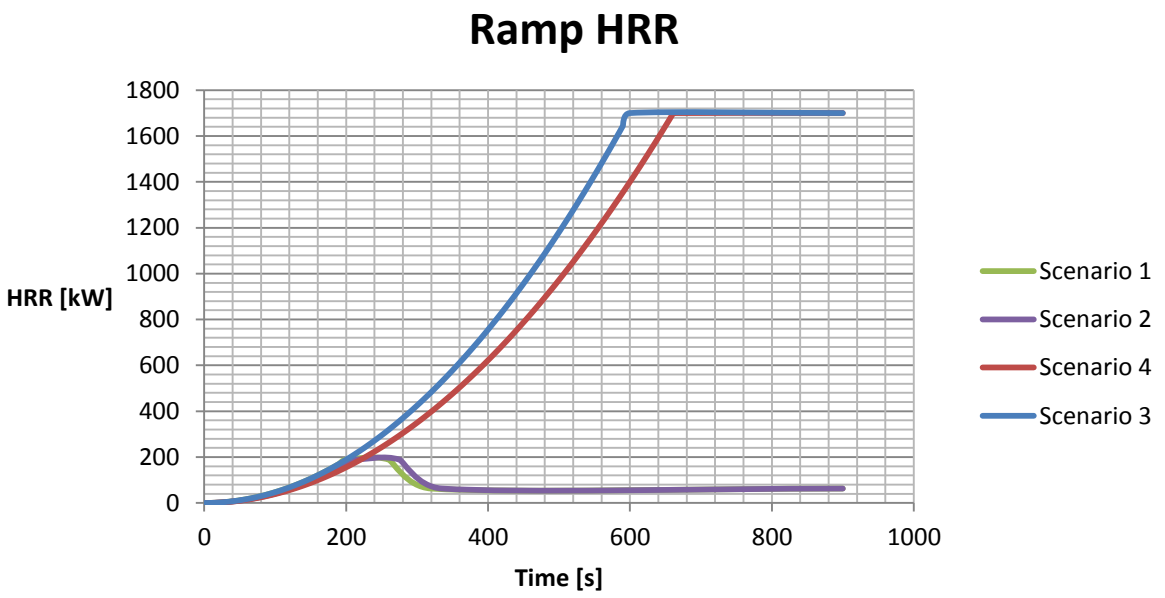

Figure 5.11 HRR for the different sprinklered and unsprinklered scenarios.

The fire in the sprinklered and unsprinklered cases had square areas of 0.64 m^2 respectively 0.09 m^2. The fuel properties were composed of the weighted average of all materials that were assumed to be involved in the fire within the cabin. Consequently, the soot yield was 0.067, the CO-yield was 0.045, the heat of combustion was 26376 kJ/kg and the number of carbon, hydrogen and oxygen atoms in the fuel was 1, 1.6 and 0.2 respectively. These calculations are presented in 0. The HRR of the different cases received different ramps, as seen in Figure 5.11. For an example of an input line, see the FDS lines below.

```
&OBST XB= 10.1,10.9,0.9,1.7, 0.0, 0.0, SURF_IDS='BURNER','INERT','INERT' / Unsprinklered
&REAC       FUEL='MYFUEL'
            SOOT_YIELD=0.067
            CO_YIELD=0.045
            IDEAL=.TRUE.
            C=1
            H=1.6
            O=0.2
            HEAT_OF_COMBUSTION=26376/
&SURF ID='BURNER',
    COLOR='RED'
    HRRPUA=2656.25,
    RAMP_Q='RAMP_HRR'/
&RAMP…
```

5.5 Miscellaneous settings

- The simulation time was set to 900 seconds.
- The ambient temperature was set to 20 °C.
- The radiative fraction was set to 0.262 (based on the materials in the cabin, see 0).
- The exterior boundaries of the computational domain were open.

– The visibility factor used was the default value of 3, which represents visibility towards light-reflecting signs[*] (McGrattan et al., 2013).

[*] According to SOLAS 13/3.2.5.1 those types of signs are allowed (IMO, 2004).

6 Results

This chapter presents output data according to what is described in chapter 2. First, results are presented for each scenario separately and then a comparison is made between the results of the two sprinklered scenarios and the two unsprinklered scenarios.

The measure points in adjacent rooms (points E, F, I, J and L) reached at the most a temperature increase of 1 °C. Because of this, risks in other spaces than the corridor have been neglected, hence the output data has not been investigated further.

6.1 Scenario 1 – Sprinklered FRP

Looking at Figure 6.1 it is possible to see that for this scenario the temperatures increase in the beginning and then, because of sprinkler activation, decrease until they stabilize so that critical temperatures can be found only in the middle of the corridor (over a length of 2 meters). Critical temperatures start occurring after 130 seconds and the stabilization of the temperatures occurs after 350-400 seconds.

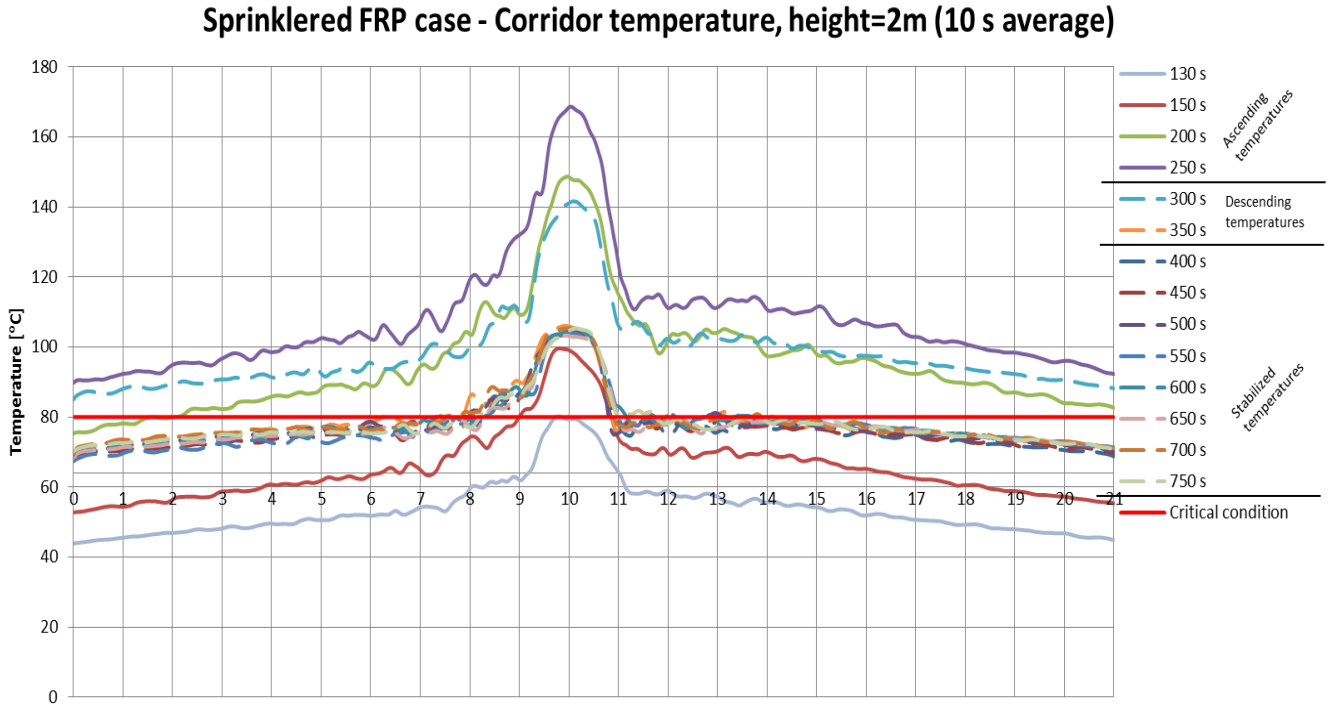

Figure 6.1. Temperature along centerline of the corridor, at the height two meters for 10 seconds intervals. The data is time averaged over 10 seconds.

The visibility (see Figure 6.2) becomes critical after 50 seconds according to the 10 m criterion. After 90 seconds the whole corridor has a visibility below the critical condition for this criterion. Although for the 5 m criterion, the visibility starts becoming critical at 60 seconds and the whole corridor has critical visibility after 100 seconds.

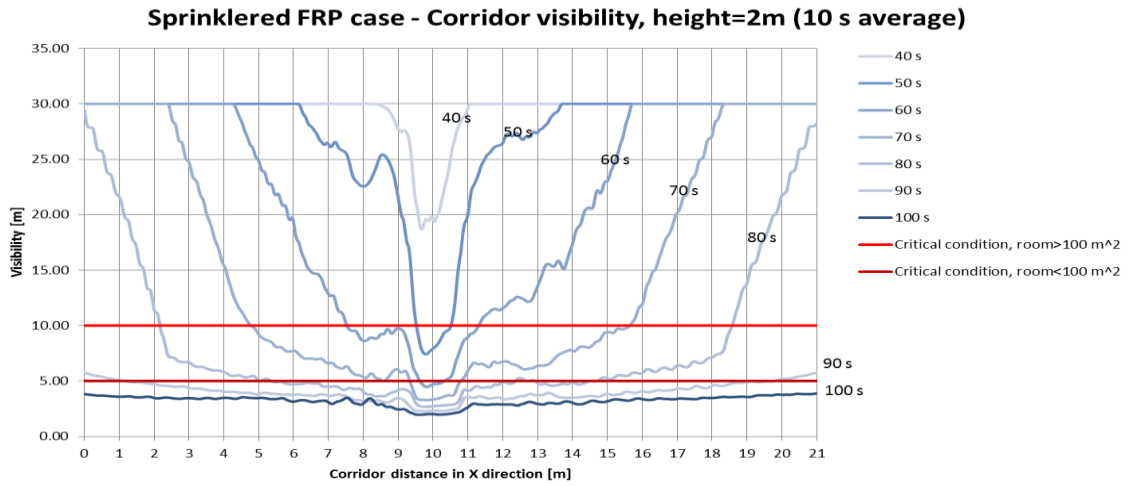

Figure 6.2. Visibility along centerline of the corridor, at the height two meters for 10 seconds intervals. The data is time averaged over 10 seconds.

6.2 Scenario 2 – Sprinklered steel

The same trend as in Scenario 1 – Sprinklered FRP can be seen for the temperatures in the corridor, see Figure 6.3. However for this scenario, the time of the first occurrence of critical temperatures is 150 seconds, which is 20 seconds later than in the other scenario. Also, the temperatures are generally slightly lower at the same time intervals in this scenario. The times at which temperatures increase and decrease is similar.

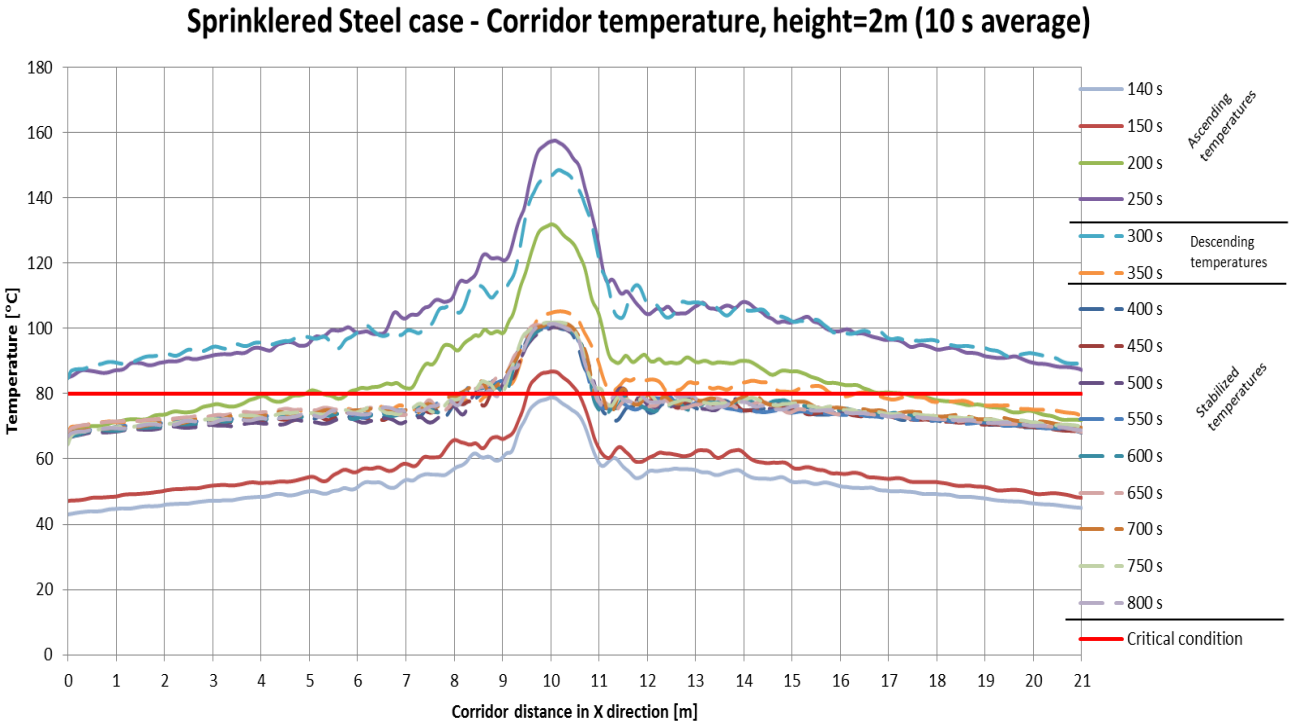

Figure 6.3. Temperature along centerline of the corridor, at the height two meters for 10 seconds intervals. The data is time averaged over 10 seconds.

The decrease in visibility is generally slower than in Scenario 1 – Sprinklered FRP. The time at which the visibility in the whole corridor is below both the 10 m and the 5 m visibility criteria is 100

respectively 110 seconds, which is 10 seconds later than in the other scenario. However the visibility starts going below the 10 m criterion at 50 seconds and the 5 m criterion at 70 seconds.

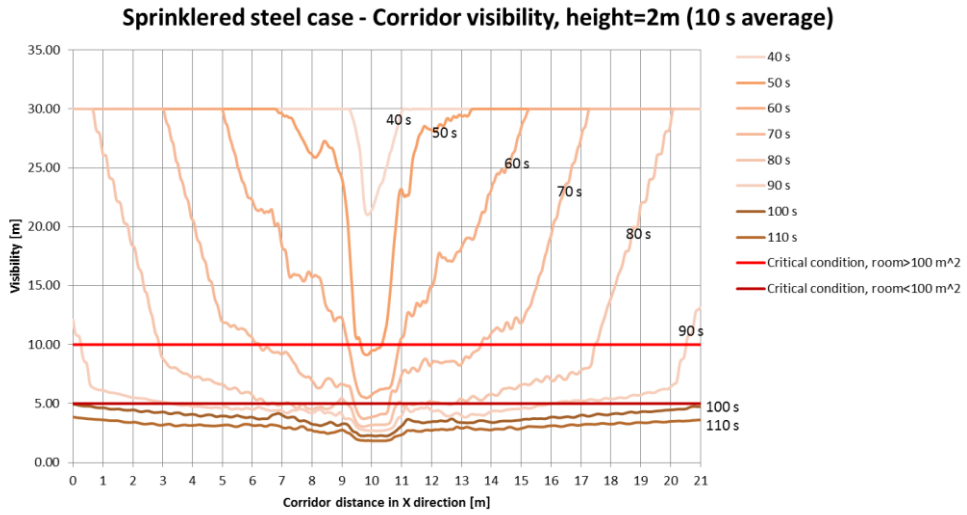

Figure 6.4. Visibility along centerline of the corridor, at the height two meters for 10 seconds intervals. The data is time averaged over 10 seconds.

6.3 Scenario 3 – Unsprinklered FRP

Looking at Figure 6.5 one can see that the temperature starts going above 80 °C in the middle of the corridor after 150 seconds and that the whole corridor has temperatures ranging from 80 to 150 °C after 220 seconds.

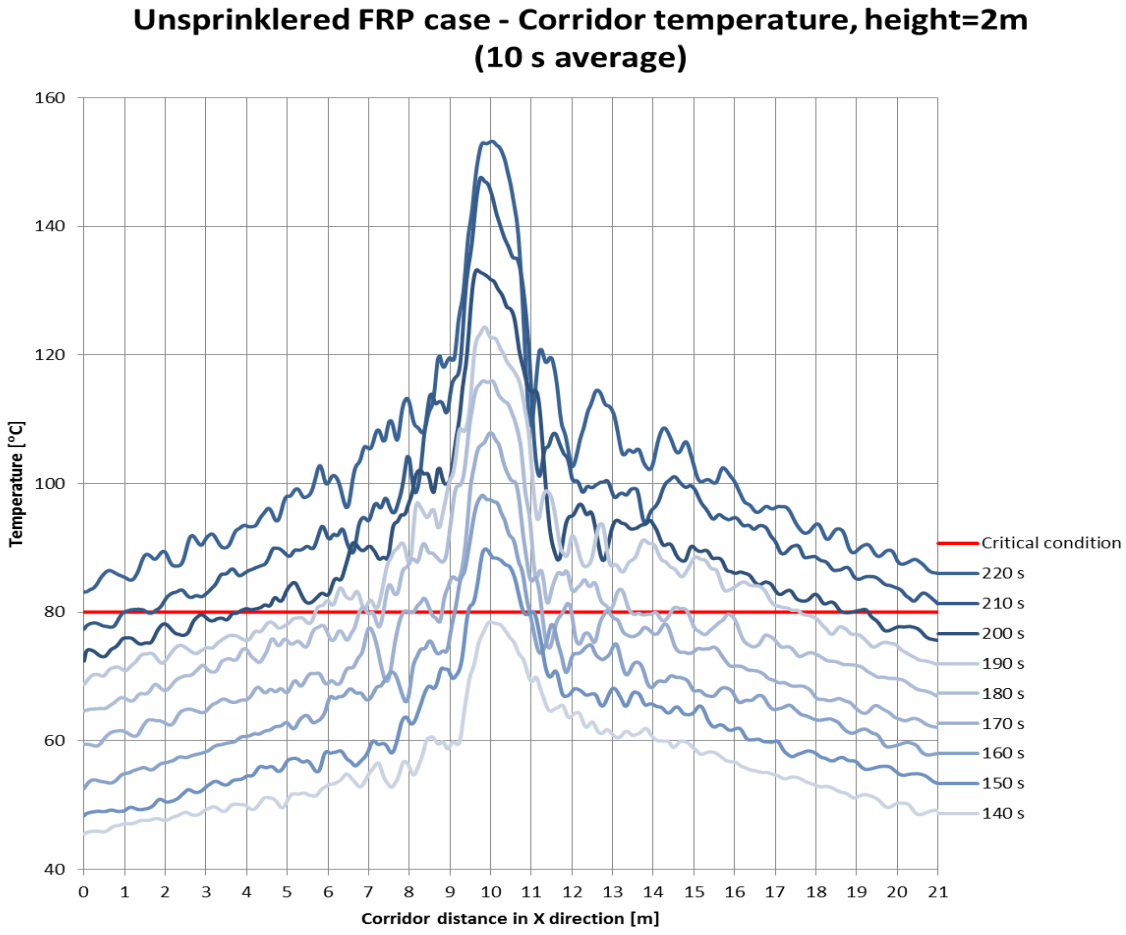

Figure 6.5. Temperature along centerline of the corridor, at the height two meters for 10 seconds intervals. The data is time averaged over 10 seconds.

Investigation of visibility showed occurrence of critical conditions in the middle of the corridor after 50 seconds according to the 10 m criterion for larger spaces. According to the 5 m criterion for smaller spaces, critical conditions occur 10 seconds later. Critical conditions were reached in the whole corridor after 90 respectively 110 seconds for the 10 m respectively 5 m criteria, see Figure 6.6.

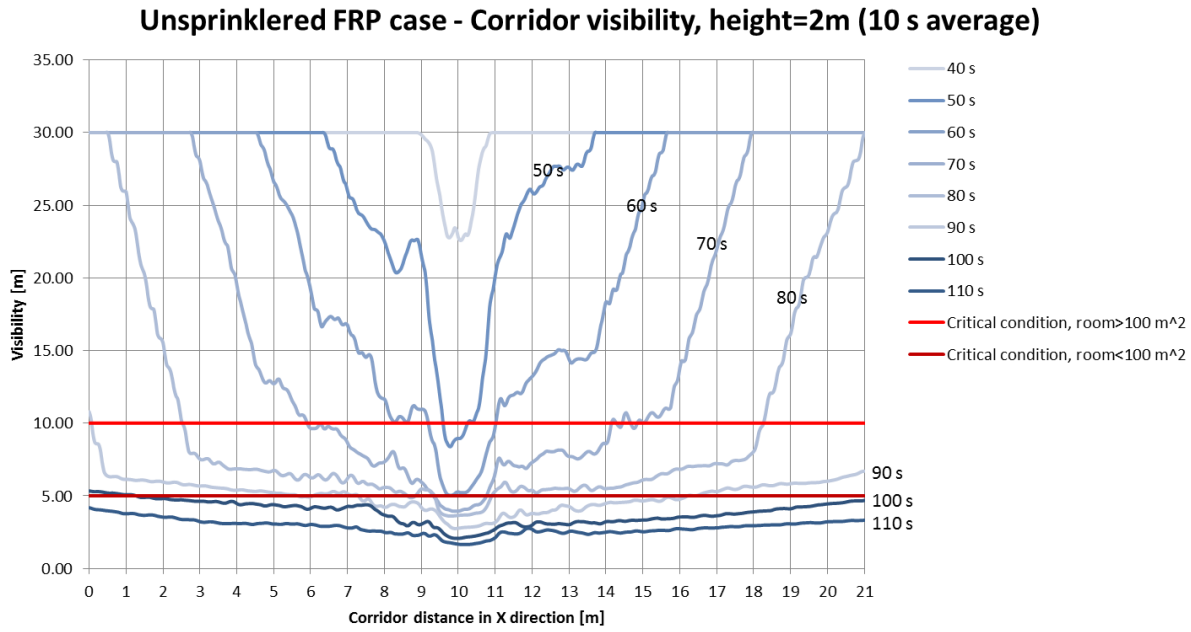

Figure 6.6. Visibility along centerline of the corridor, at the height two meters for 10 seconds intervals. The data is time averaged over 10 seconds.

6.4 Scenario 4 – Unsprinklered steel

For this scenario the critical conditions in the middle of the corridor are reached after 160 seconds, 10 seconds later than in Scenario 3 – Unsprinklered FRP. Critical conditions were reached in the whole corridor after 240 seconds, which is 20 seconds later than Scenario 3 – Unsprinklered FRP. See Figure 6.7.

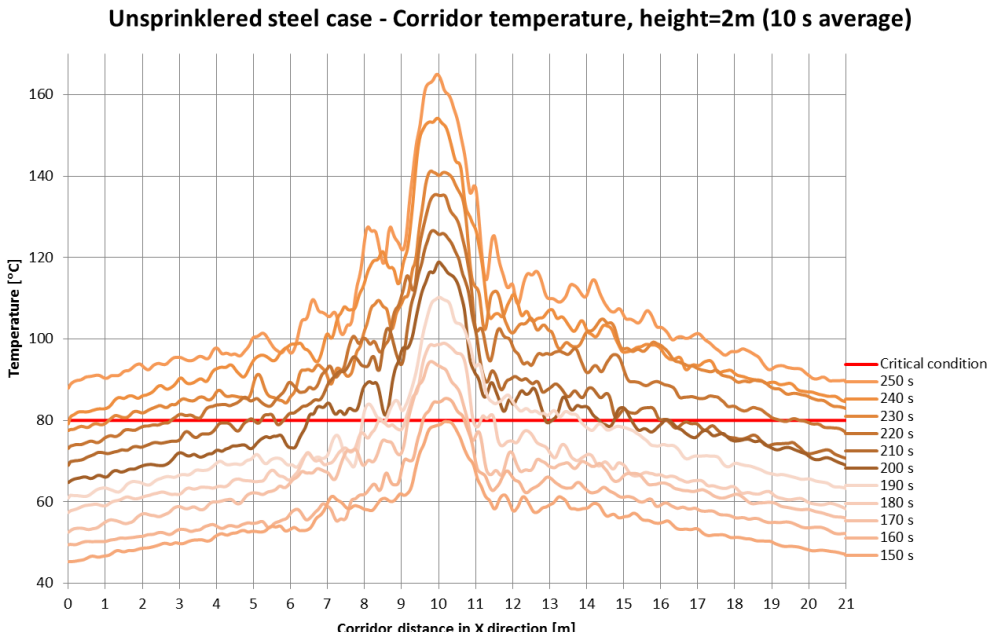

Figure 6.7. Temperature along centerline of the corridor, at the height two meters for 10 seconds intervals. The data is time averaged over 10 seconds.

The visibility starts becoming critical after 60 seconds, according to the 10 m criterion, and after 70 seconds according to the 5 m criterion. After 100 seconds the whole corridor has visibility below critical according to the 10 m criterion and after 110 seconds according to the 5 m criterion. This is 10 seconds later than for Scenario 3 – Unsprinklered FRP. See Figure 6.8.

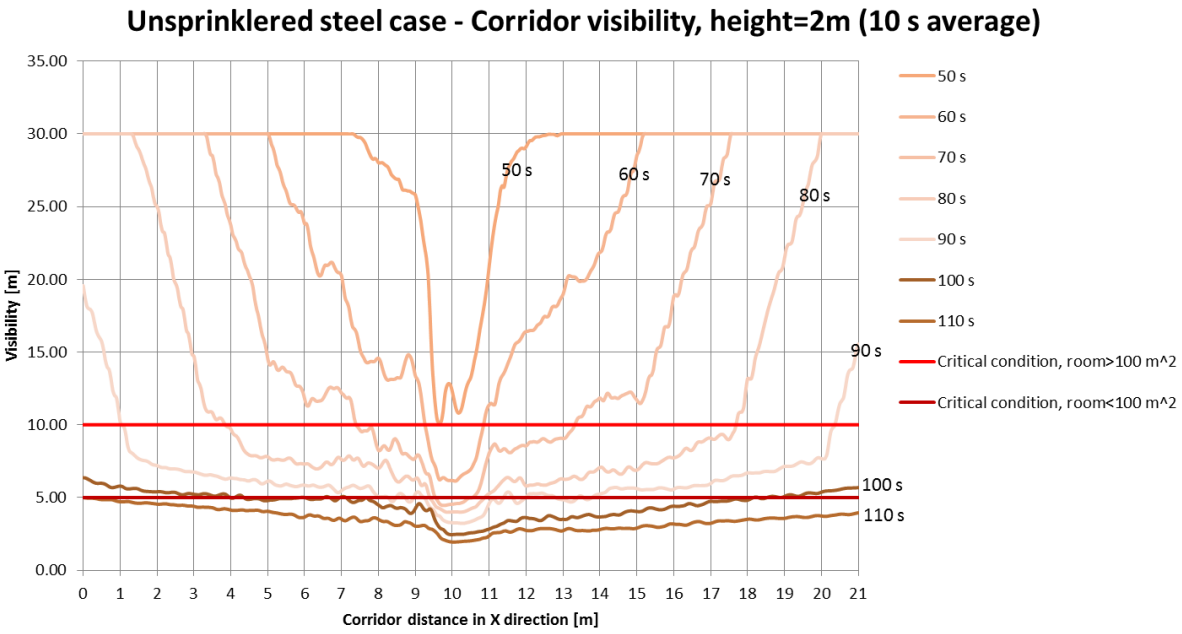

Figure 6.8. Visibility along centerline of the corridor, at the height two meters for 10 seconds intervals. The data is time averaged over 10 seconds.

6.5 Comparison of scenarios

Before reading this chapter, notice that the graphs show interpolations between different data points.

6.5.1 Scenario 1 and 2 – sprinklered.

Time until critical temperatures occur within an unacceptable fraction of the corridor is 164 seconds for the steel scenario and 156 seconds for the FRP scenario. The whole corridor holds critical temperatures twice as long in the FRP case, which is about 100 seconds, whereas it is only about 50 seconds in the steel case. However, after sprinkler activation the FRP scenario decreases more rapidly and arrives at critical temperatures in an acceptable fraction of the corridor 40 seconds earlier than the steel scenario. See Figure 6.9.

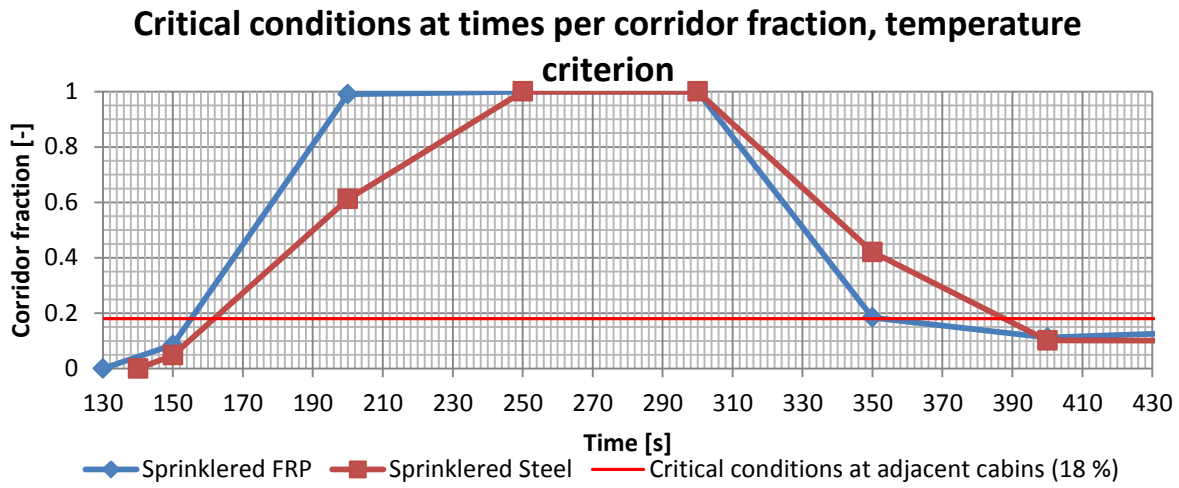

Figure 6.9. Fractions of corridor with critical temperature conditions dependent on time for scenario 1 and 2.

For the 10 m visibility criterion the steel scenario reaches the critical condition within an unacceptable fraction of the corridor at 64 seconds. For the FRP scenario this time is 61 seconds. For the 5 m criteria, the steel scenario reaches this fraction at 79 seconds, which is 5 seconds later than the FRP scenario. See Figure 6.10.

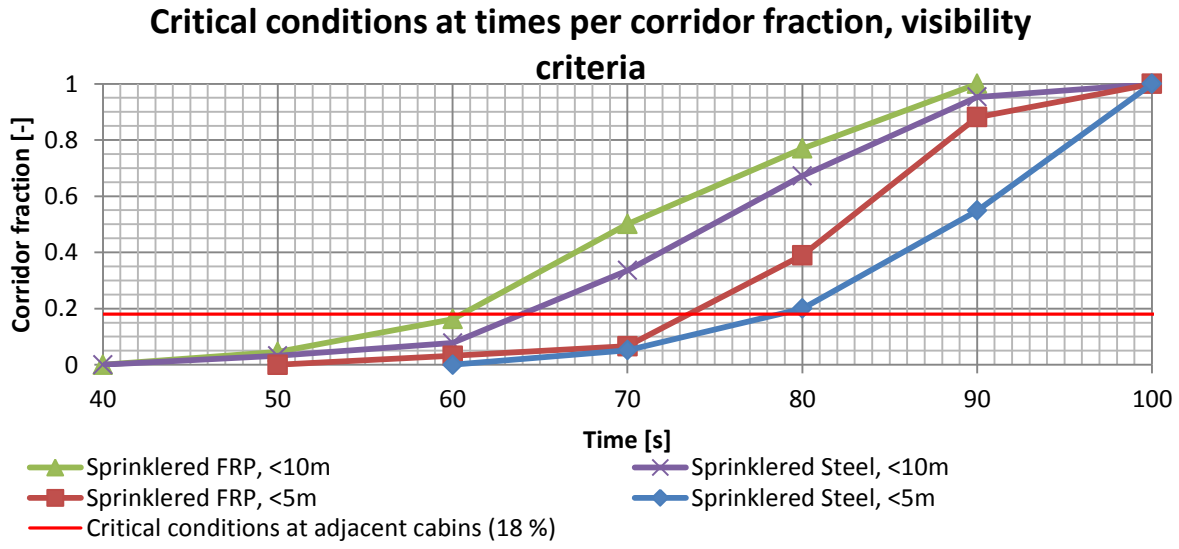

Figure 6.10. Fractions of corridor with critical visibility conditions dependent on time for scenario 1 and 2.

Contrary to the temperature the visibility does not stabilize at an acceptable level after sprinkler activation. This can be seen in Figure 6.11 where it can be observed that the visibility after 400 seconds stabilizes at less than 2 m. The differences between scenario 1 and 2 become smaller as time goes on.

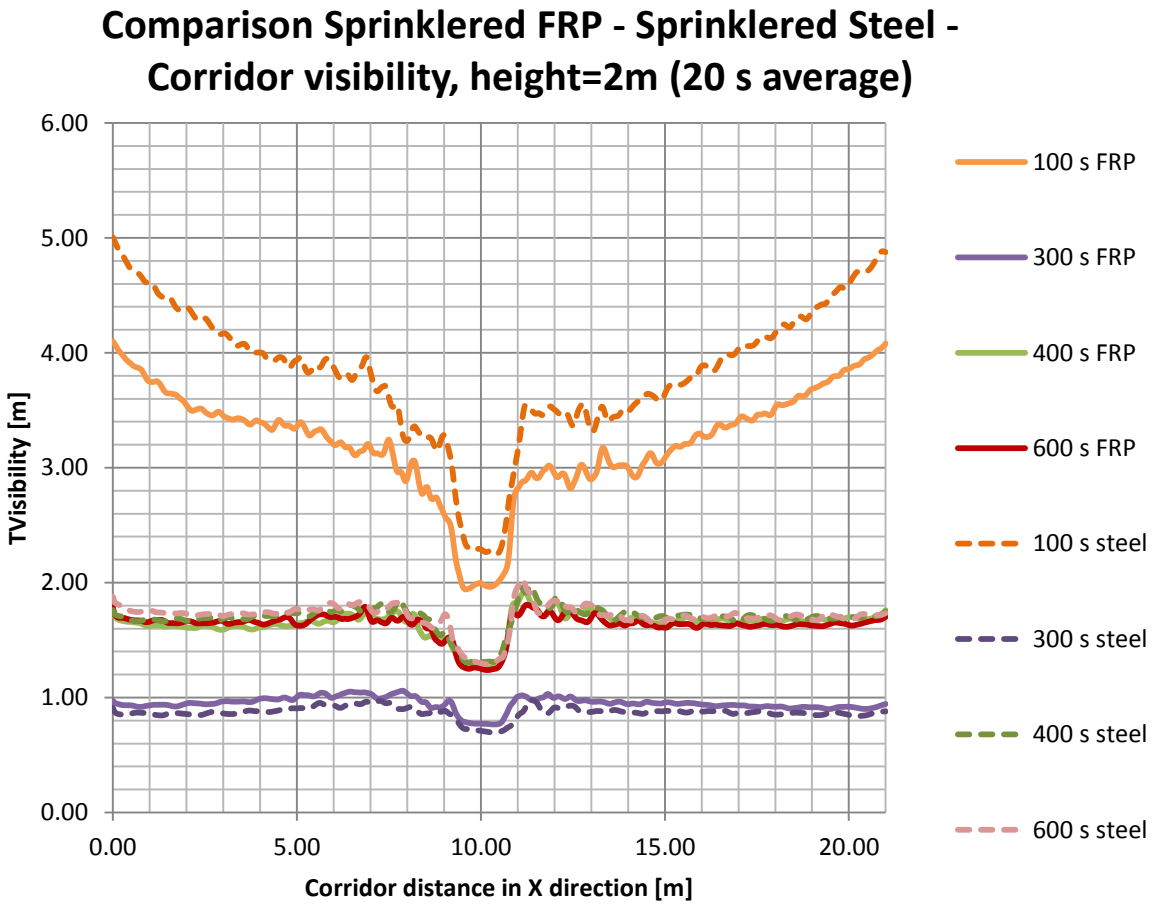

Figure 6.11. Visibility comparison scenario 1 and 2. Values for 10 minutes.

6.5.2 Scenario 3 and 4 – unsprinklered.

As stated previously the threshold where an unacceptable part of the corridor contains critical conditions is 18%. The time until the different cases reach this fraction varies. For scenario 1 and 2 this time can be read from Figure 6.12 and Figure 6.13. For the temperature criteria the time varies so that the steel scenario fills this fraction with critical temperatures at 185 seconds, which is 12 seconds after the FRP scenario. For the 10 m respectively 5 m visibility criteria, the steel scenario has critical visibility within this fraction at 2 respectively 7 seconds after the FRP scenario. It seems the time differences increase with time for the temperature criteria. In the beginning the differences for this criteria is around 10 seconds. When more than 50 percent of the corridor has critical conditions, the time differences are around 20 seconds.

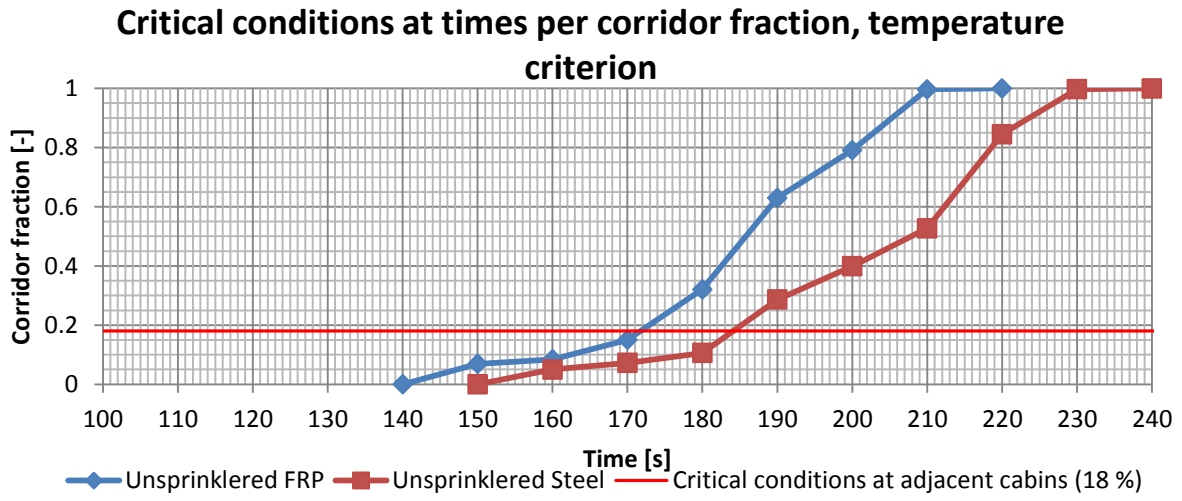

Figure 6.12. Fractions of corridor with critical temperature conditions dependent on time for scenario 3 and 4.

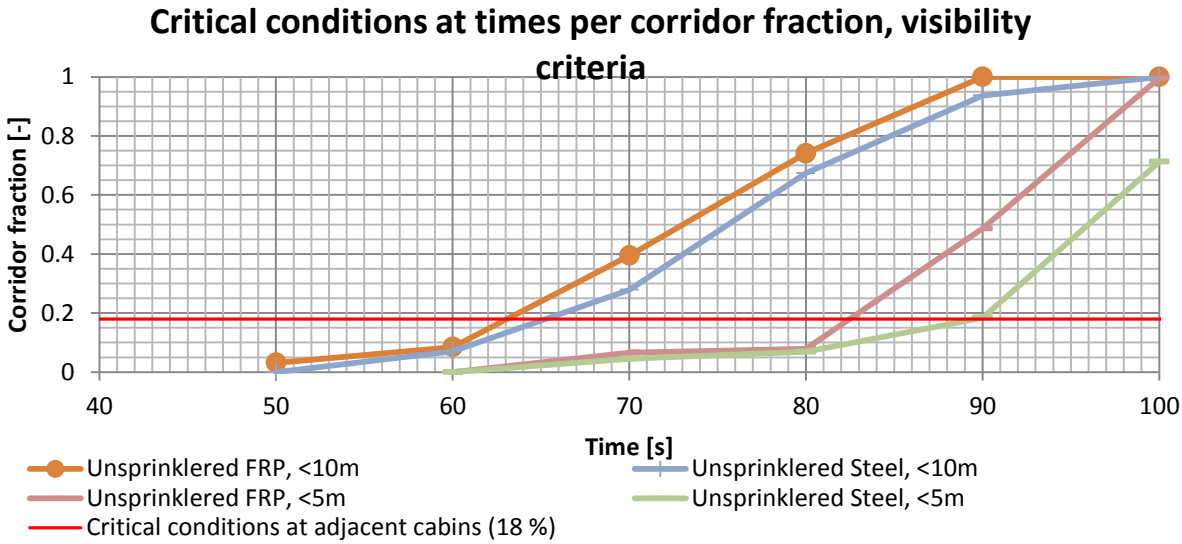

Figure 6.13. Fractions of corridor with critical visibility conditions dependent on time for scenario 3 and 4.

Figure 6.14 below gives a better overview and comparison of the temperature results the unsprinklered scenarios. The intervals are 100 seconds but show the temperatures over a larger time than the previous temperature charts. In the later stages the gas temperatures have values of several hundred degress. The maximum for the FRP case is around 760°C whereas the maximum for the steel case is around 660°C.

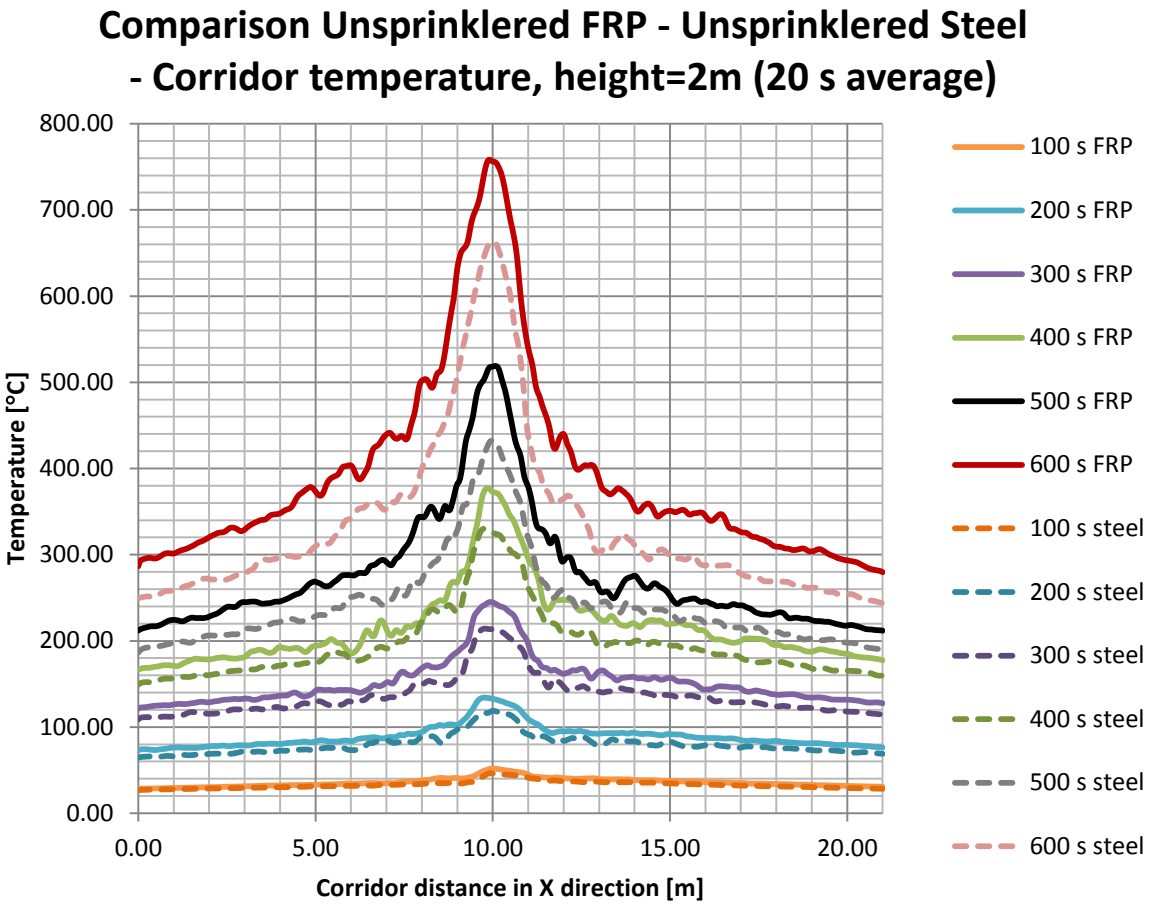

Figure 6.14. Temperature comparison scenario 3 and 4. Values for 10 minutes.

6.6 Smoke layer height

This part of the chapter presents the smoke layer heights for the early and later stages of the fire.

6.6.1 Early stages

Pictures that show output for the soot mass fraction in the corridor are presented. The times at which critical visibility conditions occur in an unacceptable fraction of the corridor have been extracted from Figure 6.10 and Figure 6.13. The times are the following for each scenario;

Scenario 1 - 61 s
Scenario 2 - 64 s
Scenario 3 - 63 s
Scenario 4 - 66 s

The pictures are extracted for these times, for each scenario respectively, and the critical smoke layer height is marked with a red line. The mentioned corridor fraction is marked with a transparent red box.

For all scenarios the actual smoke layer height inside the corridor fraction has descended below the critical smoke layer height, see Figure 6.15 - Figure 6.18. This means that the time until critical conditions is judged by the visibility criterion since only one of the two criteria has to be fulfilled according to BFS 2013:12 (Boverket, 2013).

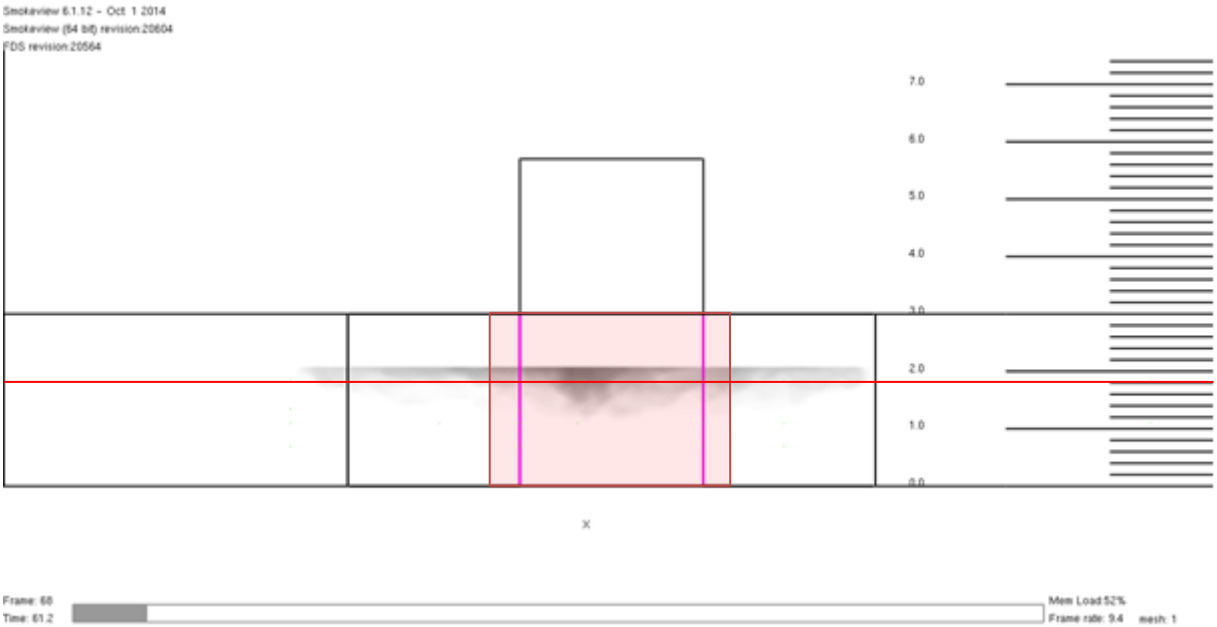

Figure 6.15. Soot mass fraction for scenario 1. Time of frame is 61 s.

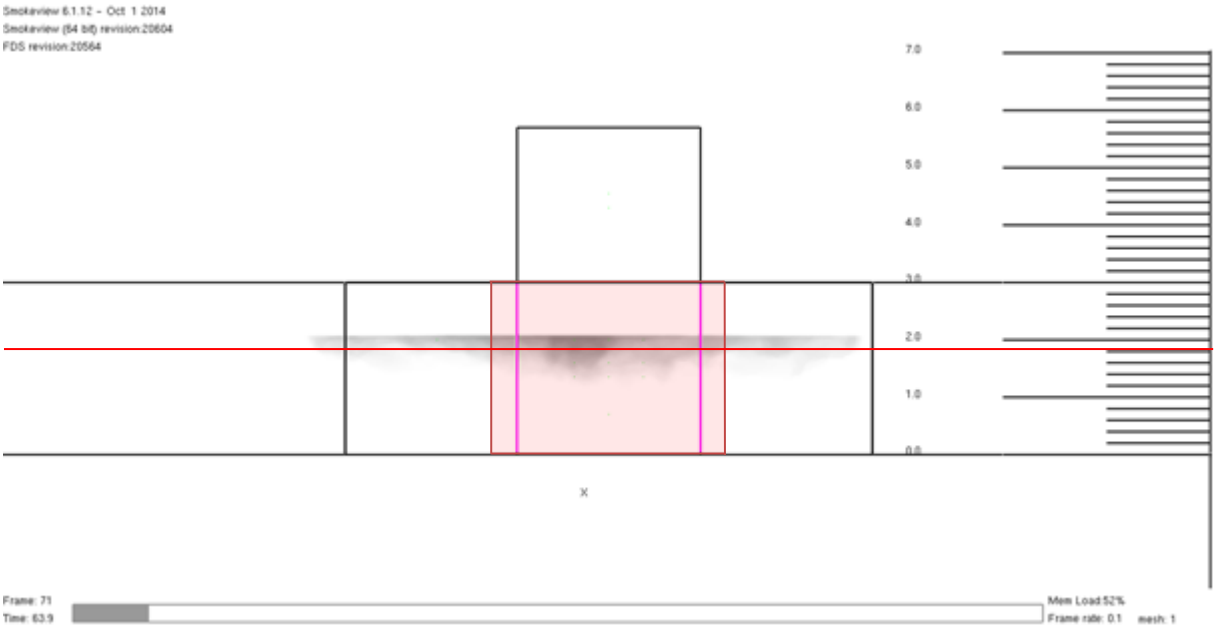

Figure 6.16. Soot mass fraction for scenario 2. Time of frame is 64 s.

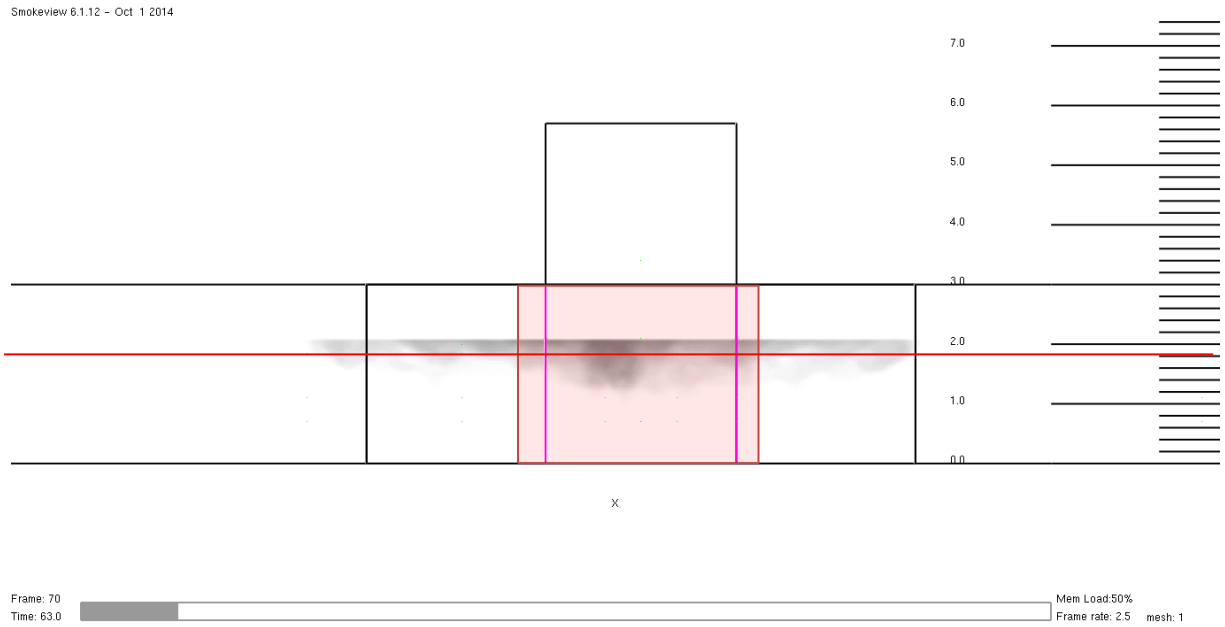

Figure 6.17. Soot mass fraction for scenario 3. Time of frame is 63 s

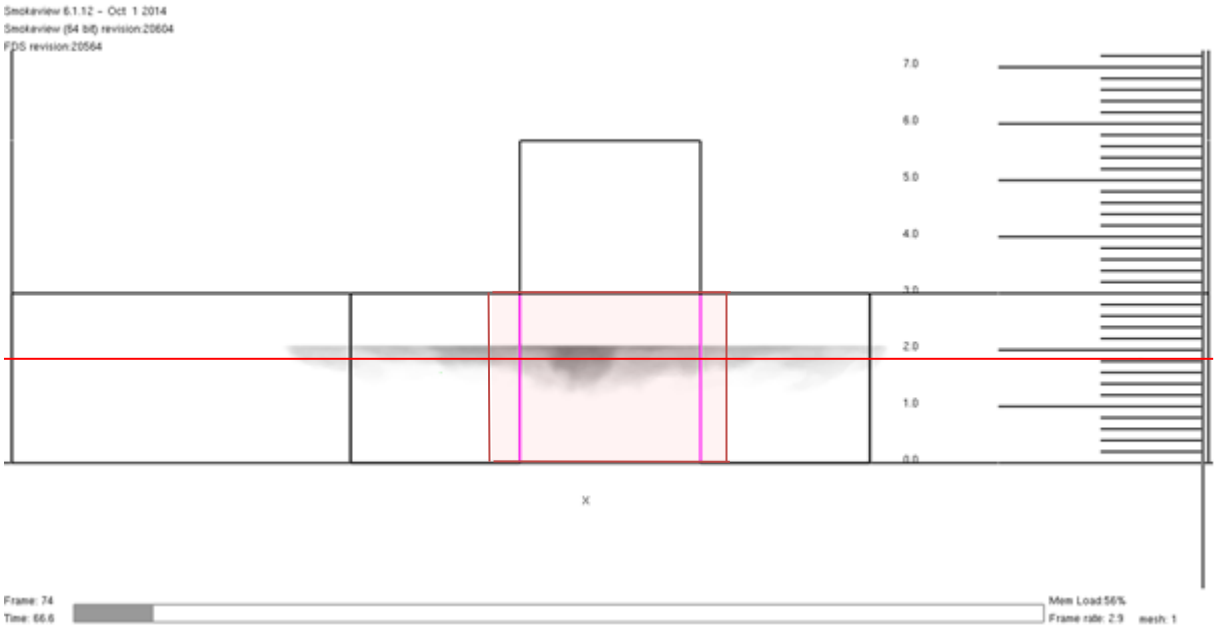

Figure 6.18. Soot mass fraction for scenario 4. Time of frame is 66 s

6.6.2 Later stages

The smoke layer stabilizes after approximately 500 seconds in scenario 1 and 2 at heights of 1.4 m above floor level. For scenario 3 and 4 the stabilization occurs after 450 seconds at heights around 1.2 m above floor level. Looking at Figure 6.19 and Figure 6.20 it is possible to distinguish a little denser smoke in scenario 1 than in scenario 2.

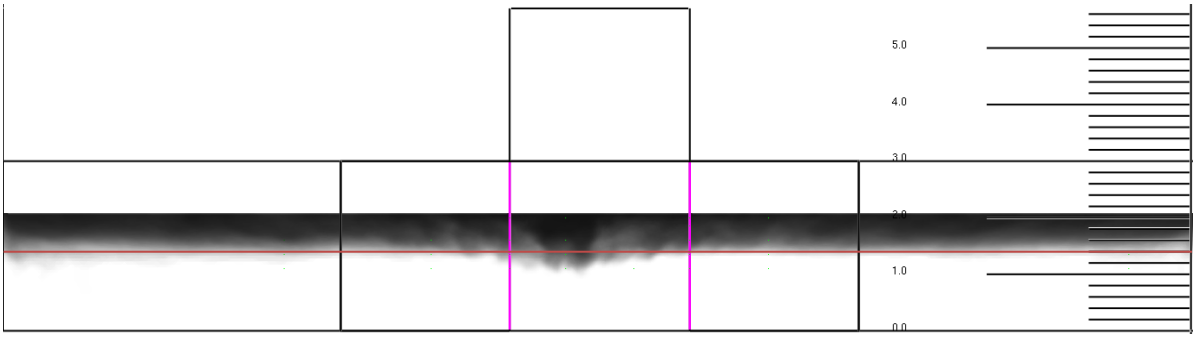

Figure 6.19. Stabilized smoke layer height for scenario 1. Time frame is 500 seconds.

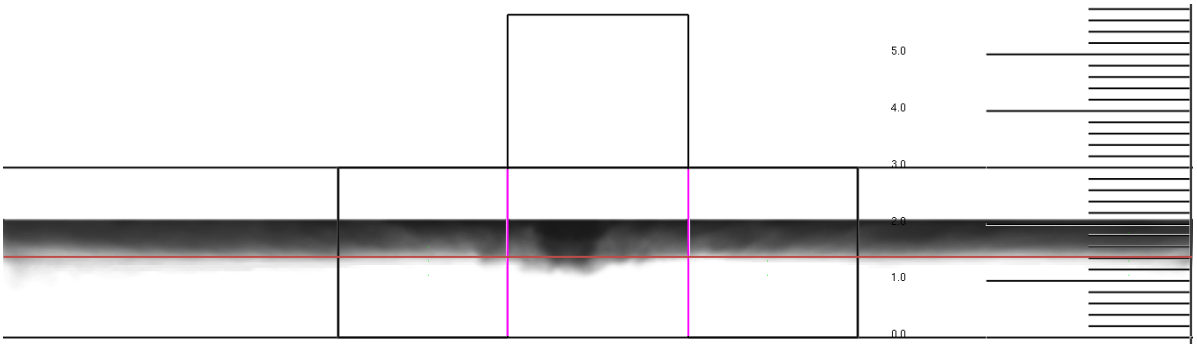

Figure 6.20. Stabilized smoke layer height for scenario 2. Time frame is 500 seconds.

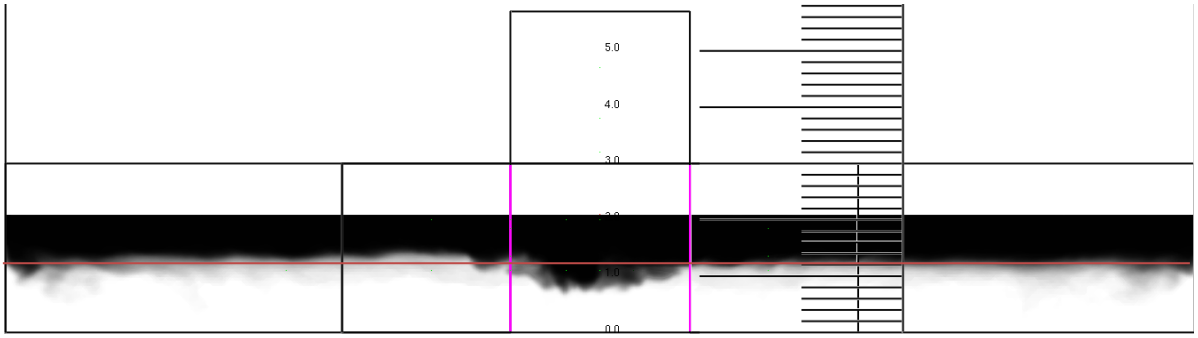

Figure 6.21. Stabilized smoke layer height for scenario 3. Time frame is 450 seconds.

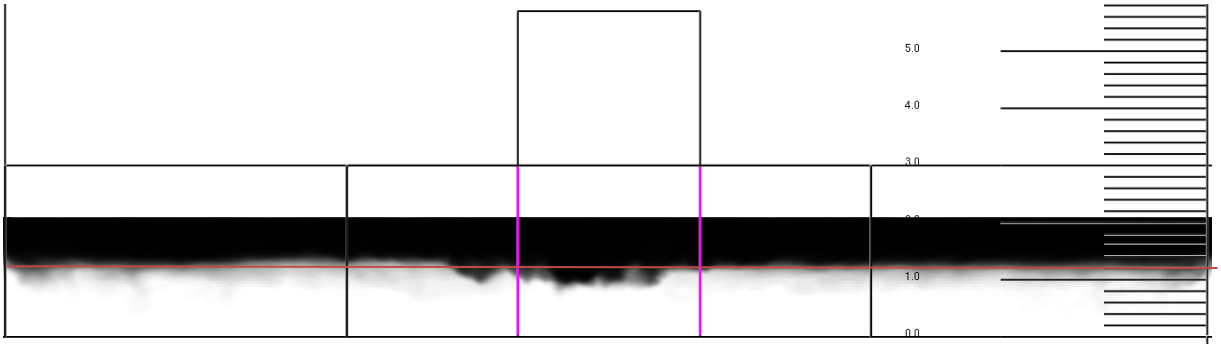

Figure 6.22. Stabilized smoke layer height for scenario 4. Time frame is 450 seconds.

7 Sensitivity analysis

The sensitivity analysis is divided into three separate chapters, the first one concerns the choice of FDS version, the second chapter is a summary of the grid independence analysis and the third and final chapter describes the sensitivity analysis of some input parameters.

7.1 Model independence analysis

The foundations of this model independence analysis can be seen in Appendix E where five different curve charts are presented. The simulations used for the analysis were:

- Scenario 3 - unsprinklered FRP case simulated with FDS 5 (version 5.3.3).
- Scenario 3 - unsprinklered FRP case simulated with FDS 6 (version 6.1.1).

The output data that was studied was taken from thermocouple and velocity probe device trees in point D and A, and thermocouple tree in point K. The simulation that was run in version 5.3.3 crashed after approximately 700 s due to numerical instability.

7.1.1 Observations from output

The velocities in measure points for D and A are more fluctuating for FDS 5 than FDS 6. The temperatures are generally higher for FDS 6. Regarding the time after the ceiling collapses (420 s) the velocities fluctuates much more in FDS 5 than in FDS 6.

The lowest placed device in point D has different directions of the flow in the different cases. The FDS 5 case has a negative velocity, whilst it is positive in FDS 6. This indicates that the neutral plane is located higher up in the FDS 5 case than in the FDS 6 case.

7.1.2 Conclusion

Since FDS 6 was more stable when calculating velocities it is wise from a time-based project perspective to use FDS 6 when simulating all other cases. Since FDS 6 generally had higher temperatures and lower neutral plane a use of FDS 6 would also be a more conservative approach. Consequently, FDS 6 was used for all other simulations.

7.2 Grid independence analysis

The foundations of this grid independence analysis can be seen in Appendix F where several graphs and pictures are presented. The simulations that were performed and used in the analysis were:

- Scenario 3 - unsprinklered FRP case with the medium grid size of 0.10 m.
- Scenario 3 - unsprinklered FRP case with the coarser grid size of 0.20 m.
- Scenario 3 - unsprinklered FRP case with the finer grid size of 0.05 m.

The studied output data came from the thermocouple and velocity probe device trees located in point D and A. The fine case had a computational time that extended outside the LUNARC maximum of 168 hours. Consequently, it ended after 623 s. The medium case had a computational time less than 72 hours and the coarse case had a computational time less than 10 hours. Both of the latter ones were simulated until finish (900 s).

In the FDS manual by McGrattan et al. (2013) it is proposed that the ratio between the characteristic diameter of the fire (D*) and the nominal grid size (δ_x) should have a value between 4 and 16 since these values have shown to give good results. An earlier published source, McGrattan (2007), states however that “Past experience has shown that a ratio of 5 to 10 usually produces favorable results at a moderate computational cost”.

The calculation of D^*/δ_x was made in accordance with the method presented in equation below. It was however calculated for every second resulting in a transient presentation of the values, see Figure 7.1. The medium case reached the lowest value proposed by McGrattan et al. (2013) after approximately 200 s, whereas the coarse case did not until about 400 s. The fine case reached the proposed value after a little under 100 s. The medium case had, in the later stages of the fire, values that correspond well with what has been stated above regarding acceptable results at an acceptable computational cost. The coarse case never passed the value 6 and the fine case was in the later stages very high regarding computational cost.

$$\frac{D^*}{\delta_x} = \left(\frac{\dot{Q}}{\rho_\infty c_p T_\infty \sqrt{g}}\right)^{\frac{2}{5}} \left(\frac{1}{\delta_x}\right)$$

$\dot{Q}$ – fire heat release rate, ρ_∞ - density of ambient air, c_p - specific heat capacity of ambient air, T_∞ - temperature of ambient air, g – gravitational acceleration (McGrattan et al., 2013).

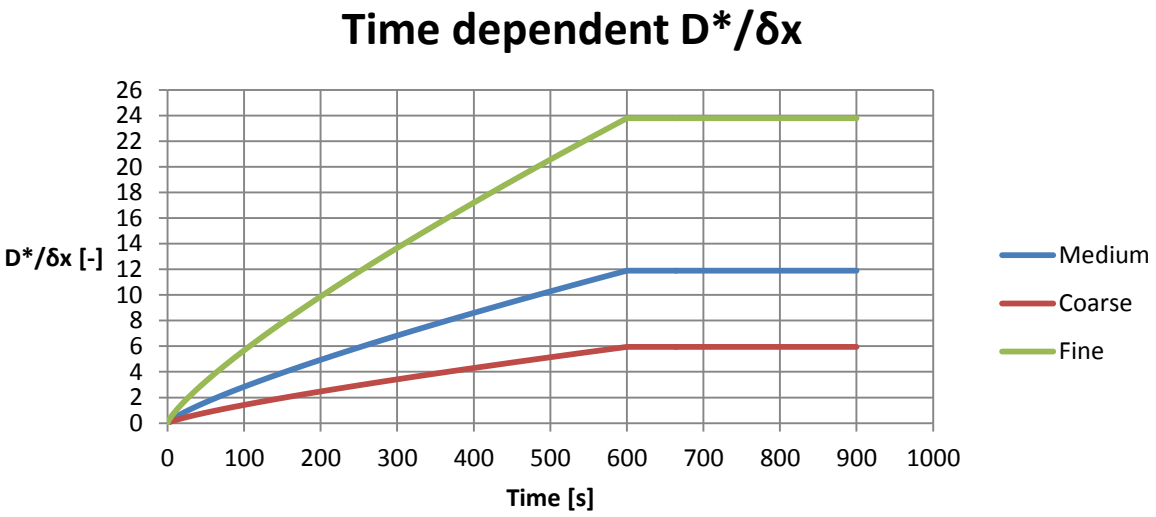

Figure 7.1. Transient representation of the calculated D^*/δ_x for Medium, Coarse and Fine grid for the unsprinklered FRP scenario.

Since the simulations are used for evaluating the conditions during evacuation from a human safety perspective it is important that the grid size is fine enough in the early stages of the fire in order to give accurate predictions of the conditions. This is important for both gas spread and temperatures to be correctly calculated during the first minutes. A D*/δx that follows the fine time dependency is therefore preferable in the early stages of the fire. As can be seen in Figure 7.1, the medium and coarse simulations do not reach a sufficient value for D*/ δx until a later stage. In a reasonable results contra reasonable computational costs point of view, the D*/δx for the medium case is decent even though it is below 4 during the first two minutes.

7.2.1 Observations from output

The overall difference between the coarse case and the other cases is large, especially in the doorway. Temperatures are lower and the velocity profile has a different shape in the doorway. The resulting neutral plane is placed much higher up in the coarse case, resulting in flows in the opposite direction for several velocity probe heights.

Most large deviations between the different cases occur around the lowest device measure point (0.7 m above floor) in the doorway. Here, even the differences between the medium and fine cases are large. The fine case has temperatures that are several hundred degrees higher. This is because the smoke

layer height is lower in the fine case than in the other simulations, which is due to the larger amount of air entrainment into the fire plume. The reason for this is that the finer grid is able to capture the smaller turbulent eddies, which allows for more entrainment to occur.

The visual difference from the slice file inside the fire room is big. In the fine simulation the turbulence is much better represented in all stages of the fire.

7.2.2 Conclusion

For the scenario analysis where it is necessary to correctly investigate the critical conditions during the time for evacuation, a fine grid was used for the fire room and the corridor.

For the sensitivity analysis, the medium grid in the fire room and the corridor was used. This is because of two reasons:

1. Exact results showing time to critical conditions are not of as great importance as gaining knowledge on how the conditions deviate given different inputs.
2. The computational cost is much lesser and consequently gives the opportunity to make sensitivity analyses on several parameters.

7.3 Input parameters analysis

The input parameters investigated in the sensitivity analysis were the soot yield and fire growth rate. The corresponding outputs that were analysed were the temperature and visibility for each one of the parameters. The scenarios used for the input parameters analysis was scenario 3 and 4 in order to gain an understanding on the parameters significance for the results in the scenario analysis.

The temperatures values were extracted from the devices and presented in both transient graphs for each device as well as time averaged[*] temperature-height profiles for every 100 s. These devices were placed in measure points A, B and C.

The visibility was extracted from the slice file at y=4.9 m(in the corridor) with FDS2ASCII. The extracted values were averaged over 20 seconds for every hundred second. They were also averaged over the lengths of the A and C parts of the corridor, at a height of 2 m above the floor. See A and C part of the corridor in Figure 7.2.

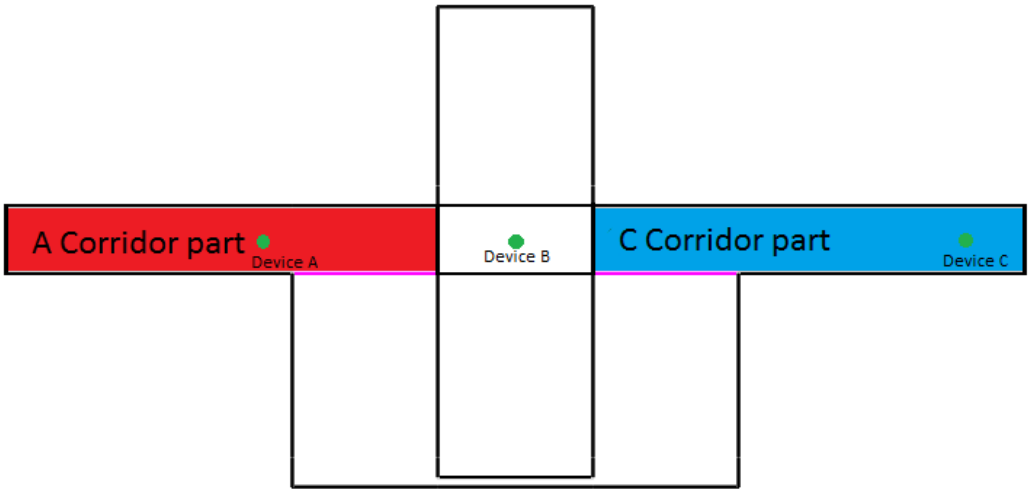

Figure 7.2. Geometry for sensitivity analysis

[*] The time average was made over 20s. For example at 100s, the time average is made for values between 90s and 110s.

7.3.1 Soot yield

The soot yield was increased by approximately 50%, from the original value 0.067 to 0.1.

Temperatures

As expected the temperatures were the same in all measure points regardless of the change in soot yield therefore these results are not presented.

Visibility

The change in soot yield had a large impact on the visibility. The visibility at 2 m was 30-41% lower for the simulation with a higher soot production. There was however no significant difference between the impact on the visibility in the FRP and steel case.

Table 7.1. Corridor part A visibility with different soot yield inputs, 20s time average, value averaged over centreline of corridor, height H=2.0. Extracted from FDS2ASCII.

	Corridor part A					
Time [s]	FRP case Visibility [m]	Higher soot yield Visibility [m]	Steel case Visibility [m]	Higher soot yield Visibility [m]	Difference FRP case Visibility change[%]	Difference steel case Visibility change[%]
100	4.03	2.55	4.80	3.14	-37	-35
200	0.92	0.58	1.04	0.67	-38	-36
300	0.53	0.33	0.60	0.38	-37	-36
400	0.37	0.23	0.42	0.27	-37	-37
500	0.27	0.17	0.32	0.20	-37	-37
600	0.23	0.15	0.25	0.16	-35	-37
700	0.24	0.16	0.24	0.15	-34	-36
800	0.25	0.16	0.25	0.16	-36	-36
900	0.25	0.16	0.27	0.17	-36	-38
				MIN DEV	**-34**	**-35**
				MAX DEV	**-38**	**-38**
				AVERAGE DEV	**-36**	**-36**

Table 7.2. Corridor part C visibility with different soot yield inputs, 20s time average, value averaged over centreline of corridor, height H=2.0. Extracted from FDS2ASCII.

	Corridor part C					
Time [s]	FRP case Visibility [m]	Higher soot yield Visibility [m]	Steel case Visibility [m]	Higher soot yield Visibility [m]	Difference FRP case Visibility change[%]	Difference Steel case Visibility change[%]
100	3.72	2.39	4.62	2.91	-36	-37
200	0.97	0.61	1.09	0.70	-37	-36
300	0.55	0.35	0.61	0.39	-37	-36
400	0.38	0.25	0.44	0.27	-36	-38
500	0.28	0.18	0.32	0.20	-36	-35
600	0.24	0.16	0.26	0.17	-34	-36
700	0.26	0.17	0.25	0.16	-36	-36
800	0.26	0.18	0.28	0.18	-30	-37
900	0.31	0.19	0.28	0.19	-41	-33
				MIN DEV	**-30**	**-33**
				MAX DEV	**-41**	**-38**
				AVERAGE DEV	**-36**	**-36**

7.3.2 Growth rate

The growth rate was varied compared to the original steel case by decreasing the value in one simulation and increasing it in two others. The changes in terms of percentages were -7.1% (alfa 1), +7.1% (alfa 2), and +14.3% (alfa 3). Table 7.3 below show how the different growth rates relate to the steel case as well as to the FRP case.

Table 7.3. Input deviations for growth rate sensitivity analysis.

	alfa 1	alfa steel	alfa 2	alfa 3	alfa FRP
Growth rate [kW/s^2]	0.00361	0.00389	0.00417	0.00444	0.00472
Change compared to steel	-7.1%	-	+7.1%	+14.3%	+21.4%
Change compared to FRP	-23.5%	-17.6%	-11.8%	-5.9%	-
HRR at 600 s [kW]	1300	1400	1500	1600	1700

Temperatures

The largest differences in shape for the temperature profiles could be observed in the early stages where the profile for the lowered growth rate had a larger impact on the temperatures than the other cases. The profiles for the later stages were more similar, but the values show that the differences in temperatures are larger. Profiles can be seen in Figure 7.3, Figure 7.4 and Figure 7.5.

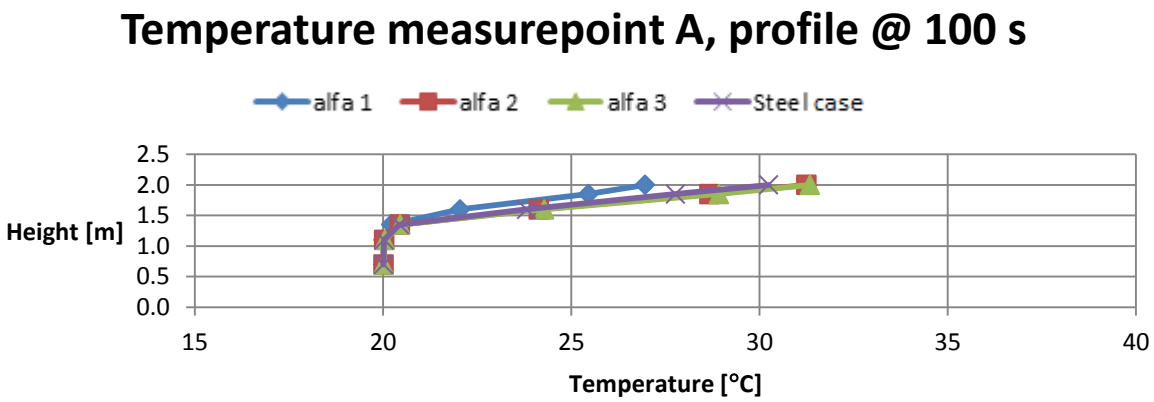

Figure 7.3. Temperature measurement in point A. Profiles are averaged over 20s at 100s.

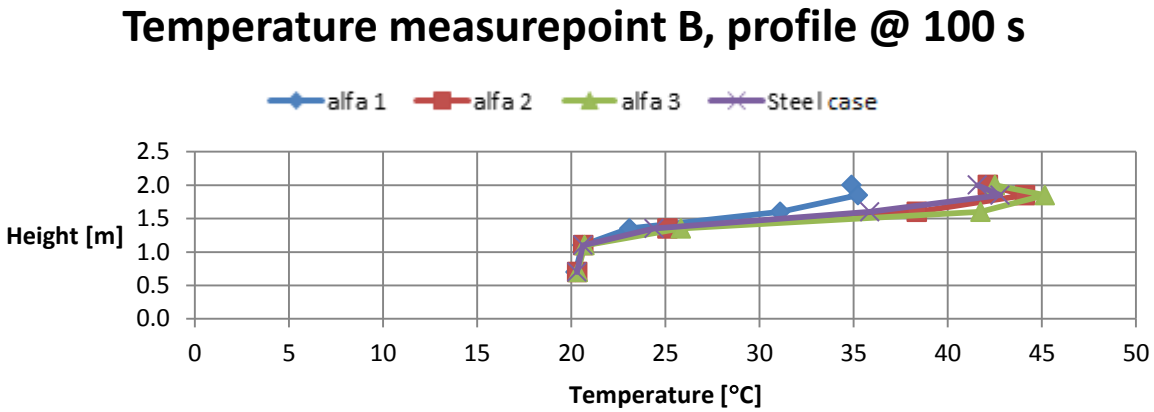

Figure 7.4. Temperature measurement in point B. Profiles are averaged over 20s at 100s.

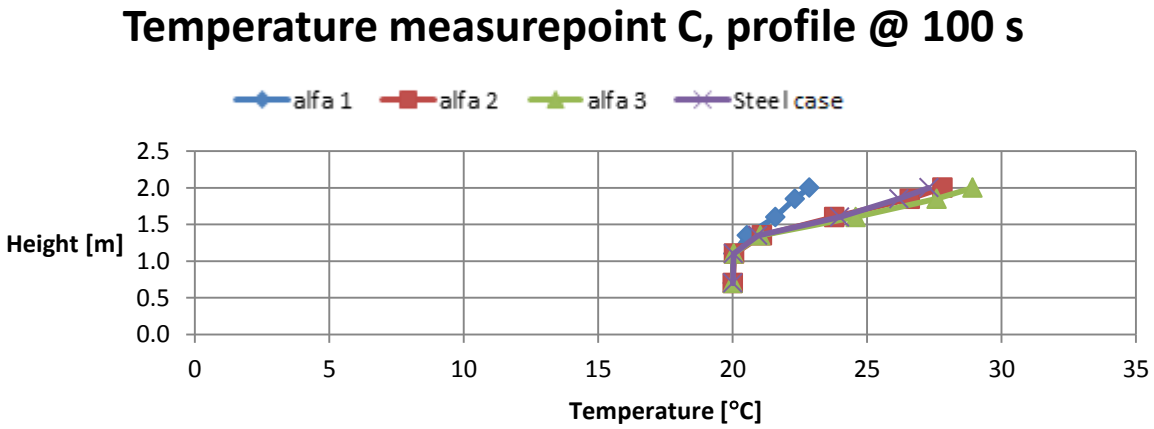

Figure 7.5. Temperature measurement in point C. Profiles are averaged over 20s at 100s.

The temperature profiles obtained in the different simulations were very similar for all other measure points and time intervals. Because of this, only an example on how the temperatures varied in the later stages is presented, see Figure 7.6, Figure 7.7 and Figure 7.8.

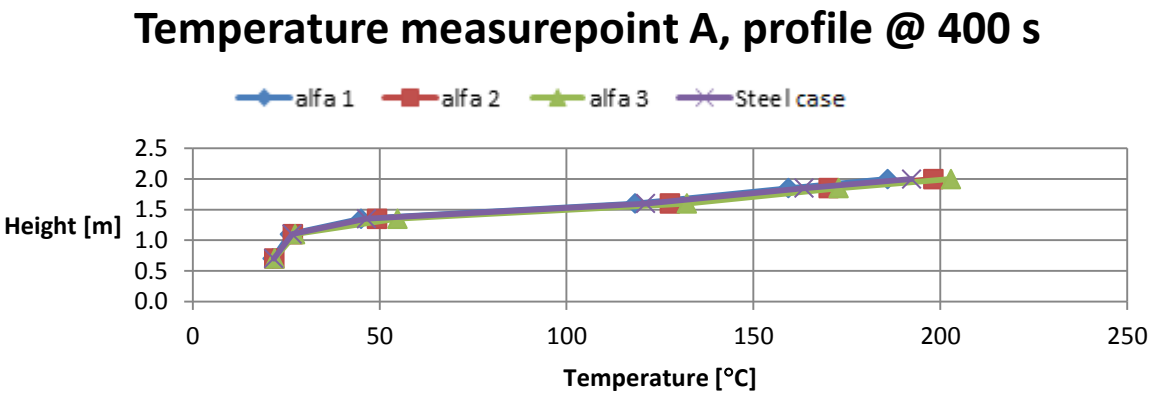

Figure 7.6. Temperature measurement in point A. Profiles are averaged over 20s at 400s.

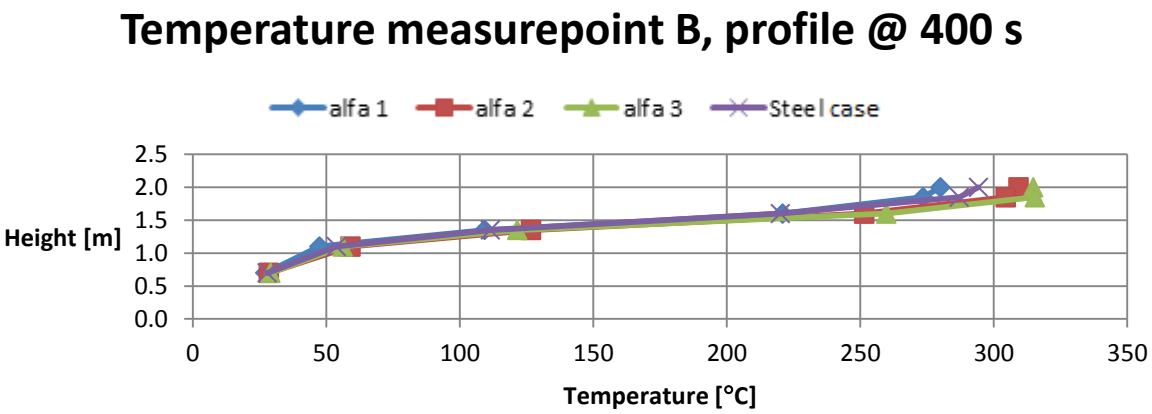

Figure 7.7. Temperature measurement in point B. Profiles are averaged over 20s at 400s.

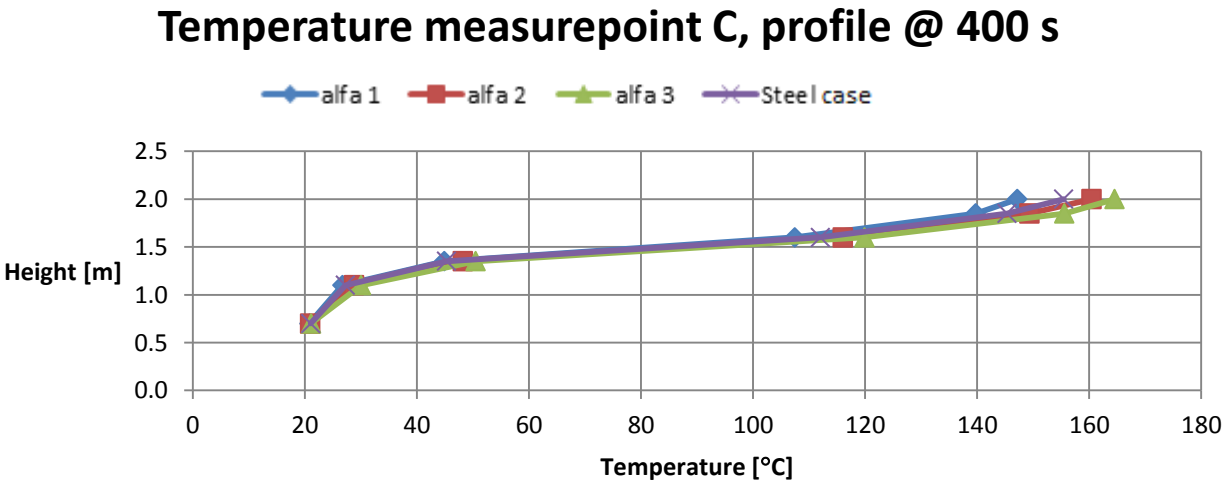

Figure 7.8. Temperature measurement in point C. Profiles are averaged over 20s at 400s.

The absolute deviations in temperatures were around 1-60°C, and in percent 0-15% from the steel case. The temperature differences are at their maximum in the later stages, at 600 seconds. For a quantification of how much temperatures varied compared to the steel case for the different times and measure points, see Table 7.4.

Table 7.4. Corridor temperatures compared to steel case for changes in growth rates (alfa 1, alfa 2 and alfa 3), 20s time average, value extracted from devices in measure points A, B and C.

Time [s]		TEMPERATURE CHANGES COMPARED TO STEEL CASE [°C]								
		Height 2.0, POINT A			Height 2.0, POINT B			Height 2.0, POINT C		
		-7.1%	+7.1%	+14.3%	-7.10%	+7.1%	+14.3%	-7.10%	+7.1%	+14.3%
100 s		-3	+1	+1	-7	+1	+1	-4	0	+2
200 s		-3	+2	+7	-4	+4	+10	-2	+3	+6
300 s		-7	+5	+10	-13	+8	+18	-1	+6	+11
400 s		-6	+6	+10	-14	+15	+21	-8	+5	+9
500 s		-7	+9	+19	-19	+19	+36	-7	+6	+11
600 s		-19	+19	+46	-34	+32	+58	-6	+12	+29
700 s		-6	+17	+19	-19	+14	+28	-5	+3	+11
800 s		-15	+11	+6	-20	+5	+13	+5	+8	+15
900 s		+5	+17	+20	-1	+12	+7	-4	+3	+5
MIN DEV	[°C]	-3	+1	+1	-1	+1	+1	-1	+0	+2
	[%]	-4	+3	+3	~0	+1	+2	~0	+2	+6
MAX DEV	[°C]	-19	+9	+46	-34	+32	+58	-8	+12	+29
	[%]	-6	+6	+15	-6	+6	+10	-5	+5	+12
AVERAGE DEV	[°C]	-8	+10	+15	-15	+12	+21	-5	+5	+11
	[%]	-3	+4	+6	-3	+3	+5	-2	+3	+5

Visibility

Looking at Table 7.5 it is possible to see that the maximum deviations between the simulations occur in the early stages of the fire. The maximum values vary in absolute numbers between 0.24 and 0.65 m. The smallest deviations are 0 and after 200 seconds the differences between the different simulations are only minor, with absolute values around 0.02-0.1 m. In percentages the maximum deviation is for alfa 3, which is 14% and the average values lies around 3-5% for alfa 1 and alfa 2 and 7% for alfa 3.

Table 7.5. Corridor visibility compared to steel case for changes in growth rates (alfa 1, alfa 2 and alfa 3), 20s time average and averaged over corridor part length. Values extracted from slice file in corridor part A and C.

Time [s]		VISIBILITY CHANGES COMPARED TO STEEL CASE [m]					
		Corridor Part A			Corridor Part C		
		-7.1%	+7.1%	+14.3%	-7.10%	+7.1%	+14.3%
100 s		+0.35	-0.39	-0.50	+0.24	-0.30	-0.65
200 s		+0.04	-0.04	-0.09	+0.05	-0.03	-0.10
300 s		+0.02	-0.03	-0.06	+0.04	-0.02	-0.04
400 s		+0.02	-0.03	-0.03	+0.02	-0.03	-0.04
500 s		+0.02	-0.01	-0.02	+0.02	-0.01	-0.02
600 s		+0.01	-0.01	-0.02	0.00	-0.01	-0.03
700 s		-0.01	0.00	0.00	-0.01	+0.01	0.01
800 s		0.00	-0.01	0.00	-0.02	0.00	-0.01
900 s		-0.02	-0.02	-0.02	-0.01	0.00	0.00
MIN DEV	[m]	0.00	0.00	0.00	0.00	0.00	0.00
	[%]	0	0	0	0	0	0
MAX DEV	[m]	+0.35	-0.39	-0.50	+0.24	-0.30	-0.65
	[%]	+7.21	-8.06	-10.40	+6.40	-6.49	-14.12
AVERAGE DEV	[m]	+0.05	-0.06	-0.08	+0.05	-0.05	-0.10
	[%]	+4.43	-4.61	-6.83	+4.88	-3.40	-7.07

8 Discussion

The discussion is divided into several parts in order to give a better overview and make it easier to follow. The choice of method as well as the results are discussed and analyzed in order to identify potential weaknesses as well as to enable the drawing of valid conclusions.

8.1 Choice of scenarios

Both the FRP and the steel case were simulated for a sprinklered and an unsprinklered scenario. The sprinklered scenario represents the most probable case because of the requirement that demands the use of sprinklers onboard large passenger ships. The unsprinklered scenario represents a probable worst case event and therefore it will result in more severe consequences. This scenario was chosen in order to evaluate the constructions based on events that are somewhat out of the ordinary. The probability of sprinkler failure is however relatively low (5-10%). This means that the resulting risk is lower than it would be if the probability would have been the same as in the sprinklered scenario.

8.2 Analysis of results

To enable a good comparison between the FRP and steel cases the time until critical conditions was not just determined for a single location. Instead the differences were, as previously explained, measured by calculating the amount of corridor length where critical conditions have occurred at different times. This was presented as the fraction of the corridor area where critical conditions were present at the given time. This approach had another benefit (besides the additional information gained from looking at several locations and times) in that the fraction could be used to define a state were critical conditions are not considered to be acceptable. If critical conditions occur in a single point, for example directly outside the doorway of the fire compartment, it does not necessarily mean that human safety is compromised. In this scenario the assumption is that any person inside the fire cabin will either evacuated on time or be beyond saving at the time when critical conditions occur in the corridor. Because of this the time to critical conditions directly outside the fire cabin is not deemed to be of interest but rather the time where people in the adjacent cabins could be affected by critical conditions. This led to the formulation of the criterion that critical conditions should be reached in less than 18% of the corridor in order for safe evacuation to be possible.

The results from the FDS simulations showed some differences in the time until critical conditions between the FRP case and the steel case. For the sprinklered cases there was a 12 second difference in the time until the critical temperature of 80°C was reached in 18% of the corridor. In both cases this occurred before sprinkler activation. The temperatures do however in both cases stabilize after around 400 seconds. This may seem strange considering that the fire growth rates differ but can be explained by the fact that a faster growth rate will lead to an earlier activation of the sprinkler. Hence, since the time to sprinkler activation is shorter for the FRP case than for the steel case the HRR at the time of sprinkler activation is similar in the two cases in this scenario, resulting in roughly the same fire behavior after sprinkler activation. It should however be stated that even though the earlier sprinkler activation leads to a faster cooling of the gases in the corridor, critical temperatures are reached earlier in the FRP case which makes it a more severe case in regard to this variable.

The differences in time until critical conditions for the visibility criteria occur were smaller than for the temperature criterion. Figures showed times for both the 10 m and the 5 m criteria, however, the discussion is based on the results from the 10 m criterion which showed a 3 second difference. The reason for only analyzing the 10 m criterion is based on the geometry. Since the length of the corridor in the setup is longer than 10 m it can be argued that it is inappropriate to allow 5 m visibility. Although a corridor is easy to orientate in for an evacuating person (because there are mostly only two

route options), it should also be possible to see emergency exit signs, which will not necessarily be the case if the visibility is only 5 m.

Sprinkler activation showed some effect when it came to increasing the visibility, however the conditions do not improve significantly and are still critical after sprinkler activation. It should also be stated that sprinkler activation can contribute to a mixing of the gases in the fire room and consequently the smoke layer in the corridor will be affected by this as well. This means that the sprinkler activation could lead to a dispersion of the gases and a disappearance of the distinct smoke layer in the corridor. This was not accounted for in the model used and therefore the resulting visibility after sprinkler activation cannot be accurately predicted.

For the unsprinklered cases there was also a difference of 12 seconds in the time until critical temperatures occurred. However in this scenario there is no sprinkler activation which will mean that there will be no decline in temperature like in the sprinklered scenario where the conditions became safe again after some time. In addition the difference between the conditions in the FRP and steel case will increase since the fire is still in the growth phase. This is due to the fact that the difference in HRR will increase with time since the fire growth rate differs in the two cases. The consequence of this is that the conditions in the unsprinklered FRP case will continue to get worse relative to the steel case as time goes on.

The difference in time until critical conditions for visibility occur was for the unsprinklered cases 2 seconds. Just as with the temperatures, there will not be a positive influence from sprinkler activation in this scenario. However there will be no significant increase in the relative difference between the FRP and steel case since the visibility at 2 m height is already very low in the early stages of the fire. If studying the visibility at lower heights there would most likely be a difference since the smoke layer will descend faster in the FRP case due to the higher HRR.

When studying the smoke layer height it was hard to determine any differences since the variations between the scenarios were very small. The pictures from Smokeview show slight differences between the sprinklered FRP and steel cases. However, the smoke layer descends below the critical value for the smoke layer height before the visibility becomes critical. Hence the visibility will be the decisive factor when determining the time until critical conditions in regard to visibility and smoke layer height. This is because both of these criteria do not have to be fulfilled in order to enable safe evacuation, according to the criteria. Just as discussed previously about visibility in sprinklered cases, the mixing of gases will lead to a disappearance of the distinct smoke layer, which means that the figures showing the smoke layer height for the sprinklered cases are wrong. They do however hint at the fact that the FRP case gives denser smoke than the steel case.

The results of the sprinklered and unsprinkered scenarios could not be directly compared since the burner area used in FDS varied between these scenarios. The reason for this was that the HRR is much lower in the sprinklered scenario which means that the burner area had to be smaller in order to represent a realistic fire. If an equally large burner area would have been used in this scenario the HRR per unit area would be too small and the flame height unrealistically low which would result in a badly simulated fire plume and thus false results. The difference in burner area is also the reason for the deviations in time until critical conditions between the sprinklered and unsprinklered scenarios.

8.3 Growth rate sensitivity

Unlike the soot yield parameter the sensitivity analysis that concerned the growth rate showed that the difference in growth rate is a highly important parameter regarding the difference of results between

the FRP and steel cases. Since the growth rate will determine the HRR of the fire at a given time during the growth phase it will have an influence on all the output variables studied. Also, the difference in growth rate between the FRP and steel case is a result of the added insulation that is used for the FRP composite structure. This means that in order to accurately compare the two structures the change in growth rate must be correctly determined in order to represent reality. The added insulation will have an effect on the growth rate but the question is "how much?". Therefore this parameter is the single most important one since the effect of the added insulation is the foundation of the project and is modeled by varying the growth rate in the two cases. In this case the design fire that was used for the FRP case was reduced by studying data from a single experiment which compared two identical fire setups in an insulated and a non-insulated container. First of all this is a weakness since it means that the difference in growth rate is determined on the basis of only one experiment. Secondly the geometry and setup was not identical to the one used in this project, for example the compartment size, the fuel used and the insulating capabilities differ. It does comply fairly well with this case, but more representative experimental data is desirable. The reason for not performing own experiments was based on the cost as well as the time frame of the project.

8.4 Geometry limitations

A limitation in the geometry is the fact that the corridor is open at both ends. This means that the results are only valid for a long corridor, where no obstructions inside the corridor can accelerate the descent of the smoke layer. Also the model should only be used in the early stages of the fire before the smoke layer reaches a potentially closed door at the end of the corridor. If the corridor had been closed at both ends it would instead represent a scenario with shut doors. The reason for having the corridor open was partly to ensure that the fire would not be ventilation controlled. Another reason was that an open corridor can in the early stages represent another longer corridor which means that the model is applicable for more than just this specific case where the corridor is 21 m long.

Another limitation is that the corridor follows a straight line. If studying a corridor with bends the gas flow will be different than in the model used. This could give other results following the bend regarding smoke layer height, visibility as well as temperatures.

No ventilation was specified in the setup. The assumption that no smoke spread occurs through the ventilation system and that the ventilation was shut off after fire detection was made. However, these are possible scenarios that would affect the outcome. For example it could enable potential smoke spread to adjacent cabins unless smoke dampers are installed and functional.

8.5 Closing discussion

As mentioned in the report risk was defined as a combination of probability and consequences for a specific scenario. However the probability of a fire does in this case not depend on the building materials used in the construction and therefore only the consequences are compared. Since the time until critical condition is coupled with human safety it was used to compare the risk level of the different cases. The results from the FDS simulations showed some differences in time to critical conditions for the different variables that were studied. The times for the temperature criterion showed larger differences between the FRP and steel case than the times for the visibility criterion did. In both the sprinklered and the unsprinklered case the difference in time until critical conditions was 12 seconds. For the 10 m visibility criterion the time differences were 3 seconds and 2 seconds for the sprinklered and unsprinklered scenarios respectively. However for the sprinklered cases the conditions stabilize at similar levels and for the temperature criterion become acceptable again after sprinkler activation. This is not the case in the unsprinklered scenarios where the relative difference between

FRP and steel increases with time and after 10 minutes reaches temperature differences of up to 100°C.

This indicates that the risk levels for the FRP and steel cases are similar since a difference of 2-12 seconds time until critical conditions for the different criteria is not necessarily a variation that means the difference between life and death for a person evacuating. This is especially true for the sprinklered case since the temperatures as mentioned stabilize below 80°C after about 400 seconds for both of the sprinklered cases. However when analyzing the results more thoroughly it becomes clear that there is a larger difference in the time until critical conditions occur at the end of the corridor for the temperature criterion. This means that a larger number of people could be exposed to critical temperatures in the sprinklered FRP case than in the sprinklered steel case. The critical conditions are also maintained in the entire corridor for about twice as long in the FRP case compared to the steel case. For a better understanding of this Figure 6.9 can be studied.

In a way the same reasoning applies to the unsprinklered cases. There is no large difference in the time until critical conditions occur but later on as the fire grows the differences in temperature between the FRP and steel case become significant, as previously mentioned. As in the sprinklered scenarios there are no large relative differences in the visibility between the FRP and steel case.

9 Conclusions

The conclusions made only apply to the geometry used in this model and cases that fulfill the assumptions mentioned 8.4. The aim of the project was to evaluate the performance of a FRP composite structure compared to a steel structure in regard to fire safety and risk during an evacuation. This was done by investigating how the added insulation used in the FRP structure influenced the temperature, visibility and smoke layer height in the early stages of a fire and what effect this had on the risk level. The project resulted in the following conclusions being drawn:

- The largest relative difference in time until critical conditions was found when comparing the gas temperature results which showed a difference of 12 seconds.
- The visibility results show small differences in time until critical conditions, 3 seconds for the sprinklered case and 2 seconds for the unsprinklered case.
- The smoke layer height was according to the FDS results similar in both cases.
- When studying the time until critical conditions close to the fire compartment the risk levels are similar for the FRP and steel case.
- If looking at the time until critical temperature conditions further away from the fire compartment the differences in risk level are larger.
- The temperature differences become larger with time for the unsprinklered scenarios, after 600 seconds the maximum difference is about 100°C.

The general conclusion is that the overall risk level is higher in the FRP case compared to the steel case. This is based on the fact that in a real life situation it is not only the critical conditions in the vicinity of the fire that are important, but also the conditions further away from the fire. In order to determine if the differences in risk level are significant further research with a wider scope is needed. The effects of the additional insulation are things that should be considered when moving from the traditional steel constructions to lightweight constructions like FRP.

10 Further research

Some ideas on future research that could be beneficial when looking deeper into this subject is presented in this chapter along with an idea that could potentially help solve some of the problems with risk in regard to fire safety when using a FRP composite structure.

- Since determining the difference in fire growth rate between when using a FRP composite structure and a steel structure was of fundamental importance it is desirable to look into this more thoroughly. Ideally experiments could be conducted for several different geometries and for different structures with varying insulation thicknesses. This would result in a better quantification of how much the added insulation used in the FRP case influences the fire growth rate which would lead to more accurate predictions on the differences in risk level.

- The simulations performed in this project focus on a single geometry. It would be interesting to look at the effects in other types of geometries and spaces. In this way a wider understanding can be gained regarding the differences between the FRP and steel cases. For example a corridor with bends could give other results, completely different geometries like public spaces onboard ships could also be studied.

- A possible way to reduce the risk level when using a FRP composite structure is to reduce the activation temperature or RTI for the sprinklers used in the compartments that are affected by the use of the FRP structures. This would of course not make any difference in the worst case scenario where sprinkler activation fails but it could still be interesting to investigate what effects this would have.

- An investigation of how the production of chemical species, such as carbon monoxide and carbon dioxide, varies when using the different material setups could be performed for a more complete analysis of the possible difference in risk level. These values can be compared to the criteria for toxicity given in the IMO guidelines.

11 References

Arvidson, M., Axelsson, J. & Hertzberg, T., 2008. *Large-scale fire tests in a passenger cabin*. SP Report 2008:33. Borås: SP Technical Research Institute of Sweden Department of Fire Technology.

Back, A., 2012. *Fire development in insulated compartments: Effects from improved thermal insulation*. Lund University Publications Report 5387. Lund: Lund University Department of Fire Safety Engineering and Systems Safety.

BIV, 2013. *BIV:s Tillämpningsdokument 2/2013 – Utgåva 1 - CFD-beräkningar med FDS*. Malmö: BIV.

Boverket, 2013. *Boverkets ändring av verkets allmänna råd (2011:27) om analytisk dimensionering av byggnaders brandskydd*. BFS 2013:12 BBRAD 3. Karlskrona: Boverket.

Drysdale, D., 2011. *An Introduction to Fire Dynamics*. Third Edition ed. Chichester, West Sussex, United Kingdom: John Wiley & Sons Ltd.

Eckert, E.R.G. & Drake, R.M., 1987. *Analysis of Heat and Mass Transfer*. New York: Hemisphere Publishing Corporation.

Engineering Toolbox, 2014. *Mineral Wool Insulation - Thermal conductivity - Temperature and k-values*. [Online] Available at: http://www.engineeringtoolbox.com/mineral-wool-insulation-k-values-d_815.html [Accessed 7 October 2014].

Evans, D.D., 1993. *Sprinkler Fire Supression Algorithm for HAZARD*. NISTIR 5254. Gaithersburg, MD: National Institute of Standards and Technology Building and Fire Research Laboratory, National Institute of Standards and Technology.

Hens, H.S.L.C., 2012. *Performance based building design 1 - From below grade construction to cavity walls*. Berlin: Ernst & Sohn.

Hertzberg, T. et al., 2009. *LASS, Lightweight Construction Applications at Sea*. SP Report 2009:13. Borås: SP Technical Research Institute of Sweden Department of Fire Technology.

IMO, 1993. RECOMMENDATION ON FIRE RESISTANCE TESTS FOR "A", "B" and "F" CLASS DIVISIONS. In *Resolution A.754(18).*, 1993.

IMO, 1995. REVISED GUIDELINES FOR APPROVAL OF SPRINKLER SYSTEMS EQUIVALENT TO THAT REFERRED TO IN SOLAS REGULATION II-2/12. In *Resolution A.800(19).*, 1995.

IMO, 2004. *SOLAS - Consolidated Edition*. London: The Bath Press.

ISO 31000, 2009. *Risk management - Principles and guidelines*. Geneva, Switzerland: ISO.

Karlsson, B. & Quintiere, J.G., 2000. *Enclosure Fire Dynamics*. Boca Raton: CRC Press.

Madrzykowski , D. & Vettori, R.L., 1992. *A Sprinkler Fire Supression Algorithm for the GSA Engineering Fire Assessment System*. NISTIR 4833. Gaithersburg, MD: National Institute of Standards and Technology Building and Fire Research Laboratory, National Institute of Standards and Technology.

Maritime and Coastguard Agency, 2000. *International Code of Safety for High-Speed Craft*. London: TSO.

McGrattan, K., 2007. *Verification and Validation of Selected Fire Models for Nuclear Power Plant Applications, Volume 7: Fire Dynamics Simulator (FDS)*. U.S. Nuclear Regulatory Commission, Office of Nuclear Regulatory Research (RES), Rockville, MD, 2007, and Electric Power Research Institute (EPRI), Palo Alto, CA, NUREG-1824 and EPRI 1011999.

McGrattan, K. et al., 2013. *Fire Dynamics User's Guide*. NIST Special Publication 1019 Sixth Edition. Baltimore, Maryland: National Institute of Standards and Technology National Institute of Standards and Technology.

Molinelli, L., 2012. *DETector ACTuation - Time squared*. [Online] Available at: http://www.molinelli.org/DetAct.aspx [Accessed 18 November 2014].

Nystedt, F., 2011. *Verifying Fire Safety Design in Sprinklered Buildings*. Lund: Lund University Department of Fire Safety Engineering and Systems Safety.

Robbins, A.P. & Wade, C.A., 2007. *Soot Yield Values for Modelling Purposes - Residential Occupancies*. BRANZ Study Report 185. Porirua, New Zealand: BRANZ ltd.

Rodríguez Panagiotopoulos, A.E., 2014. *Modelling the Effect of the Use of Fiber Reinforeced Plastics on the Evacuation of a Ro-Pax Passenger Vessel*. Lund University Publications Report 5453. Lund: Lund University Department of Fire Safety Engineering.

S-LÄSS, 2014. *LÄSS Reports and papers*. [Online] Available at: http://www.s-lass.com/en/projects/completed/lass/Sidor/default.aspx [Accessed 29 August 2014].

Staffansson, L., 2010. *Selecting Design Fires*. Lund University Publications Report 7032. Lund: Lund University Department of Fire Safety Engineering and Systems Safety.

Tewardson, A., 2002. Section 3 - Chapter 4 - Generation of Heat and Chemical Compounds in Fires. In W.D. Walton, ed. *SFPE Handbook of Fire Protection Engineering*. 3rd ed. Quincy, Massachusetts: National Fire Protection Association. pp.82 - 161.

Tuovinen, H. & Hertzberg, T., 2009. *Simulation of fires in a RoPax vessel*. SP Report 2009:02. Borås: SP Technical Research Institute of Sweden Department of Fire Technology.

Wade, C.A., 2001. *Regulation of Smoke Generation Properties of Interior Lining Materials*. BRANZ Report FCR 6. Porirua, New Zealand: BRANZ Ltd.

Appendix A: FDS Script

Lines are marked in gray where changes between different simulations are made. This script is for scenario 1.

```
&HEAD CHID='sprinklered_frp_finer' TITLE='sprinklered_frp_finer'/
&TIME T_END=900.0/
&MESH ID='MESH_1', MPI_PROCESS=0, IJK= 64, 120, 60, XB= 8.9, 12.1, 0.0, 6.0, 0.0, 3.0 / FIREROOM
&MESH ID='MESH_2', MPI_PROCESS=1, IJK= 180, 24, 60, XB=-0.1,8.9,4.3,5.5,0.0,3.0/ CORRIORLEFT
&MESH ID='MESH_3', MPI_PROCESS=2, IJK= 180, 24, 60, XB=12.1,21.1,4.3,5.5,0.0,3.0/CORRIDORRIGHT
&MESH ID='MESH_4', MPI_PROCESS=3, IJK= 40,40,40, XB=-8.1,-0.1,0.9,8.9,0.0,8.0/LEFT AIRBOX
&MESH ID='MESH_5', MPI_PROCESS=3, IJK= 30, 45, 30, XB=5.9,8.9,-0.2,4.3,0.0,3.0/ LEFTADJACENTR
&MESH ID='MESH_6', MPI_PROCESS=3, IJK= 30, 45, 30, XB=12.1,15.1,-0.2,4.3,0.0,3.0/ RIGHTADJACENTR
&MESH ID='MESH_7', MPI_PROCESS=3, IJK= 40,40,40, XB=21.1,28.1,0.9,8.9,0.0,8.0/RIGHT AIRBOX
&MESH ID='MESH_8', MPI_PROCESS=3, IJK= 64, 4,60, XB= 8.9, 12.1, -0.2, 0.0, 0.0, 3.0/SMALLWALLMESH
&MESH ID='MESH_9', MPI_PROCESS=3, IJK= 32, 38, 30, XB=8.9,12.1,6.0,9.8,0.0,3.0/OPPOSITEROOM
&MESH ID='MESH_10', MPI_PROCESS=3, IJK= 32, 45, 27, XB= 8.9, 12.1, 0.0, 4.5, 3.0, 5.7/ 2NDPLANEROOM
==================
OPEN BOUNDARIES==
&VENT XB=-0.1,-0.1,4.3,5.5,0.0,3.0, SURF_ID='OPEN',/
&VENT XB=21.1,21.1,4.3,5.5,0.0,3.0, SURF_ID='OPEN',/
&VENT XB=-0.1,8.9,5.5,5.5,0.0,3.0, SURF_ID='OPEN',/
&VENT XB=12.1,21.1,5.5,5.5,0.0,3.0, SURF_ID='OPEN',/
&VENT XB=-0.1,8.9,4.3,4.3,0.0,3.0, SURF_ID='OPEN',/
&VENT XB=12.1,21.1,4.3,4.3,0.0,3.0, SURF_ID='OPEN',/

&VENT XB=-8.1,-0.1,0.9,8.9,8.0,8.0, SURF_ID='OPEN',/
&VENT XB=-8.1,-8.1,0.9,8.9,0.0,8.0, SURF_ID='OPEN'/
&VENT XB=-8.1,-8.1,0.9,0.9,0.0,8.0, SURF_ID='OPEN'/
&VENT XB=-8.1,-8.1,8.9,8.9,0.0,8.0, SURF_ID='OPEN'/
&VENT XB=-0.1,-0.1,0.9,4.3,0.0,8.0, SURF_ID='OPEN'/
&VENT XB=-0.1,-0.1,5.5,8.9,0.0,8.0, SURF_ID='OPEN'/
&VENT XB=-0.1,-0.1,4.3,5.5,3.0,8.0, SURF_ID='OPEN'/

&VENT XB=21.1,29.1,0.9,8.9,8.0,8.0, SURF_ID='OPEN',/
&VENT XB=29.1,29.1,0.9,8.9,0.0,8.0, SURF_ID='OPEN'/
&VENT XB=29.1,29.1,0.9,0.9,0.0,8.0, SURF_ID='OPEN'/
&VENT XB=29.1,29.1,8.9,8.9,0.0,8.0, SURF_ID='OPEN'/
&VENT XB=21.1,21.1,0.9,4.3,0.0,8.0, SURF_ID='OPEN'/
&VENT XB=21.1,21.1,5.5,8.9,0.0,8.0, SURF_ID='OPEN'/
&VENT XB=21.1,21.1,4.3,5.5,3.0,8.0, SURF_ID='OPEN'/
===============
===MATERIALS===
&MATL          ID='Laminate'
               CONDUCTIVITY_RAMP='laminate_k_ramp'
               SPECIFIC_HEAT_RAMP='laminate_cp_ramp'
               DENSITY=1870.0/ [SP Report 2009:02] interpolated both
&MATL          ID='DivinycellH80'
               CONDUCTIVITY_RAMP='DivinycellH80_k_ramp'
               SPECIFIC_HEAT_RAMP='DivinycellH80_cp_ramp'
               DENSITY=80.0/ [SP Report 2009:02] interpolated both
&MATL          ID='Firemaster'
               CONDUCTIVITY_RAMP='Firemaster_k_ramp'
               SPECIFIC_HEAT=0.8
               DENSITY=100.0/ [SP Report 2009:02] interpolated conductivity, Cp constant
&MATL          ID='Steel'
               CONDUCTIVITY_RAMP='Steel_k_ramp'
               SPECIFIC_HEAT=0.5
```

```
                DENSITY=7850.0/ [SP Report 2009:02] interpolated conductivity, Cp constant
&MATL           ID='Aluminium'
                CONDUCTIVITY_RAMP='Aluminium_k_ramp'
                SPECIFIC_HEAT=0.896
                DENSITY=2707.0/
[SFPE TAB B6],
[http://books.google.se/books?id=1Mh9XoMoPRQC&pg=PA772&hl=sv&source=gbs_toc_r&cad=4#v=onepage&q
&f=false]
&MATL           ID='RockWool'
                CONDUCTIVITY_RAMP='RockWool_k_ramp'
                SPECIFIC_HEAT=0.84
                DENSITY=190/  Interpolated conductivity, Cp constant
[http://www.engineeringtoolbox.com/thermal-conductivity-d_429.html] - conductivity
[http://books.google.se/books?id=U3-
9vP4IDJIC&pg=PR21&lpg=PR21&dq=mineral+wool+specific+heat&source=bl&ots=nS9C2g7y_P&sig=u_zUwyru
Q4c3yl8YxdNGjdTskYU&hl=sv&sa=X&ei=TncJVIHOOcesPf6XgcAJ&ved=0CGcQ6AEwBw#v=onepage&q=miner
al%20wool%20specific%20heat&f=false]
=======
RAMPS==
::::::::::::::::::::::::LAMINATE K RAMP::::::::::::::::::::::::

&RAMP ID='laminate_k_ramp',    T=    20 ,F=   0.0425   /
&RAMP ID='laminate_k_ramp',    T=    30 ,F=   0.04375 /
&RAMP ID='laminate_k_ramp',    T=    40 ,F=   0.045    /
&RAMP ID='laminate_k_ramp',    T=    50 ,F=   0.04625 /
&RAMP ID='laminate_k_ramp',    T=    60 ,F=   0.0475   /
&RAMP ID='laminate_k_ramp',    T=    70 ,F=   0.04875 /
&RAMP ID='laminate_k_ramp',    T=    80 ,F=   0.05     /
::::::::::::::::::::::::LAMINATE Cp RAMP::::::::::::::::::::::::

&RAMP ID='laminate_cp_ramp',  T=    20 ,F=0.7425     /
&RAMP ID='laminate_cp_ramp',  T=    30 ,F=0.74375    /
&RAMP ID='laminate_cp_ramp',  T=    40 ,F=0.745      /
&RAMP ID='laminate_cp_ramp',  T=    50 ,F=0.74625    /
&RAMP ID='laminate_cp_ramp',  T=    60 ,F=0.7475     /
&RAMP ID='laminate_cp_ramp',  T=    70 ,F=0.74875    /
&RAMP ID='laminate_cp_ramp',  T=    80 ,F=0.75       /
:::::::::::::::::::::::: Divinycell Core H80 K RAMP::::::::::::::::::::::::

&RAMP ID='DivinycellH80_k_ramp', T=    20 ,F=   0.029            /
&RAMP ID='DivinycellH80_k_ramp', T=    30 ,F=   0.028702722    /
&RAMP ID='DivinycellH80_k_ramp', T=    40 ,F=   0.028703444    /
&RAMP ID='DivinycellH80_k_ramp', T=    50 ,F=   0.028704167    /
&RAMP ID='DivinycellH80_k_ramp', T=    60 ,F=   0.028704889    /
&RAMP ID='DivinycellH80_k_ramp', T=    70 ,F=   0.028705611    /
&RAMP ID='DivinycellH80_k_ramp', T=    80 ,F=   0.028706333    /
:::::::::::::::::::::::: Divinycell Core H80 Cp RAMP::::::::::::::::::::::::

&RAMP ID='DivinycellH80_cp_ramp',  T= 20 ,F=2.12             /
&RAMP ID='DivinycellH80_cp_ramp',  T= 30 ,F=2.163333333    /
&RAMP ID='DivinycellH80_cp_ramp',  T= 40 ,F=2.206666667    /
&RAMP ID='DivinycellH80_cp_ramp',  T= 50 ,F=2.25             /
&RAMP ID='DivinycellH80_cp_ramp',  T= 60 ,F=2.293333333    /
&RAMP ID='DivinycellH80_cp_ramp',  T= 70 ,F=2.336666667    /
&RAMP ID='DivinycellH80_cp_ramp',  T= 80 ,F=2.38             /
:::::::::::::::::::::::: Firemaster K RAMP::::::::::::::::::::::::

&RAMP ID='Firemaster_k_ramp', T= 20    ,F=   0.0335   /
```

```
&RAMP ID='Firemaster_k_ramp', T= 30   ,F=  0.034   /
&RAMP ID='Firemaster_k_ramp', T= 40   ,F=  0.0345  /
&RAMP ID='Firemaster_k_ramp', T= 50   ,F=  0.035   /
&RAMP ID='Firemaster_k_ramp', T= 60   ,F=  0.037   /
&RAMP ID='Firemaster_k_ramp', T= 70   ,F=  0.039   /
&RAMP ID='Firemaster_k_ramp', T= 80   ,F=  0.041   /
&RAMP ID='Firemaster_k_ramp', T= 90   ,F=  0.043   /
&RAMP ID='Firemaster_k_ramp', T= 100  ,F=  0.045   /
&RAMP ID='Firemaster_k_ramp', T= 110  ,F=  0.0466  /
&RAMP ID='Firemaster_k_ramp', T= 120  ,F=  0.0482  /
&RAMP ID='Firemaster_k_ramp', T= 130  ,F=  0.0498  /
&RAMP ID='Firemaster_k_ramp', T= 140  ,F=  0.0514  /
&RAMP ID='Firemaster_k_ramp', T= 150  ,F=  0.053   /
&RAMP ID='Firemaster_k_ramp', T= 160  ,F=  0.055   /
&RAMP ID='Firemaster_k_ramp', T= 170  ,F=  0.057   /
&RAMP ID='Firemaster_k_ramp', T= 180  ,F=  0.059   /
&RAMP ID='Firemaster_k_ramp', T= 190  ,F=  0.061   /
&RAMP ID='Firemaster_k_ramp', T= 200  ,F=  0.063   /
&RAMP ID='Firemaster_k_ramp', T= 210  ,F=  0.0655  /
&RAMP ID='Firemaster_k_ramp', T= 220  ,F=  0.068   /
&RAMP ID='Firemaster_k_ramp', T= 230  ,F=  0.0705  /
&RAMP ID='Firemaster_k_ramp', T= 240  ,F=  0.073   /
&RAMP ID='Firemaster_k_ramp', T= 250  ,F=  0.0755  /
&RAMP ID='Firemaster_k_ramp', T= 260  ,F=  0.078   /
&RAMP ID='Firemaster_k_ramp', T= 270  ,F=  0.0805  /
&RAMP ID='Firemaster_k_ramp', T= 280  ,F=  0.083   /
&RAMP ID='Firemaster_k_ramp', T= 290  ,F=  0.0855  /
&RAMP ID='Firemaster_k_ramp', T= 300  ,F=  0.088   /
:::::::::::::::::::::::: Steel K RAMP::::::::::::::::::::::::

&RAMP ID='Steel_k_ramp',   T= 20   ,F=  60           /
&RAMP ID='Steel_k_ramp',   T= 30   ,F=  59.57692308  /
&RAMP ID='Steel_k_ramp',   T= 40   ,F=  59.15384615  /
&RAMP ID='Steel_k_ramp',   T= 50   ,F=  58.73076923  /
&RAMP ID='Steel_k_ramp',   T= 60   ,F=  58.30769231  /
&RAMP ID='Steel_k_ramp',   T= 70   ,F=  57.88461538  /
&RAMP ID='Steel_k_ramp',   T= 80   ,F=  57.46153846  /
&RAMP ID='Steel_k_ramp',   T= 90   ,F=  57.03846154  /
&RAMP ID='Steel_k_ramp',   T= 100  ,F=  56.61538462  /
&RAMP ID='Steel_k_ramp',   T= 110  ,F=  56.19230769  /
&RAMP ID='Steel_k_ramp',   T= 120  ,F=  55.76923077  /
&RAMP ID='Steel_k_ramp',   T= 130  ,F=  55.34615385  /
&RAMP ID='Steel_k_ramp',   T= 140  ,F=  54.92307692  /
&RAMP ID='Steel_k_ramp',   T= 150  ,F=  54.5         /
&RAMP ID='Steel_k_ramp',   T= 160  ,F=  54.07692308  /
&RAMP ID='Steel_k_ramp',   T= 170  ,F=  53.65384615  /
&RAMP ID='Steel_k_ramp',   T= 180  ,F=  53.23076923  /
&RAMP ID='Steel_k_ramp',   T= 190  ,F=  52.80769231  /
&RAMP ID='Steel_k_ramp',   T= 200  ,F=  52.38461538  /
&RAMP ID='Steel_k_ramp',   T= 210  ,F=  51.96153846  /
&RAMP ID='Steel_k_ramp',   T= 220  ,F=  51.53846154  /
&RAMP ID='Steel_k_ramp',   T= 230  ,F=  51.11538462  /
&RAMP ID='Steel_k_ramp',   T= 240  ,F=  50.69230769  /
&RAMP ID='Steel_k_ramp',   T= 250  ,F=  50.26923077  /
&RAMP ID='Steel_k_ramp',   T= 260  ,F=  49.84615385  /
&RAMP ID='Steel_k_ramp',   T= 270  ,F=  49.42307692  /
&RAMP ID='Steel_k_ramp',   T= 280  ,F=  49           /
&RAMP ID='Steel_k_ramp',   T= 290  ,F=  48.57692308  /
```

```
&RAMP ID='Steel_k_ramp',   T= 300  ,F=   48.15384615   /
&RAMP ID='Steel_k_ramp',   T= 310  ,F=   47.73076923   /
&RAMP ID='Steel_k_ramp',   T= 320  ,F=   47.30769231   /
&RAMP ID='Steel_k_ramp',   T= 330  ,F=   46.88461538   /
&RAMP ID='Steel_k_ramp',   T= 340  ,F=   46.46153846   /
&RAMP ID='Steel_k_ramp',   T= 350  ,F=   46.03846154   /
&RAMP ID='Steel_k_ramp',   T= 360  ,F=   45.61538462   /
&RAMP ID='Steel_k_ramp',   T= 370  ,F=   45.19230769   /
&RAMP ID='Steel_k_ramp',   T= 380  ,F=   44.76923077   /
&RAMP ID='Steel_k_ramp',   T= 390  ,F=   44.34615385   /
&RAMP ID='Steel_k_ramp',   T= 400  ,F=   43.92307692   /
&RAMP ID='Steel_k_ramp',   T= 410  ,F=   43.5          /
&RAMP ID='Steel_k_ramp',   T= 420  ,F=   43.07692308   /
&RAMP ID='Steel_k_ramp',   T= 430  ,F=   42.65384615   /
&RAMP ID='Steel_k_ramp',   T= 440  ,F=   42.23076923   /
&RAMP ID='Steel_k_ramp',   T= 450  ,F=   41.80769231   /
&RAMP ID='Steel_k_ramp',   T= 460  ,F=   41.38461538   /
&RAMP ID='Steel_k_ramp',   T= 470  ,F=   40.96153846   /
&RAMP ID='Steel_k_ramp',   T= 480  ,F=   40.53846154   /
&RAMP ID='Steel_k_ramp',   T= 490  ,F=   40.11538462   /
&RAMP ID='Steel_k_ramp',   T= 500  ,F=   39.69230769   /
&RAMP ID='Steel_k_ramp',   T= 510  ,F=   39.26923077   /
&RAMP ID='Steel_k_ramp',   T= 520  ,F=   38.84615385   /
&RAMP ID='Steel_k_ramp',   T= 530  ,F=   38.42307692   /
&RAMP ID='Steel_k_ramp',   T= 540  ,F=   38            /
&RAMP ID='Steel_k_ramp',   T= 550  ,F=   37.57692308   /
&RAMP ID='Steel_k_ramp',   T= 560  ,F=   37.15384615   /
&RAMP ID='Steel_k_ramp',   T= 570  ,F=   36.73076923   /
&RAMP ID='Steel_k_ramp',   T= 580  ,F=   36.30769231   /
&RAMP ID='Steel_k_ramp',   T= 590  ,F=   35.88461538   /
&RAMP ID='Steel_k_ramp',   T= 600  ,F=   35.46153846   /
&RAMP ID='Steel_k_ramp',   T= 610  ,F=   35.03846154   /
&RAMP ID='Steel_k_ramp',   T= 620  ,F=   34.61538462   /
&RAMP ID='Steel_k_ramp',   T= 630  ,F=   34.19230769   /
&RAMP ID='Steel_k_ramp',   T= 640  ,F=   33.76923077   /
&RAMP ID='Steel_k_ramp',   T= 650  ,F=   33.34615385   /
&RAMP ID='Steel_k_ramp',   T= 660  ,F=   32.92307692   /
&RAMP ID='Steel_k_ramp',   T= 670  ,F=   32.5          /
&RAMP ID='Steel_k_ramp',   T= 680  ,F=   32.07692308   /
&RAMP ID='Steel_k_ramp',   T= 690  ,F=   31.65384615   /
&RAMP ID='Steel_k_ramp',   T= 700  ,F=   31.23076923   /
&RAMP ID='Steel_k_ramp',   T= 710  ,F=   30.80769231   /
&RAMP ID='Steel_k_ramp',   T= 720  ,F=   30.38461538   /
&RAMP ID='Steel_k_ramp',   T= 730  ,F=   29.96153846   /
&RAMP ID='Steel_k_ramp',   T= 740  ,F=   29.53846154   /
&RAMP ID='Steel_k_ramp',   T= 750  ,F=   29.11538462   /
&RAMP ID='Steel_k_ramp',   T= 760  ,F=   28.69230769   /
&RAMP ID='Steel_k_ramp',   T= 770  ,F=   28.26923077   /
&RAMP ID='Steel_k_ramp',   T= 780  ,F=   27.84615385   /
&RAMP ID='Steel_k_ramp',   T= 790  ,F=   27.42307692   /
&RAMP ID='Steel_k_ramp',   T= 800  ,F=   27            /
:::::::::::::::::::::::: RockWool K RAMP::::::::::::::::::::::::

&RAMP ID='RockWool_k_ramp',   T= 20     ,F=0.049754955   /
&RAMP ID='RockWool_k_ramp',   T= 37.8   ,F=0.052         /
&RAMP ID='RockWool_k_ramp',   T= 40     ,F=0.052277477   /
&RAMP ID='RockWool_k_ramp',   T= 60     ,F=0.0548        /
&RAMP ID='RockWool_k_ramp',   T= 80     ,F=0.057322523   /
```

```
&RAMP ID='RockWool_k_ramp',   T= 93.3   ,F=0.059          /
&RAMP ID='RockWool_k_ramp',   T= 100    ,F=0.059964029  /
&RAMP ID='RockWool_k_ramp',   T= 120    ,F=0.062841727  /
&RAMP ID='RockWool_k_ramp',   T= 140    ,F=0.065719424  /
&RAMP ID='RockWool_k_ramp',   T= 148.9  ,F=0.067        /
&RAMP ID='RockWool_k_ramp',   T= 160    ,F=0.0688       /
&RAMP ID='RockWool_k_ramp',   T= 180    ,F=0.072043243  /
&RAMP ID='RockWool_k_ramp',   T= 200    ,F=0.075286486  /
&RAMP ID='RockWool_k_ramp',   T= 204.4  ,F=0.076        /
&RAMP ID='RockWool_k_ramp',   T= 220    ,F=0.079086331  /
&RAMP ID='RockWool_k_ramp',   T= 240    ,F=0.083043165  /
&RAMP ID='RockWool_k_ramp',   T= 260    ,F=0.087        /
&RAMP ID='RockWool_k_ramp',   T= 280    ,F=0.091316547  /
&RAMP ID='RockWool_k_ramp',   T= 300    ,F=0.095633094  /
&RAMP ID='RockWool_k_ramp',   T= 315.6  ,F=0.099        /


:::::::::::::::::::::::: ALUMINIUM K RAMP::::::::::::::::::::::::

&RAMP ID='Aluminium_k_ramp',   T= 20    ,F=202.8  /
&RAMP ID='Aluminium_k_ramp',   T= 40    ,F=203.6  /
&RAMP ID='Aluminium_k_ramp',   T= 60    ,F=204.4  /
&RAMP ID='Aluminium_k_ramp',   T= 80    ,F=205.2  /
&RAMP ID='Aluminium_k_ramp',   T= 100   ,F=206    /
&RAMP ID='Aluminium_k_ramp',   T= 120   ,F=207.8  /
&RAMP ID='Aluminium_k_ramp',   T= 140   ,F=209.6  /
&RAMP ID='Aluminium_k_ramp',   T= 160   ,F=211.4  /
&RAMP ID='Aluminium_k_ramp',   T= 180   ,F=213.2  /
&RAMP ID='Aluminium_k_ramp',   T= 200   ,F=215    /
&RAMP ID='Aluminium_k_ramp',   T= 220   ,F=217.6  /
&RAMP ID='Aluminium_k_ramp',   T= 240   ,F=220.2  /
&RAMP ID='Aluminium_k_ramp',   T= 260   ,F=222.8  /
&RAMP ID='Aluminium_k_ramp',   T= 280   ,F=225.4  /
&RAMP ID='Aluminium_k_ramp',   T= 300   ,F=228    /
&RAMP ID='Aluminium_k_ramp',   T= 320   ,F=232.2  /
&RAMP ID='Aluminium_k_ramp',   T= 340   ,F=236.4  /
&RAMP ID='Aluminium_k_ramp',   T= 360   ,F=240.6  /
&RAMP ID='Aluminium_k_ramp',   T= 380   ,F=244.8  /
&RAMP ID='Aluminium_k_ramp',   T= 400   ,F=249    /

SURF===
===unexposed backing====
&SURF ID= 'B-class panel', COLOR='BLUE', TRANSPARENCY=0.2, MATL_ID='Steel','Firemaster','Steel',
THICKNESS=0.0007,0.0486,0.0007/ symmetric
&SURF ID= 'FRP inside', COLOR='RED', TRANSPARENCY=0.2,
MATL_ID='Firemaster','Laminate','DivinycellH80','Laminate', THICKNESS=0.1,001,0.05,0.001/
&SURF ID= 'FRP outside', COLOR='RED' TRANSPARENCY=0.2,
MATL_ID='Laminate','DivinycellH80','Laminate','Firemaster', THICKNESS=0.001,0.05,0.001,0.1/
&SURF ID= 'FLOOR+CEILING_upwards', COLOR='RED', TRANSPARENCY=0.2,
MATL_ID='Firemaster','Laminate','DivinycellH80','Laminate','RockWool','Aluminium',
THICKNESS=0.1,0.001,0.05,0.001,0.02,0.002/
&SURF ID= 'FLOOR+CEILING_downwards', COLOR='RED', TRANSPARENCY=0.2,
MATL_ID='Aluminium','RockWool','Laminate','DivinycellH80','Laminate','Firemaster',
THICKNESS=0.002,0.02,0.001,0.05,0.001,0.1/
====backing exposed====
&SURF ID= 'B-class panel_exp', COLOR='BLUE', TRANSPARENCY=0.2, MATL_ID='Steel','Firemaster','Steel',
THICKNESS=0.0007,0.0486,0.0007, BACKING='EXPOSED'/ symmetric
```

&SURF ID= 'FRP inside_exp', COLOR='RED', TRANSPARENCY=0.2,
MATL_ID='Firemaster','Laminate','DivinycellH80','Laminate', THICKNESS=0.1,001,0.05,0.001,
BACKING='EXPOSED'/
&SURF ID= 'FRP outside_exp', COLOR='RED', TRANSPARENCY=0.2,
MATL_ID='Laminate','DivinycellH80','Laminate','Firemaster', THICKNESS=0.001,0.05,0.001,0.1,
BACKING='EXPOSED'/
&SURF ID= 'FLOOR+CEILING_upwards_exp', COLOR='RED', TRANSPARENCY=0.2,
MATL_ID='Firemaster','Laminate','DivinycellH80','Laminate','RockWool','Aluminium',
THICKNESS=0.1,0.001,0.05,0.001,0.02,0.002, BACKING='EXPOSED'/
&SURF ID= 'FLOOR+CEILING_downwards_exp', COLOR='RED', TRANSPARENCY=0.2,
MATL_ID='Aluminium','RockWool','Laminate','DivinycellH80','Laminate','Firemaster'
THICKNESS=0.002,0.02,0.001,0.05,0.001,0.1, BACKING='EXPOSED'/

==========
Geometry 1st floor==
&OBST XB=0.0,9.0,5.5,5.5,0.0,2.7, SURF_ID6='INERT','INERT','B-class panel','B-class panel','INERT','INERT'/
longside corridor 1.1
&OBST XB=9.0,12.0,5.5,5.5,0.0,2.7, SURF_ID6='INERT','INERT','B-class panel_exp','B-class
panel_exp','INERT','INERT'/ longside corridor 1.2
&OBST XB=12.0,21.0,5.5,5.5,0.0,2.7, SURF_ID6='INERT','INERT','B-class panel','B-class
panel','INERT','INERT'/ longside corridor 1.3
&OBST XB=9.0,12.0,9.8,9.8,0.0,2.7, SURF_ID6='INERT','INERT','B-class panel_exp','B-class
panel_exp','INERT','INERT'/ shortside room other sidde
&OBST XB=9.0,9.0,5.5,9.8,0.0,2.7, SURF_ID6='B-class panel','B-class panel','INERT','INERT','INERT','INERT'/
side room other side
&OBST XB=12.0,12.0,5.5,9.8,0.0,2.7, SURF_ID6='B-class panel','B-class
panel','INERT','INERT','INERT','INERT'/ side room other side
&OBST XB=9.0,12.0,5.5,9.8,0.0,0.0,
SURF_ID6='INERT','INERT','INERT','INERT','FLOOR+CEILING_upwards','FLOOR+CEILING_downwards'/ floor
other side
&OBST XB=9.0,12.0,5.5,9.8,2.7,2.7,
SURF_ID6='INERT','INERT','INERT','INERT','FLOOR+CEILING_upwards','FLOOR+CEILING_downwards'/ outer
ceiling other side
&OBST XB=0.0,9.0,4.3,4.3,0.0,2.7, SURF_ID6='INERT','INERT','B-class panel','B-class panel','INERT','INERT'/
longside corridor 2.1
&OBST XB=9.0,12.0,4.3,4.3,0.0,2.7, SURF_ID6='INERT','INERT','B-class panel_exp','B-class
panel_exp','INERT','INERT'/ longside corridor 2.2 ___Backing exposed
&OBST XB=12.0,21.0,4.3,4.3,0.0,2.7, SURF_ID6='INERT','INERT','B-class panel','B-class
panel','INERT','INERT', / longside corridor 2.3
&OBST XB=6.0,6.0,-0.2,4.3,0.0,2.7, SURF_ID6='B-class panel','B-class panel','INERT','INERT','INERT','INERT'/
cabin dividing wall 1
&OBST XB=9.0,9.0,-0.2,4.3,0.0,2.7, SURF_ID6='B-class panel_exp','B-class
panel_exp','INERT','INERT','INERT','INERT'/ cabin dividing wall 2 ___Backing exposed
&OBST XB=12.0,12.0,-0.2,4.3,0.0,2.7, SURF_ID6='B-class panel_exp','B-class
panel_exp','INERT','INERT','INERT','INERT'/ cabin dividing wall 3 ___Backing exposed
&OBST XB=15.0,15.0,-0.2,4.3,0.0,2.7, SURF_ID6='B-class panel','B-class
panel','INERT','INERT','INERT','INERT'/ cabin wall 4
&OBST XB=6.0,15.0,0.0,0.0,0.0,2.7, BNDF_OBST=.TRUE., SURF_ID6='INERT','INERT','B-class panel_exp','B-
class panel_exp','INERT','INERT'/ cabin shortsidewall
&OBST XB=6.0,15.0,-0.2,-0.2,0.0,2.7, BNDF_OBST=.TRUE., SURF_ID6='INERT','INERT','FRP outside','FRP
inside','INERT','INERT'/cabin shortside wall outer
&OBST XB=0.0,21.0,4.3,5.5,2.7,2.7,
SURF_ID6='INERT','INERT','INERT','INERT','FLOOR+CEILING_upwards','FLOOR+CEILING_downwards'/
bigroof
&OBST XB=6.0,15.0,-0.2,4.3,2.7,2.7,
SURF_ID6='INERT','INERT','INERT','INERT','FLOOR+CEILING_upwards_exp','FLOOR+CEILING_downwards_e
xp'/ littleroof

&OBST XB=0.0,21.0,4.3,5.5,0.0,0.0,
SURF_ID6='INERT','INERT','INERT','INERT','FLOOR+CEILING_upwards','FLOOR+CEILING_downwards'/
bigfloor
&OBST XB=6.0,15.0,-0.2,4.3,0.0,0.0,
SURF_ID6='INERT','INERT','INERT','INERT','FLOOR+CEILING_upwards','FLOOR+CEILING_downwards'/
littlefloor

&OBST XB=0.0,0.0,4.3,5.5,2.1,2.7, SURF_ID6='B-class panel','B-class panel','INERT','INERT','INERT','INERT'/
leftsideceilingconnector
&OBST XB=21.0,21.0,4.3,5.5,2.1,2.7, SURF_ID6='B-class panel','B-class panel','INERT','INERT','INERT','INERT'/
rightsideceilingconnector

&OBST XB=10.8,10.8,2.5,4.3,0.0,2.7, SURF_ID6='B-class panel_exp','B-class
panel_exp','INERT','INERT','INERT','INERT'/ toilet longside
&OBST XB=10.8,12.0,2.5,2.5,0.0,2.7, SURF_ID6='INERT','INERT','B-class panel_exp','B-class
panel_exp','INERT','INERT'/ toilet shortside

&HOLE XB=9.5,10.3,4.0,4.5,0.0,2.0/ door cabin 4 (mitten)
&HOLE XB=10.8,10.9,3.4,3.5,0.0,0.1/ 0.0125*1 m2 toilet door chink
&HOLE XB=1.5,1.6,4.2,4.4,0.0,0.1/ 0.0125*1 m2 door chink cabin 1
&HOLE XB=4.5,4.6,4.2,4.4,0.0,0.1/ 0.0125*1 m2 door chink cabin 2
&HOLE XB=7.5,7.6,4.2,4.4,0.0,0.1/ 0.0125*1 m2 door chink cabin 3
&HOLE XB=13.5,13.6,4.2,4.4,0.0,0.1/ 0.0125*1 m2 door chink cabin 5
&HOLE XB=16.5,16.6,4.2,4.4,0.0,0.1/ 0.0125*1 m2 door chink cabin 6
&HOLE XB=19.5,19.6,4.2,4.4,0.0,0.1/ 0.0125*1 m2 door chink cabin 7
&HOLE XB=2.1,2.2,5.4,5.6,0.0,0.1/ 0.0125*1 m2 door chink cabin 8
&HOLE XB=5.1,5.2,5.4,5.6,0.0,0.1/ 0.0125*1 m2 door chink cabin 9
&HOLE XB=8.1,8.2,5.4,5.6,0.0,0.1/ 0.0125*1 m2 door chink cabin 10
&HOLE XB=11.1,11.2,5.4,5.6,0.0,0.1/ 0.0125*1 m2 door chink cabin 11
&HOLE XB=14.1,14.2,5.4,5.6,0.0,0.1/ 0.0125*1 m2 door chink cabin 12
&HOLE XB=17.1,17.2,5.4,5.6,0.0,0.1/ 0.0125*1 m2 door chink cabin 13
&HOLE XB=20.1,20.2,5.4,5.6,0.0,0.1/ 0.0125*1 m2 door chink cabin 14

INNER CEILING===
&OBST XB=9.0,12.0,-0.2,4.3,2.1,2.1, SURF_ID6='INERT','INERT','INERT','INERT','B-class panel_exp','B-class
panel_exp'/ Middle cabin
&OBST XB=6.0,9.0,-0.2,4.3,2.1,2.1, SURF_ID6='INERT','INERT','INERT','INERT','B-class panel','B-class panel'/
Left cabin
&OBST XB=12.0,15.0,-0.2,4.3,2.1,2.1, SURF_ID6='INERT','INERT','INERT','INERT','B-class panel','B-class
panel'/ right cabin
&OBST XB=0.0,21.0,4.3,5.5,2.1,2.1, SURF_ID6='INERT','INERT','INERT','INERT','B-class panel','B-class panel'/
corridor
&OBST XB=9.0,12.0,5.5,9.8,2.1,2.1, SURF_ID6='INERT','INERT','INERT','INERT','B-class panel','B-class panel'/
other side

ONLY IN UNSPRINKLERED CASES:

==CEILING COLLAPSE – TIME DEPENDENT OPENING==========
&HOLE XB=9.0,12.0,0.0,4.3,2.0,2.2, DEVC_ID='collapse_timer', COLOR='YELLOW',
TRANSPARENCY=0.2/ceiling collapses
&DEVC XYZ=10.5,2.15,2.1, ID='collapse_timer', SETPOINT=420.0, QUANTITY='TIME',
INITIAL_STATE=.FALSE./timer for ceiling collapse (time dependent on HRR)

==========
==2nd floor==
&OBST XB=9.0,9.0,0.0,4.3,2.7,5.4, SURF_ID6='B-class panel','B-class panel','INERT','INERT','INERT','INERT'/
cabin wall1
&OBST XB=12.0,12.0,0.0,4.3,2.7,5.4, SURF_ID6='B-class panel','B-class
panel','INERT','INERT','INERT','INERT'/ cabin wall 2

```
&OBST XB=9.0,12.0,4.3,4.3,2.7,5.4,  SURF_ID6='INERT','INERT','B-class panel','B-class panel','INERT','INERT'/
cabinwall 3
&OBST XB=9.0,12.0,0.0,0.0,2.7,5.4,  SURF_ID6='INERT','INERT','B-class panel','B-class panel','INERT','INERT'/
cabinwall 4
&OBST XB=9.0,12.0,0.0,4.3,5.4,5.4,
SURF_ID6='INERT','INERT','INERT','INERT','FLOOR+CEILING_upwards_exp','FLOOR+CEILING_downwards_e
xp'/cabin outter ceiling
&OBST XB=9.0,12.0,0.0,4.3,4.8,4.8, SURF_ID6='INERT','INERT','INERT','INERT','B-class panel_exp','B-class
panel_exp'/ cabin inner ceiling
==================================
===BRAND====
&OBST XB= 10.35,10.65,1.15,1.45, 0.0, 0.0, SURF_IDS='BURNER','INERT','INERT' /
&REAC           FUEL='MYFUEL'
                SOOT_YIELD=0.067
                CO_YIELD=0.045
                IDEAL=.TRUE.
                C=1
                H=1.6
                O=0.2
                HEAT_OF_COMBUSTION=26376/
&SURF ID='BURNER',
    COLOR='RED',
    HRRPUA=2098.765,
    RAMP_Q='RAMP_HRR'/
&RAMP ID='RAMP_HRR', T=   0    , F=  0              /
&RAMP ID='RAMP_HRR', T=   10   , F=  0.002500001  /
&RAMP ID='RAMP_HRR', T=   20   , F=  0.010000002  /
&RAMP ID='RAMP_HRR', T=   30   , F=  0.022500005  /
&RAMP ID='RAMP_HRR', T=   40   , F=  0.040000008  /
&RAMP ID='RAMP_HRR', T=   50   , F=  0.062500013  /
&RAMP ID='RAMP_HRR', T=   60   , F=  0.090000019  /
&RAMP ID='RAMP_HRR', T=   70   , F=  0.122500025  /
&RAMP ID='RAMP_HRR', T=   80   , F=  0.160000033  /
&RAMP ID='RAMP_HRR', T=   90   , F=  0.202500042  /
&RAMP ID='RAMP_HRR', T=   100  , F=  0.250000051  /
&RAMP ID='RAMP_HRR', T=   110  , F=  0.302500062  /
&RAMP ID='RAMP_HRR', T=   120  , F=  0.360000074  /
&RAMP ID='RAMP_HRR', T=   130  , F=  0.422500087  /
&RAMP ID='RAMP_HRR', T=   140  , F=  0.490000101  /
&RAMP ID='RAMP_HRR', T=   150  , F=  0.562500116  /
&RAMP ID='RAMP_HRR', T=   160  , F=  0.640000132  /
&RAMP ID='RAMP_HRR', T=   170  , F=  0.722500149  /
&RAMP ID='RAMP_HRR', T=   180  , F=  0.810000167  /
&RAMP ID='RAMP_HRR', T=   190  , F=  0.902500186  /
&RAMP ID='RAMP_HRR', T=   200  , F=  1.000000206  /
&RAMP ID='RAMP_HRR', T=   260  , F=  1              /
&RAMP ID='RAMP_HRR', T=   320  , F=  0.333333333  /
&RAMP ID='RAMP_HRR', T=   900  , F=  0.333333333  /

============
===DEVICES=

::::::::::::::::::::FIRE THERMOCOUPLES::::::::::::::::::::::::::

&DEVC  ID='FireTC       1       ',  XYZ=  10.5 , 1.3 , 2      , QUANTITY='THERMOCOUPLE'/
&DEVC  ID='FireTC       2       ',  XYZ=  10.5 , 1.3 , 1.85   , QUANTITY='THERMOCOUPLE'/
&DEVC  ID='FireTC       3       ',  XYZ=  10.5 , 1.3 , 1.6    , QUANTITY='THERMOCOUPLE'/
&DEVC  ID='FireTC       4       ',  XYZ=  10.5 , 1.3 , 1.35   , QUANTITY='THERMOCOUPLE'/
```

```
&DEVC ID='FireTC        5       ',  XYZ=  10.5 , 1.3 , 1.1    , QUANTITY='THERMOCOUPLE'/
&DEVC ID='FireTC        6       ',  XYZ=  10.5 , 1.3 , 0.7    , QUANTITY='THERMOCOUPLE'/
::::::::::::::::::DOOR THERMOCOUPLES::::::::::::::::::::

&DEVC ID='DoorTC        1       ',  XYZ=  9.9  , 4.3 , 2      , QUANTITY='THERMOCOUPLE'/
&DEVC ID='DoorTC        2       ',  XYZ=  9.9  , 4.3 , 1.85   , QUANTITY='THERMOCOUPLE'/
&DEVC ID='DoorTC        3       ',  XYZ=  9.9  , 4.3 , 1.6    , QUANTITY='THERMOCOUPLE'/
&DEVC ID='DoorTC        4       ',  XYZ=  9.9  , 4.3 , 1.35   , QUANTITY='THERMOCOUPLE'/
&DEVC ID='DoorTC        5       ',  XYZ=  9.9  , 4.3 , 1.1    , QUANTITY='THERMOCOUPLE'/
&DEVC ID='DoorTC        6       ',  XYZ=  9.9  , 4.3 , 0.7    , QUANTITY='THERMOCOUPLE'/
::::::::::::::::::CORRIDOR B THERMOCOUPLES::::::::::::::::::::

&DEVC ID='CorridorBTC 1         ',  XYZ=  9.9  , 4.9 , 2      , QUANTITY='THERMOCOUPLE'/
&DEVC ID='CorridorBTC 2         ',  XYZ=  9.9  , 4.9 , 1.85   , QUANTITY='THERMOCOUPLE'/
&DEVC ID='CorridorBTC 3         ',  XYZ=  9.9  , 4.9 , 1.6    , QUANTITY='THERMOCOUPLE'/
&DEVC ID='CorridorBTC 4         ',  XYZ=  9.9  , 4.9 , 1.35   , QUANTITY='THERMOCOUPLE'/
&DEVC ID='CorridorBTC 5         ',  XYZ=  9.9  , 4.9 , 1.1    , QUANTITY='THERMOCOUPLE'/
&DEVC ID='CorridorBTC 6         ',  XYZ=  9.9  , 4.9 , 0.7    , QUANTITY='THERMOCOUPLE'/
::::::::::::::::::CORRIDOR A THERMOCOUPLES::::::::::::::::::::

&DEVC ID='CorridorATC 1         ',  XYZ=  4.9  , 4.9 , 2      , QUANTITY='THERMOCOUPLE'/
&DEVC ID='CorridorATC 2         ',  XYZ=  4.9  , 4.9 , 1.85   , QUANTITY='THERMOCOUPLE'/
&DEVC ID='CorridorATC 3         ',  XYZ=  4.9  , 4.9 , 1.6    , QUANTITY='THERMOCOUPLE'/
&DEVC ID='CorridorATC 4         ',  XYZ=  4.9  , 4.9 , 1.35   , QUANTITY='THERMOCOUPLE'/
&DEVC ID='CorridorATC 5         ',  XYZ=  4.9  , 4.9 , 1.1    , QUANTITY='THERMOCOUPLE'/
&DEVC ID='CorridorATC 6         ',  XYZ=  4.9  , 4.9 , 0.7    , QUANTITY='THERMOCOUPLE'/
::::::::::::::::::CORRIDOR C THERMOCOUPLES::::::::::::::::::::

&DEVC ID='CorridorCTC 1         ',  XYZ=  19.9 , 4.9 , 2      , QUANTITY='THERMOCOUPLE'/
&DEVC ID='CorridorCTC 2         ',  XYZ=  19.9 , 4.9 , 1.85   , QUANTITY='THERMOCOUPLE'/
&DEVC ID='CorridorCTC 3         ',  XYZ=  19.9 , 4.9 , 1.6    , QUANTITY='THERMOCOUPLE'/
&DEVC ID='CorridorCTC 4         ',  XYZ=  19.9 , 4.9 , 1.35   , QUANTITY='THERMOCOUPLE'/
&DEVC ID='CorridorCTC 5         ',  XYZ=  19.9 , 4.9 , 1.1    , QUANTITY='THERMOCOUPLE'/
&DEVC ID='CorridorCTC 6         ',  XYZ=  19.9 , 4.9 , 0.7    , QUANTITY='THERMOCOUPLE'/
::::::::::::::::DOOR VELOCITY::::::::::::::::::::
&DEVC ID='DoorVelo      1       ',  XYZ=  9.9  , 4.3 , 2      , QUANTITY='V-VELOCITY'       /
&DEVC ID='DoorVelo      2       ',  XYZ=  9.9  , 4.3 , 1.85   , QUANTITY='V-VELOCITY'       /
&DEVC ID='DoorVelo      3       ',  XYZ=  9.9  , 4.3 , 1.6    , QUANTITY='V-VELOCITY'       /
&DEVC ID='DoorVelo      4       ',  XYZ=  9.9  , 4.3 , 1.35   , QUANTITY='V-VELOCITY'       /
&DEVC ID='DoorVelo      5       ',  XYZ=  9.9  , 4.3 , 1.1    , QUANTITY='V-VELOCITY'       /
&DEVC ID='DoorVelo      6       ',  XYZ=  9.9  , 4.3 , 0.7    , QUANTITY='V-VELOCITY'       /
::::::::::::::::::CORRIDOR A VELOCITY::::::::::::::::::::

&DEVC ID='CorridorAVelo   1     ',  XYZ=  4.9  , 4.9 , 2      , QUANTITY='U-VELOCITY'       /
&DEVC ID='CorridorAVelo   2     ',  XYZ=  4.9  , 4.9 , 1.85   , QUANTITY='U-VELOCITY'       /
&DEVC ID='CorridorAVelo   3     ',  XYZ=  4.9  , 4.9 , 1.6    , QUANTITY='U-VELOCITY'       /
&DEVC ID='CorridorAVelo   4     ',  XYZ=  4.9  , 4.9 , 1.35   , QUANTITY='U-VELOCITY'       /
&DEVC ID='CorridorAVelo   5     ',  XYZ=  4.9  , 4.9 , 1.1    , QUANTITY='U-VELOCITY'       /
&DEVC ID='CorridorAVelo   6     ',  XYZ=  4.9  , 4.9 , 0.7    , QUANTITY='U-VELOCITY'       /
::::::::::::::::::CORRIDOR C VELOCITY::::::::::::::::::::
                                                          /
&DEVC ID='CorridorCTVelo  1     ',  XYZ=  18   , 4.9 , 2      , QUANTITY='U-VELOCITY'       /
&DEVC ID='CorridorCTVelo  2     ',  XYZ=  19.9 , 4.9 , 1.85   , QUANTITY='U-VELOCITY'       /
&DEVC ID='CorridorCTVelo  3     ',  XYZ=  19.9 , 4.9 , 1.6    , QUANTITY='U-VELOCITY'       /
&DEVC ID='CorridorCTVelo  4     ',  XYZ=  19.9 , 4.9 , 1.35   , QUANTITY='U-VELOCITY'       /
&DEVC ID='CorridorCTVelo  5     ',  XYZ=  19.9 , 4.9 , 1.1    , QUANTITY='U-VELOCITY'       /
&DEVC ID='CorridorCTVelo  6     ',  XYZ=  19.9 , 4.9 , 0.7    , QUANTITY='U-VELOCITY'       /
::::::::::::::::::ADJACENT ROOM A::::::::::::::::::::::::
```

```
-Wall-
&DEVC ID='ADROOMAW1_TC  ',  XYZ=  8.9  , 2.1 , 2      , QUANTITY='THERMOCOUPLE'/
&DEVC ID='ADROOMAW2_TC  ',  XYZ=  8.9  , 2.1 , 1.85   , QUANTITY='THERMOCOUPLE'/
&DEVC ID='ADROOMAW3_TC  ',  XYZ=  8.9  , 2.1 , 1.6    , QUANTITY='THERMOCOUPLE'/
&DEVC ID='ADROOMAW4_TC  ',  XYZ=  8.9  , 2.1 , 1.35   , QUANTITY='THERMOCOUPLE'/
&DEVC ID='ADROOMAW5_TC  ',  XYZ=  8.9  , 2.1 , 1.1    , QUANTITY='THERMOCOUPLE'/
&DEVC ID='ADROOMAW6_TC  ',  XYZ=  8.9  , 2.1 , 0.7    , QUANTITY='THERMOCOUPLE'/
-Center-
&DEVC ID='ADROOMAC1_TC  ',  XYZ=  7.5  , 2.1 , 2      , QUANTITY='THERMOCOUPLE'/
&DEVC ID='ADROOMAC2_TC  ',  XYZ=  7.5  , 2.1 , 1.85   , QUANTITY='THERMOCOUPLE'/
&DEVC ID='ADROOMAC3_TC  ',  XYZ=  7.5  , 2.1 , 1.6    , QUANTITY='THERMOCOUPLE'/
&DEVC ID='ADROOMAC4_TC  ',  XYZ=  7.5  , 2.1 , 1.35   , QUANTITY='THERMOCOUPLE'/
&DEVC ID='ADROOMAC5_TC  ',  XYZ=  7.5  , 2.1 , 1.1    , QUANTITY='THERMOCOUPLE'/
&DEVC ID='ADROOMAC6_TC  ',  XYZ=  7.5  , 2.1 , 0.7    , QUANTITY='THERMOCOUPLE'/
::::::::::::::::::ADJACENT ROOM B::::::::::::::::::::::::::::

-Wall
&DEVC ID='ADROOMBW1_TC  ',  XYZ=  12.1 , 2.1 , 2      , QUANTITY='THERMOCOUPLE'/
&DEVC ID='ADROOMBW2_TC  ',  XYZ=  12.1 , 2.1 , 1.85   , QUANTITY='THERMOCOUPLE'/
&DEVC ID='ADROOMBW3_TC  ',  XYZ=  12.1 , 2.1 , 1.6    , QUANTITY='THERMOCOUPLE'/
&DEVC ID='ADROOMBW4_TC  ',  XYZ=  12.1 , 2.1 , 1.35   , QUANTITY='THERMOCOUPLE'/
&DEVC ID='ADROOMBW5_TC  ',  XYZ=  12.1 , 2.1 , 1.1    , QUANTITY='THERMOCOUPLE'/
&DEVC ID='ADROOMBW6_TC  ',  XYZ=  12.1 , 2.1 , 0.7    , QUANTITY='THERMOCOUPLE'/
-Center-
&DEVC ID='ADROOMBC1_TC  ',  XYZ=  13.5 , 2.1 , 2      , QUANTITY='THERMOCOUPLE'/
&DEVC ID='ADROOMBC2_TC  ',  XYZ=  13.5 , 2.1 , 1.85   , QUANTITY='THERMOCOUPLE'/
&DEVC ID='ADROOMBC3_TC  ',  XYZ=  13.5 , 2.1 , 1.6    , QUANTITY='THERMOCOUPLE'/
&DEVC ID='ADROOMBC4_TC  ',  XYZ=  13.5 , 2.1 , 1.35   , QUANTITY='THERMOCOUPLE'/
&DEVC ID='ADROOMBC5_TC  ',  XYZ=  13.5 , 2.1 , 1.1    , QUANTITY='THERMOCOUPLE'/
&DEVC ID='ADROOMBC6_TC  ',  XYZ=  13.5 , 2.1 , 0.7    , QUANTITY='THERMOCOUPLE'/
::::::::::::SECOND FLOOR::::::
&DEVC ID='SecFloor1_TC',    XYZ=    10.5 , 2.1 , 4.7    , QUANTITY='THERMOCOUPLE'/
&DEVC ID='SecFloor2_TC',    XYZ=    10.5 , 2.1 , 4.55   , QUANTITY='THERMOCOUPLE'/
&DEVC ID='SecFloor3_TC',    XYZ=    10.5 , 2.1 , 4.3    , QUANTITY='THERMOCOUPLE'/
&DEVC ID='SecFloor4_TC',    XYZ=    10.5 , 2.1 , 4.05   , QUANTITY='THERMOCOUPLE'/
&DEVC ID='SecFloor5_TC',    XYZ=    10.5 , 2.1 , 3.8    , QUANTITY='THERMOCOUPLE'/
&DEVC ID='SecFloor6_TC',    XYZ=    10.5 , 2.1 , 3.4    , QUANTITY='THERMOCOUPLE'/
-
&DEVC ID='SecFloor7_TC',    XYZ=    10.5 , 2.1 , 2.8    , QUANTITY='THERMOCOUPLE'/
&DEVC ID='SecFloor8_TC',    XYZ=    10.5 , 2.1 , 3.0    , QUANTITY='THERMOCOUPLE'/
&DEVC ID='SecFloor9_TC',    XYZ=    10.5 , 2.1 , 3.2    , QUANTITY='THERMOCOUPLE'/
::::::::::::::::::ADJACENT ROOM C- over the corridor::::::::::::::::::::::::::::

-Wall
&DEVC ID='ADROOMC1_TC   ',  XYZ=  11.1 , 5.6 , 2      , QUANTITY='THERMOCOUPLE'/
&DEVC ID='ADROOMC2_TC   ',  XYZ=  11.1 , 5.6 , 1.85   , QUANTITY='THERMOCOUPLE'/
&DEVC ID='ADROOMC3_TC   ',  XYZ=  11.1 , 5.6 , 1.6    , QUANTITY='THERMOCOUPLE'/
&DEVC ID='ADROOMC4_TC   ',  XYZ=  11.1 , 5.6 , 1.35   , QUANTITY='THERMOCOUPLE'/
&DEVC ID='ADROOMC5_TC   ',  XYZ=  11.1 , 5.6 , 1.1    , QUANTITY='THERMOCOUPLE'/
&DEVC ID='ADROOMC6_TC   ',  XYZ=  11.1 , 5.6 , 0.7    , QUANTITY='THERMOCOUPLE'/


============
SLiceFiles==

&SLCF PBY=4.9, QUANTITY='U-VELOCITY'/
&SLCF PBY=4.9, QUANTITY='TEMPERATURE'/
&SLCF PBX=10.5, QUANTITY='V-VELOCITY'/
```

```
&SLCF PBX=10.5, QUANTITY='TEMPERATURE'/
&SLCF PBY=1.3, QUANTITY='TEMPERATURE'/
&SLCF PBY=1.3, QUANTITY='U-VELOCITY'/
&SLCF PBZ=1.81, QUANTITY='TEMPERATURE'/
&SLCF PBZ=9.9, QUANTITY='VISIBILITY'/
&SLCF PBZ=10.5, QUANTITY='VISIBILITY'/
&SLCF PBZ=5.2, QUANTITY='VISIBILITY'/
&SLCF PBZ=15.8, QUANTITY='VISIBILITY'/
&SLCF PBY=4.9, QUANTITY='VISIBILITY'/
&SLCF PBY=-0.1, QUANTITY='TEMPERATURE'/
&SLCF PBY=-0.1, QUANTITY='VELOCITY'/
==============
RADIATION=====
&RADI RADIATIVE_FRACTION=0.262/

==================
BOUNDARY FILES====
&BNDF QUANTITY='INCIDENT HEAT FLUX'/
&BNDF QUANTITY='WALL TEMPERATURE'/

=============
MISC========

&MISC TMPA=20, BNDF_DEFAULT=.FALSE./

&TAIL/
```

Appendix B: Material data

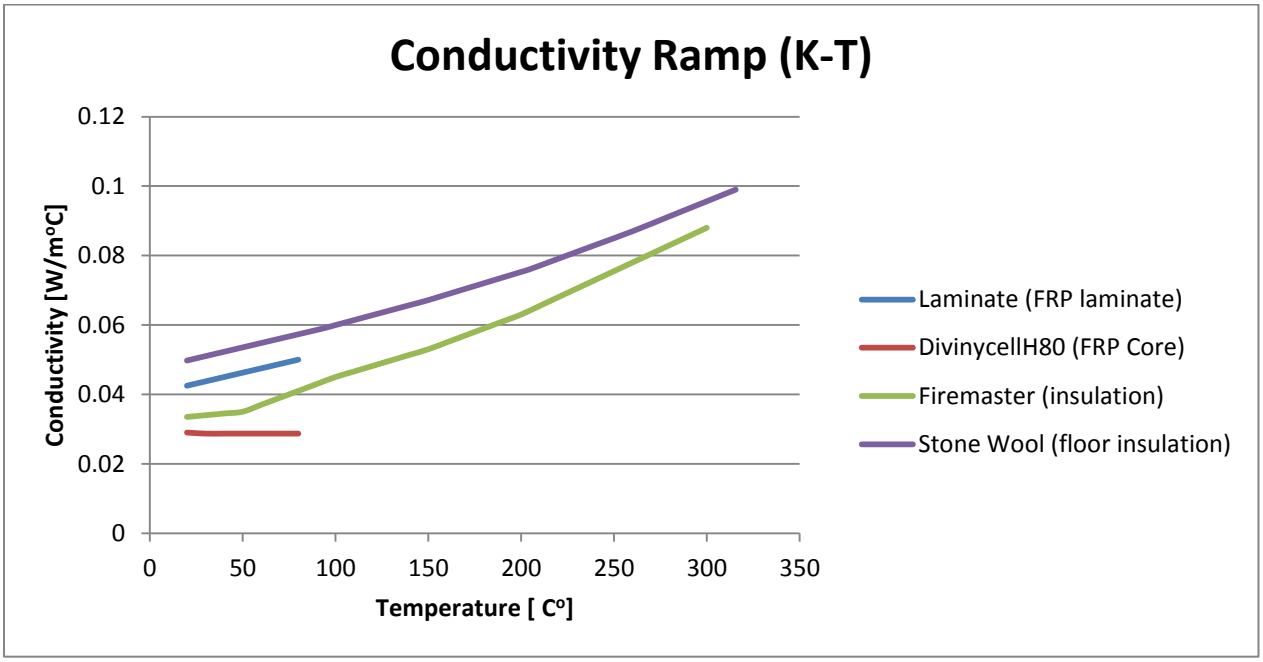

Figure B.1. Ramp for conductivity for non-metal materials.

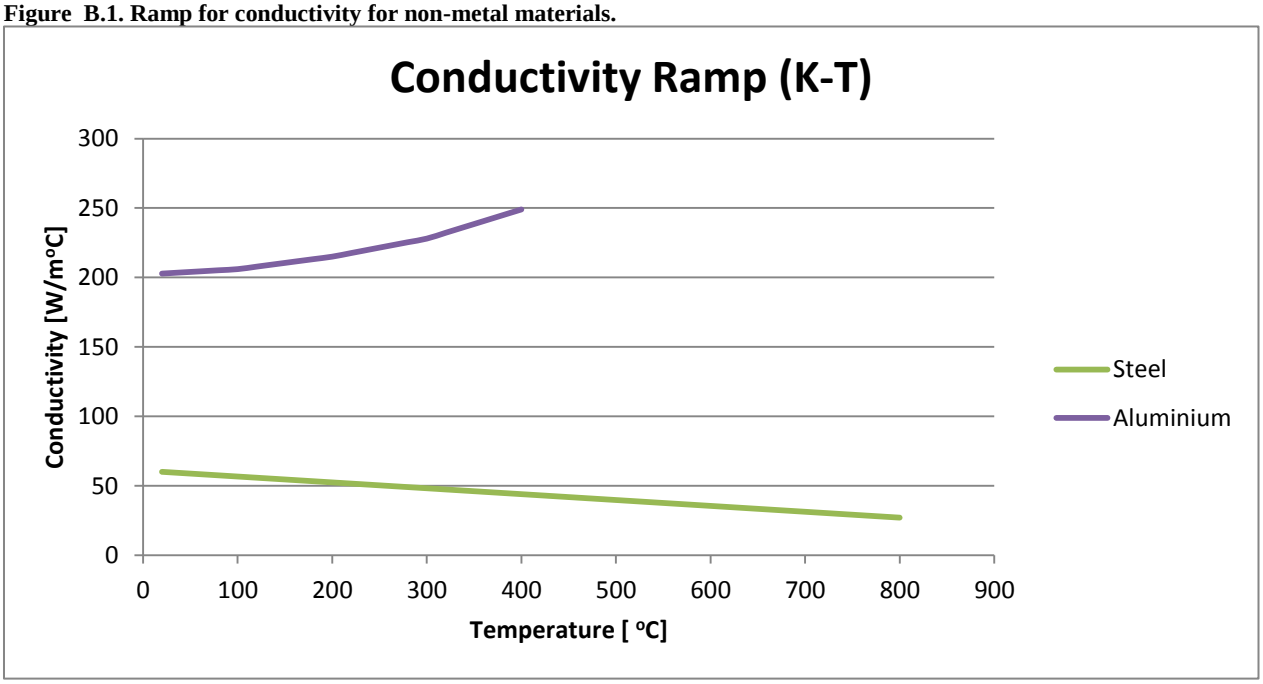

Figure B.2. Ramp for conductivity for metal materials.

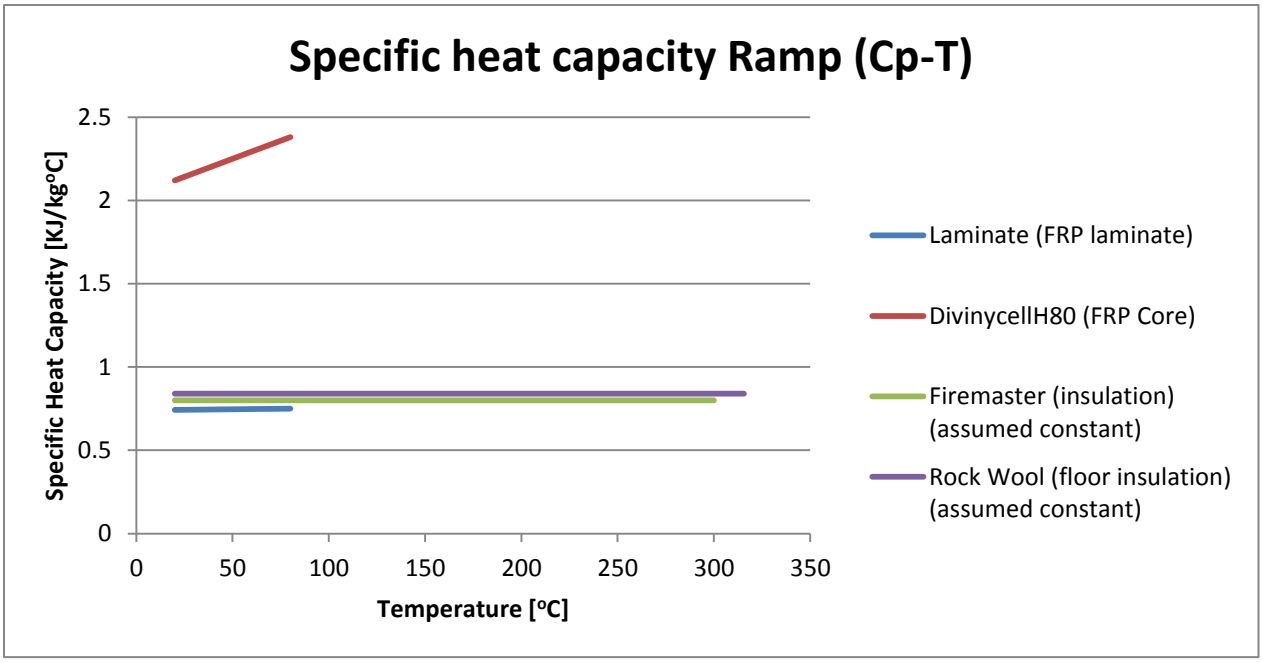

Figure B.3. Ramp for specific heat capacity for non-metal materials.

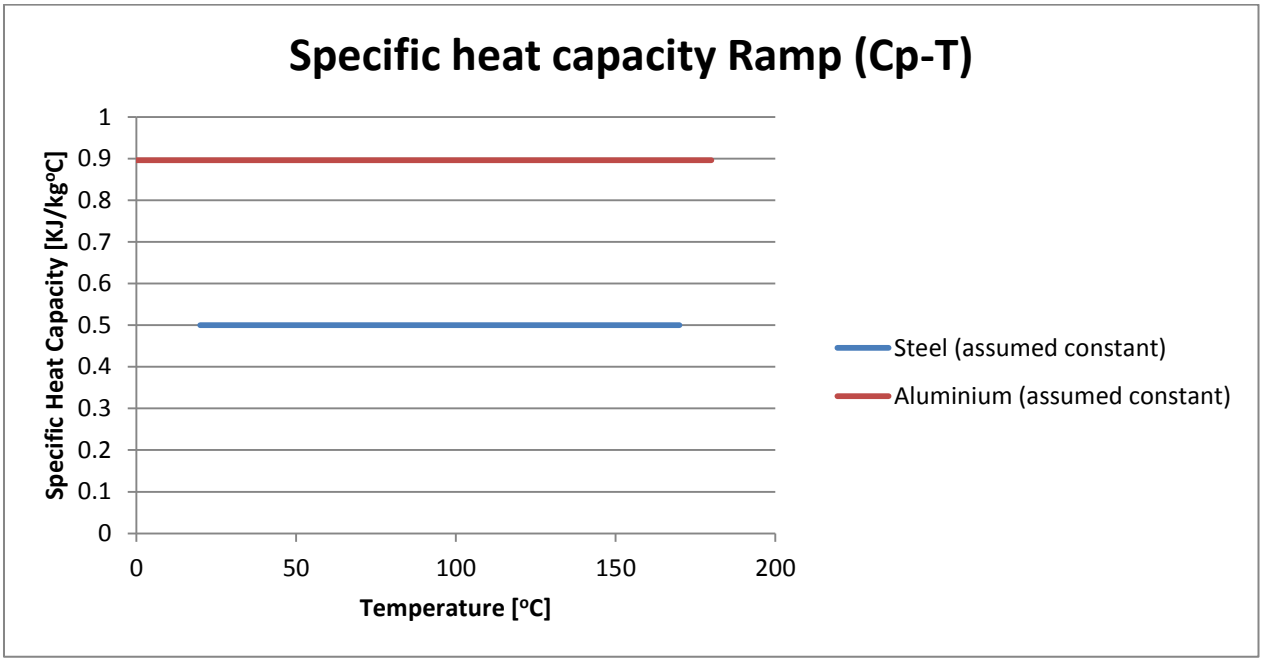

Figure B.4. Ramp (constant) for specific heat capacity for metal materials.

Table B.1. Density used for materials.

Material	Density [kg/m^3]
Laminate (on FRP wall)	1870
DivinycellH80 (FRP wall core)	80
Firemaster insulation	100
Steel	7850
Aluminium	2707
Rockwool insulation	190

Table B.2. References for presented material properties.

Material	Density reference	Specific heat capacity reference	Conductivity reference
Laminate (on FRP wall)	(Tuovinen & Hertzberg, 2009)	(Tuovinen & Hertzberg, 2009)	(Tuovinen & Hertzberg, 2009)
DivinycellH80 (FRP wall core)	(Tuovinen & Hertzberg, 2009)	(Tuovinen & Hertzberg, 2009)	(Tuovinen & Hertzberg, 2009)
Firemaster insulation	(Tuovinen & Hertzberg, 2009)	(Tuovinen & Hertzberg, 2009)	(Tuovinen & Hertzberg, 2009)
Steel	(Tuovinen & Hertzberg, 2009)	(Tuovinen & Hertzberg, 2009)	(Tuovinen & Hertzberg, 2009)
Aluminium	Table B-1 in (Eckert & Drake, 1987)	Table B-1 in (Eckert & Drake, 1987)	Table B-1 in (Eckert & Drake, 1987)
Rockwool insulation (Mineral wool)	(Hens, 2012, p.xxi)	(Hens, 2012, p.xxi)	(Engineering Toolbox, 2014)

Appendix C: Backing exposed

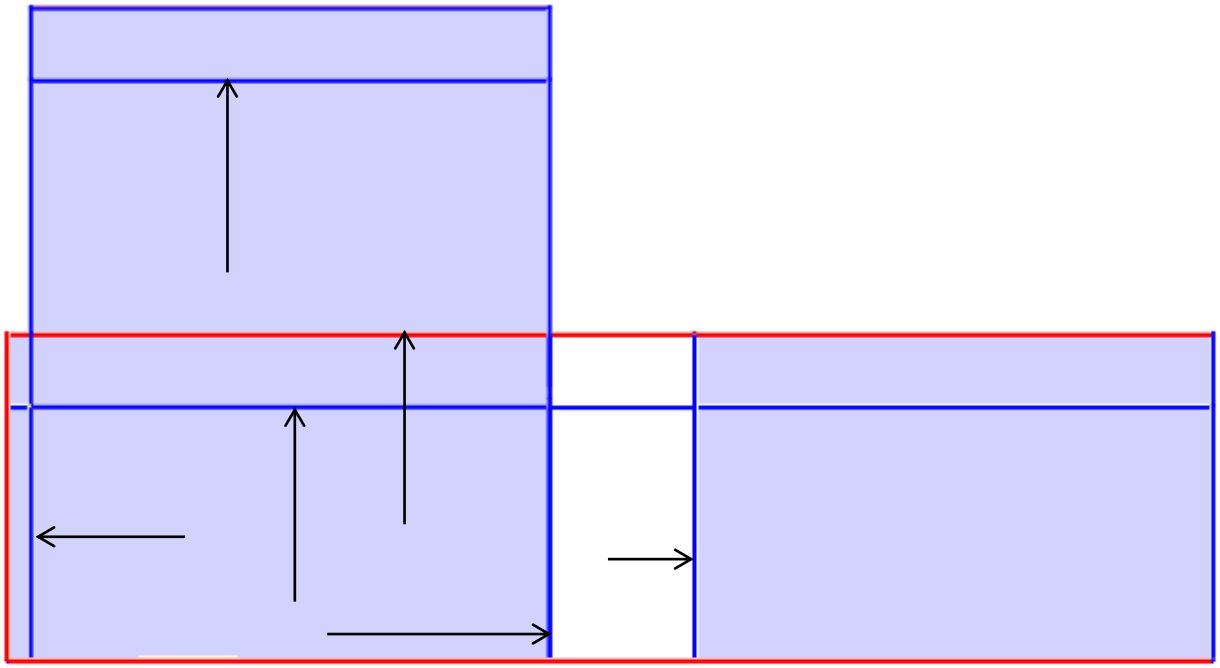

Figure C.1. Constructions with backing exposed are marked with black arrows. 2D view from side.

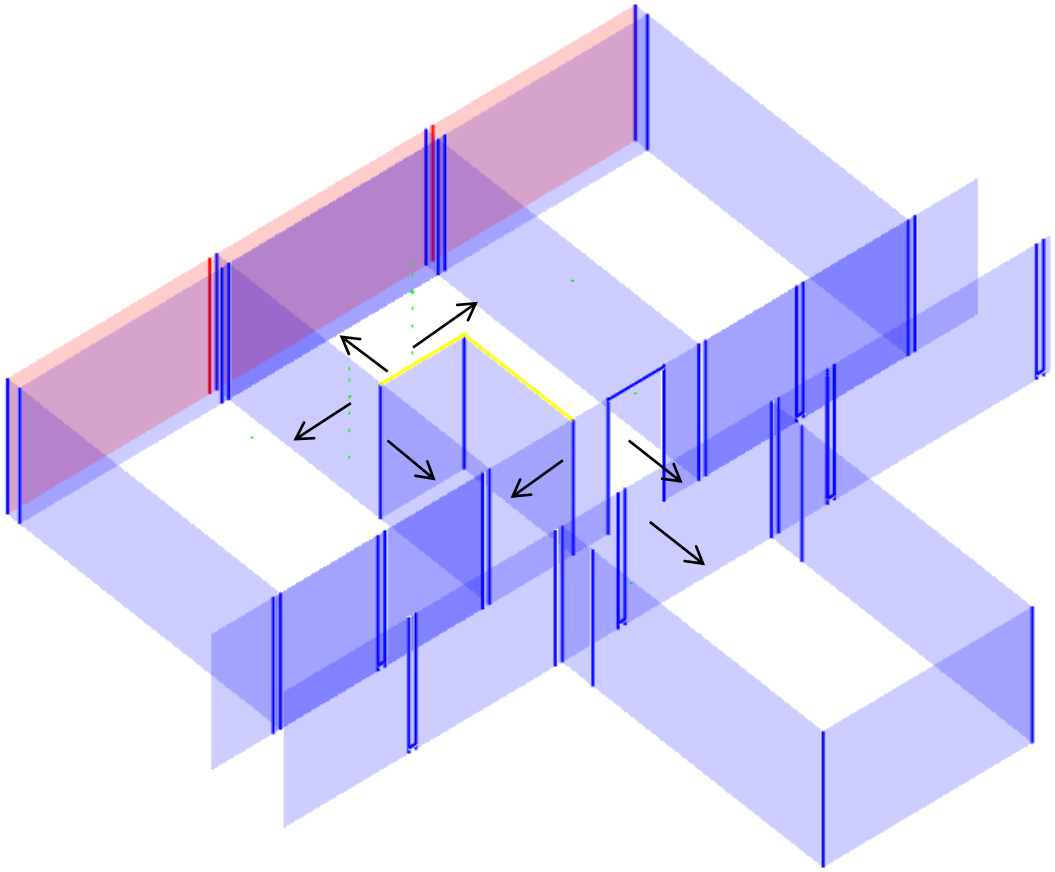

Figure C.2. Constructions with backing exposed are marked with black arrows. 3D view, parts of the geometry are cut off .

Appendix D: Fire input data

Table D.1. Assumed material leading to values for soot yield, given materials from experiment by Arvidson et al. (2008).

Items of interior *	Combustible mass [kg] *	Material	y_s	Weighted y_s
Walls (PVC foil)	6,1	PVC	0,172±	0,006582
Ceiling (PVC foil)	2,8	PVC	0,172±	0,003021
Floor (PVC carpet)	38,1	PVC flooring	0,028+	0,006693
Foam mattresses	6,4	PU	0,230#	0,009235
Spring mattresses	13,4	POLYESTER	0,090±	0,007566
Bedding mattresses	5,9	POLYESTER	0,090±	0,003331
Sheets	2,1	POLYESTER	0,090±	0,001186
Quilts	5	PE FOAMS	0,100±	0,003137
Quilt cases	2,5	POLYESTER	0,090±	0,001412
Pillows	2,3	PE FOAMS	0,100±	0,001443
Pillow cases	0,3	POLYESTER	0,090±	0,000169
Chair	1,5	WOOD	0,015#	0,000141
Table	14,4	WOOD	0,015#	0,001355
Hat rack	1	WOOD	0,015#	9,41E-05
Decorative bars	3,7	WOOD	0,015#	0,000348
Coats	4,6	POLYESTER	0,090±	0,002597
Large suitcases (PE)	12,2	PE	0,060±	0,004592
Medium suitcases (PE)	9,8	PE	0,060±	0,003689
Large suitcases (Clothes)	16	POLYESTER	0,090±	0,009034
Medium suitcases (Clothes)	11,3	COTTON (CELLULOSA)	0,025ɜ	0,001772
Σ	**159,4**			**0,067397**

* (Arvidson et al., 2008).

± Values from table 3-4.14 (Tewardson, 2002).

\+ Value from (Wade, 2001).

\# Values from table 9.2 (Karlsson & Quintiere, 2000).

ɜ Value from table 7 (Robbins & Wade, 2007).

Table D.2. Assumed materials leading to values for heat of combustion, and radiative fraction.

Material	Mass [kg]	ΔH_c [kJ/kg]	Weighted ΔH_c [kJ/kg]	ΔH_{rad} [kJ/kg]	χ_r	Weighted χ_r
PVC	8,9	16400+	916	2600+	0,16	0,009
PVC (flooring)	38,1	16400+	3920	2600+	0,16	0,038
PU (GM23)	6,4	27200+	1092	8700+	0,32	0,013
POLYESTER	44,8	32500+	9134	9800+	0,30	0,085
PE FOAM	7,3	40800+	1869	15500+	0,38	0,017
WOOD	20,6	17700+	2287	4600+	0,26	0,034
PE	22,0	43600+	6018	16600+	0,38	0,053
COTTON	11,3	16090±	1141	-	0,20*	0,014
	159,4		**26376**			**0,262**

* Assumed value, since most materials range from 0.1-0.4 for fuels with low soot production (Drysdale, 2011).

± Value from table 1.13 (Drysdale, 2011).

\+ Values from table 3-4.14 (Tewardson, 2002).

Table D.3. Assumed materials leading to coefficiencts of C, H, O and N.

Material	Combustible mass [kg]	Coefficients*				Weighted Coefficients			
		C	H	O	N	C	H	O	N
PVC	8.9	1	1.5	0	0	1	0.084	0	0
PVC flooring (PVC)	38.1	1	1.5	0	0	1	0.359	0	0
PU (GM23)	6.4	1	1.8	0.35	0.06	1	0.072	0.014	0.002
POLYESTER	44.8	1	1.4	0.22	0	1	0.393	0.062	0
POLYETHYLENE FOAMS±	7.3	1	2	0	0	1	0.092	0	0
WOOD+	20.6	1	1.7	0.72	0	1	0.22	0.093	0
PE	22	1	2	0	0	1	0.276	0	0
COTTON+	11.3	1	1.7	0.72	0	1	0.121	0.051	0
Σ	**159.4**					**1**	**1.6**	**0.2**	**0.002**

* Values in column from table 3-4.13 (Tewardson, 2002).

± Material assumed equal to "PE" in table 3-4.13 (Tewardson, 2002)

+ Material assumed equal to "red oak" in table 3-4.13 (Tewardson, 2002)

Table D.4. Assumed material leading to values for CO-yield.

Material	Combustible mass	y_{co}*	Weighted y_{co}
PVC	8.9	0.063	0.003518
PVC flooring (PVC)	38.1	0.063	0.015058
PU (GM23)	6.4	0.031	0.001245
POLYESTER	44.8	0.07	0.019674
POLYETHYLENE FOAMS	7.3	0.026	0.001191
WOOD	20.6	0.004	0.000517
PE	22	0.024	0.003312
COTTON	11.3	0.004	0.000284
Σ	**159.4**		**0.045**

* Values in column from table 3-4.14 (Tewardson, 2002).

Appendix E: FDS5 and FDS6 comparison

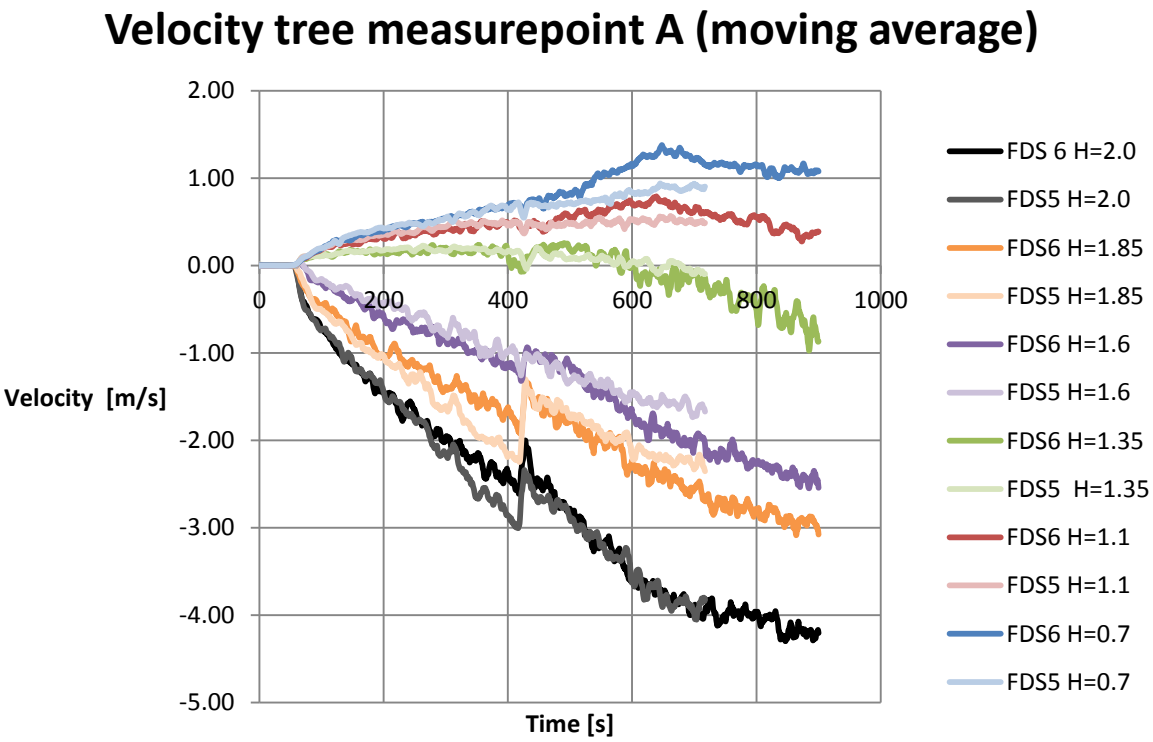

Figure E.1. Transient velocity output in measure point A from FDS 5 and FDS 6.

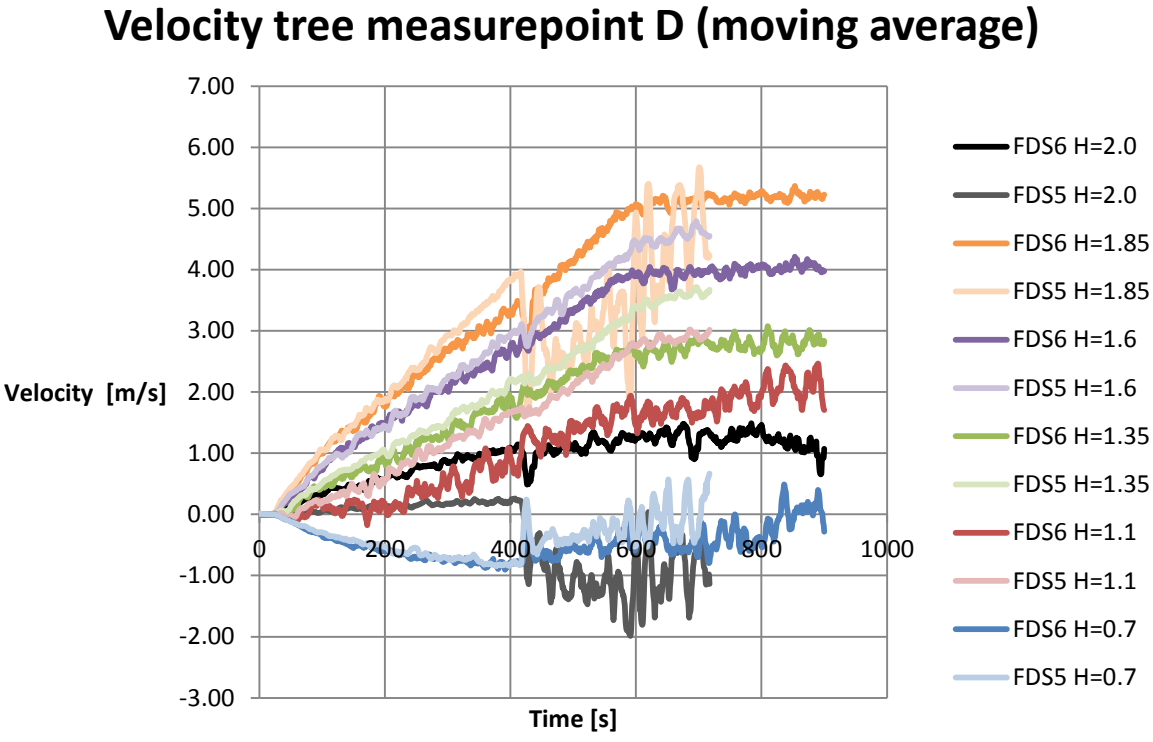

Figure E.2. Transient velocity output in measure point D from FDS 5 and FDS 6.

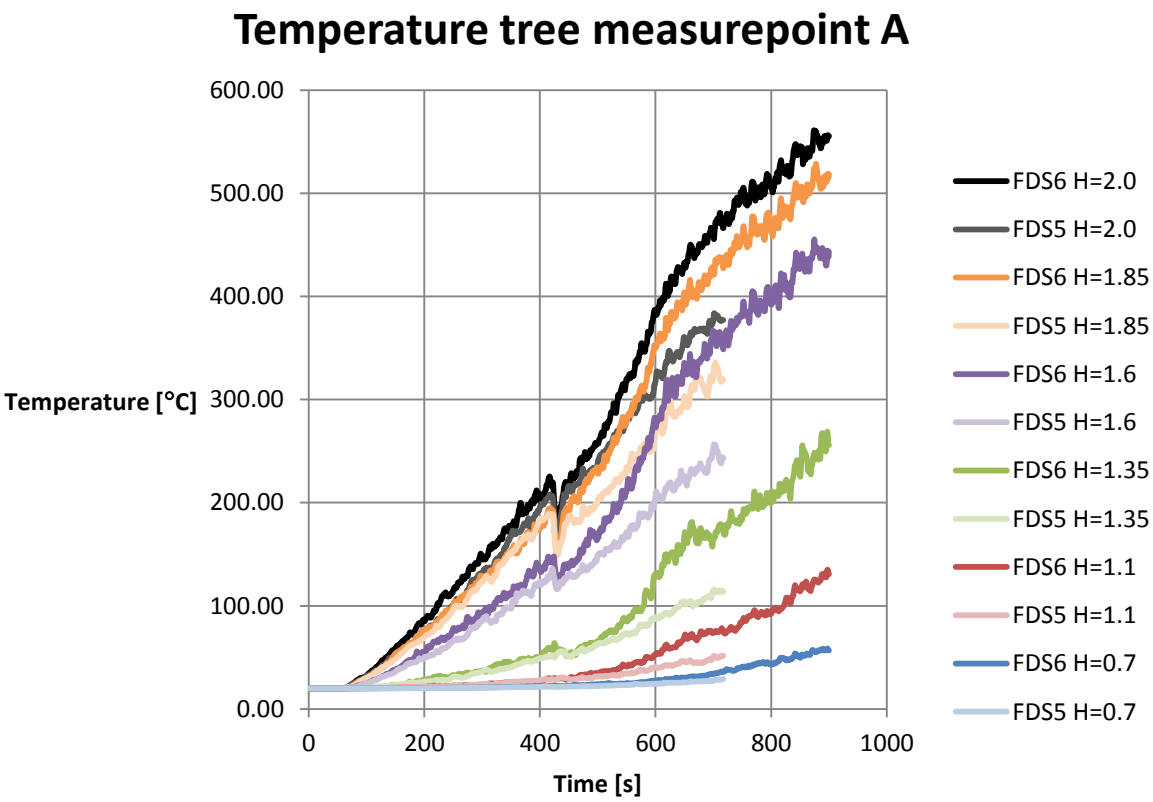

Figure E.3. Transient temperature output in measure point A from FDS 5 and FDS 6.

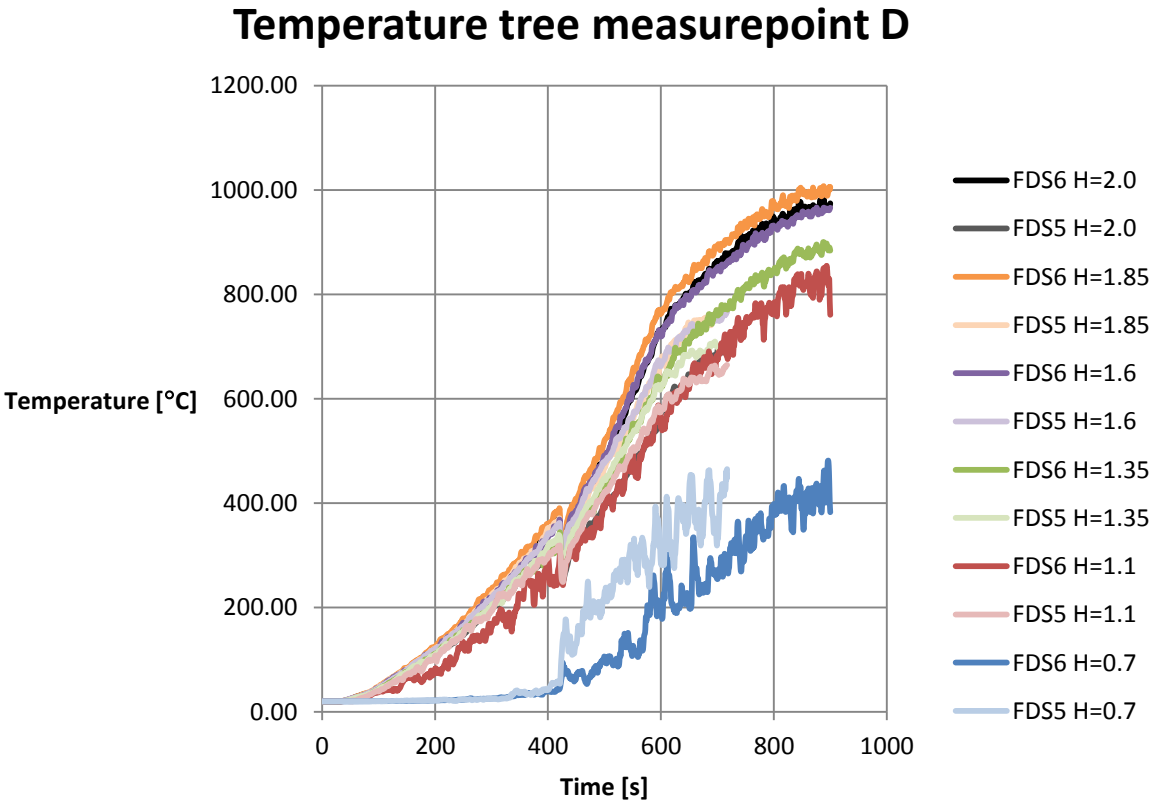

Figure E.4. Transient velocity output in measure point D from FDS 5 and FDS 6.

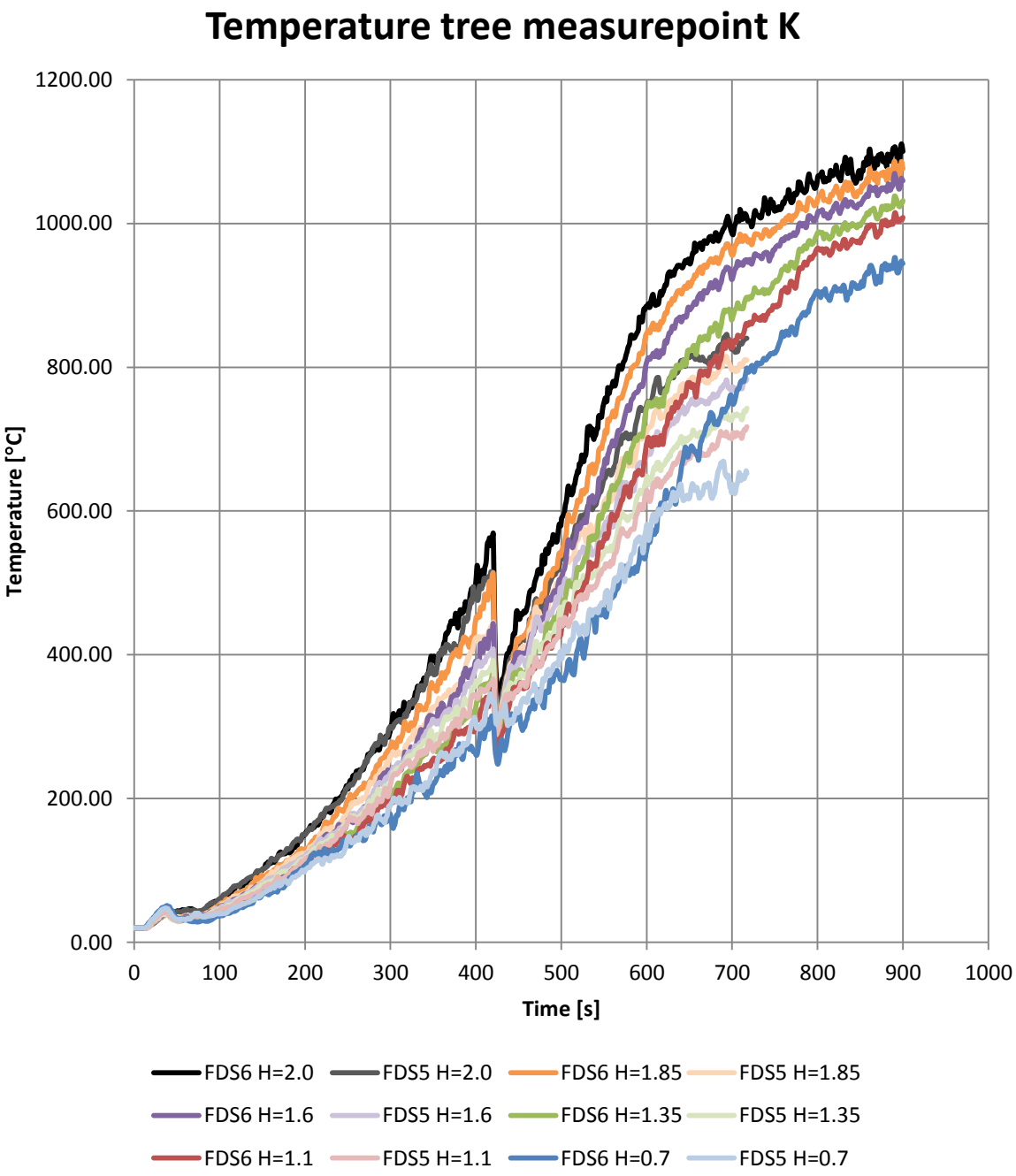

Figure E.5. Transient temperature output in measure point K from FDS 5 and FDS 6.

Appendix F: Grid independence

This appendix is divided into several sections in order to make the observations from the different device trees distinguishable.

Velocity probe tree in point D

All graph lines from the medium case, except the ones for the lowest point (0.7 m), follow the fine case well. The lines from the lowest device point have a good fit regarding magnitude and shape until approximately 430 seconds. After this time it is possible to distinguish a better fit between the coarse and fine cases than in the medium and fine cases. See graphs in Figure F.1 - Figure F.6.

Thermocouple tree in point D

All lines have a similar shape, except by the lowest device point. At this point (0.7 m) the fine case reaches higher temperatures earlier than the other two cases. The magnitudes for devices placed at 2 m are more similar for the coarse and fine cases than for the medium and fine cases. However, for devices at heights 1.85-1.1 m the medium is a better fit. For devices at heights 1.85-0.7 m following observations are made:

- The temperatures for the medium case differentiate 0-50 °C from the fine cases, except in the lowest point (0.7 m) where the difference is several hundred degrees.
- The temperatures from the coarse case differentiate 50-150°C from the fine case, except in the lowest point (0.7 m) where the difference is several hundred degrees.

See graphs in Figure F.7 - Figure F.12.

Profiles in point D

The temperature and velocity profiles for trees point A can be seen in Figure F.13 and Figure F.14. What can be observed is that the velocity profiles for the medium and fine cases have a good fit, whereas the temperature profiles are more deviating. The temperatures for highest and lowest devices differentiate about 150°C respectively 400°C for medium and fine temperatures. For the rest of the heights, the differences are in the vicinity of 30-100°C.

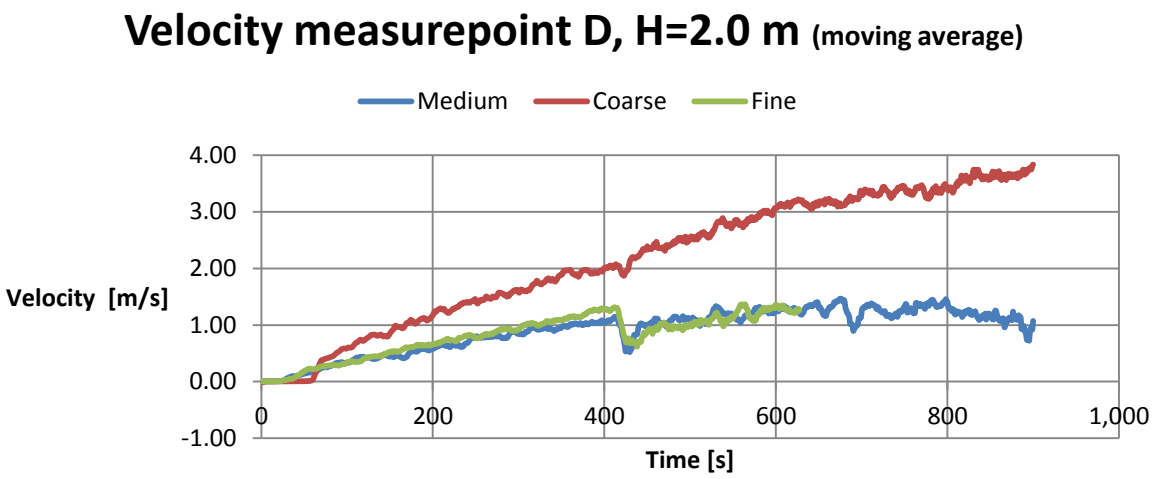

Figure F.1. Velocity in measurepoint D, H=2.0 m.

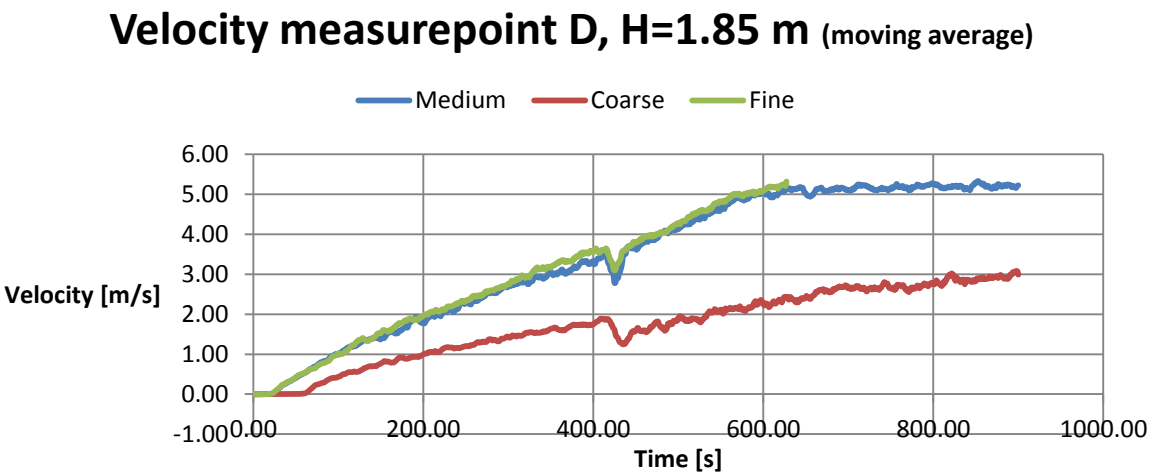

Figure F.2. Velocity in measurepoint D, H=1.85 m.

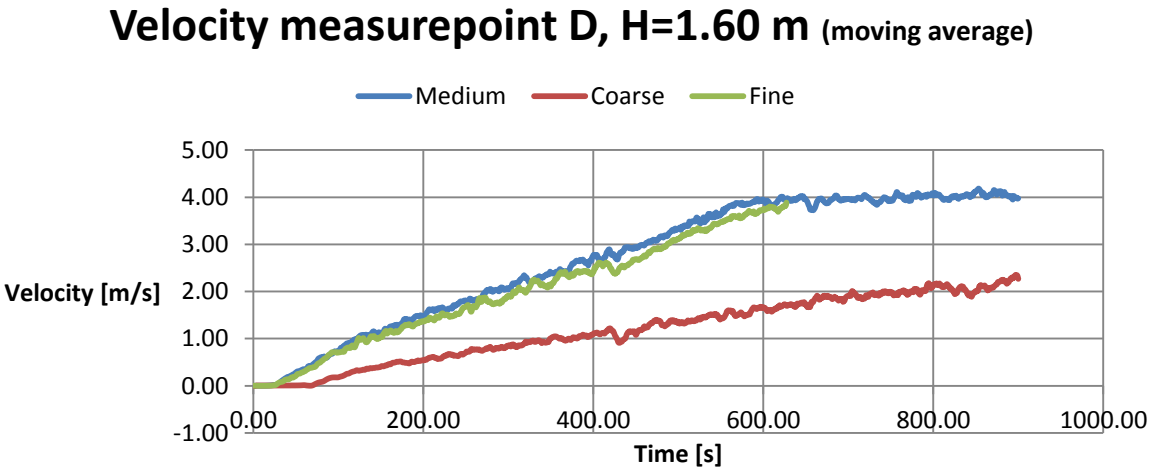

Figure F.3. Velocity in measurepoint D, H=1.60 m.

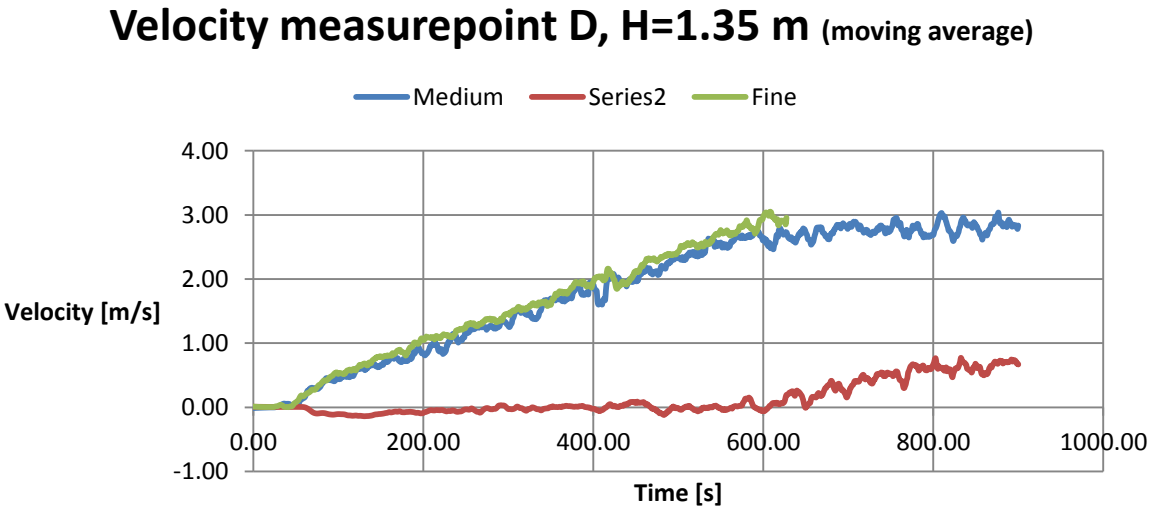

Figure F.4. Velocity in measurepoint D, H=1.35 m.

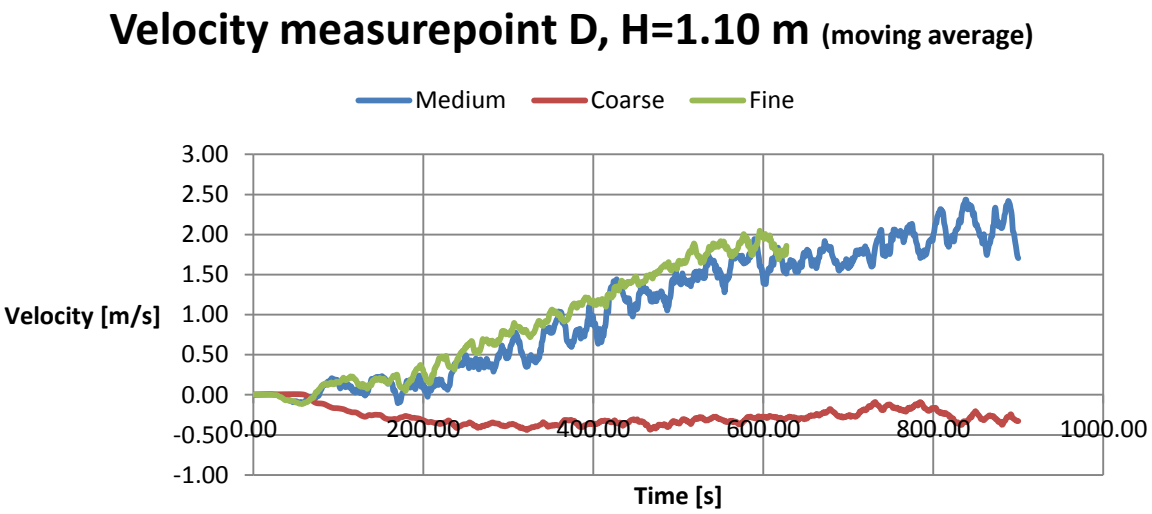

Figure F.5. Velocity in measurepoint D, H=1.10 m.

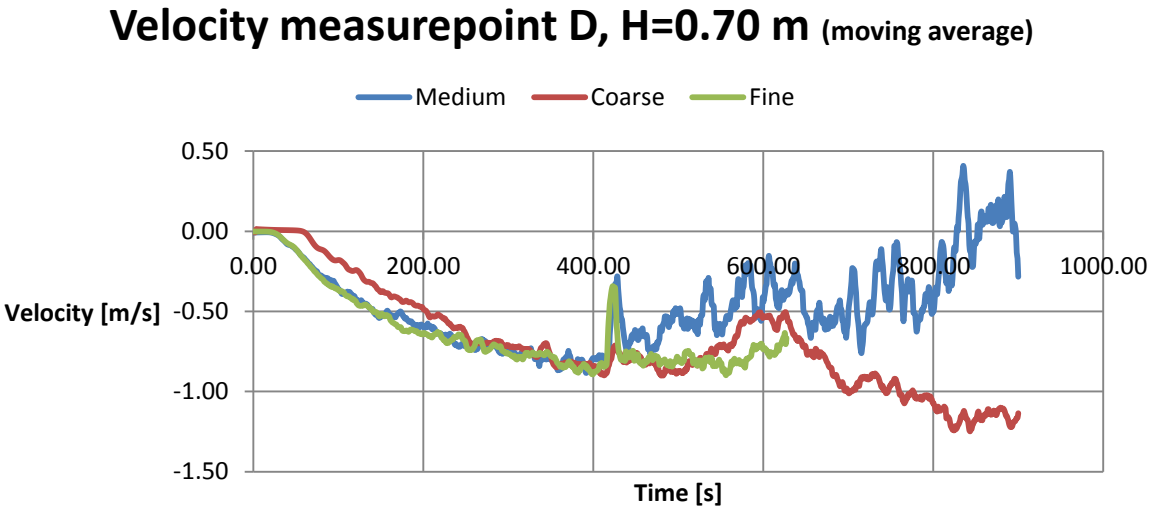

Figure F.6. Velocity in measurepoint D, H=0.70 m.

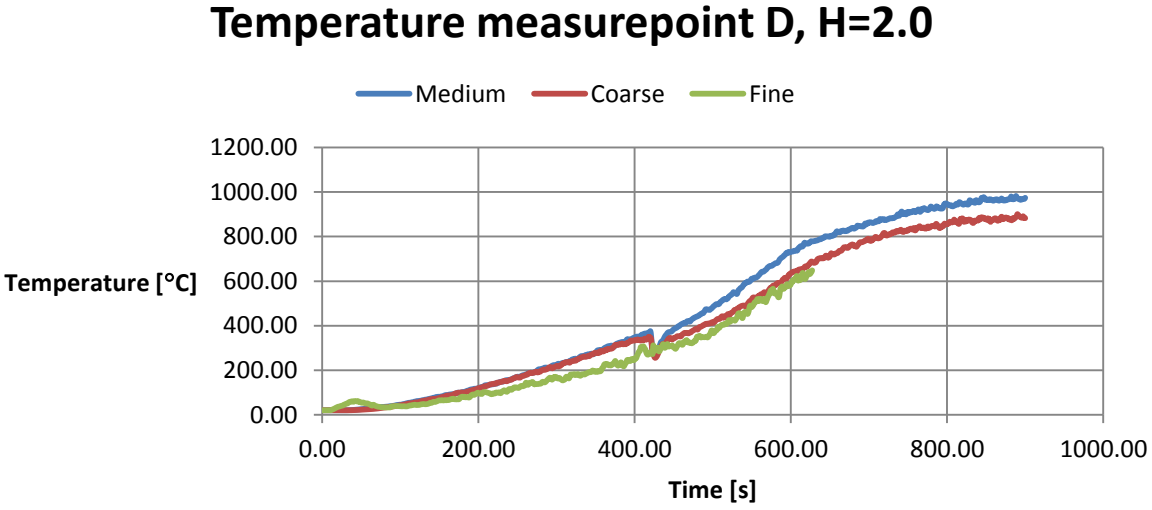

Figure F.7. Temperature in measurepoint D, H=2.0 m.

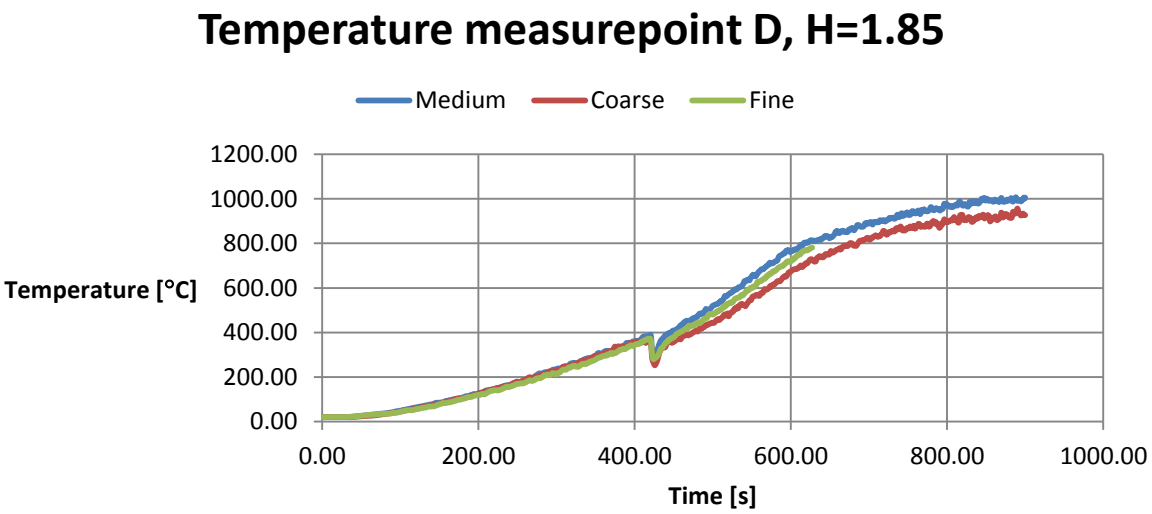

Figure F.8. Temperature in measurepoint D, H=1.85 m.

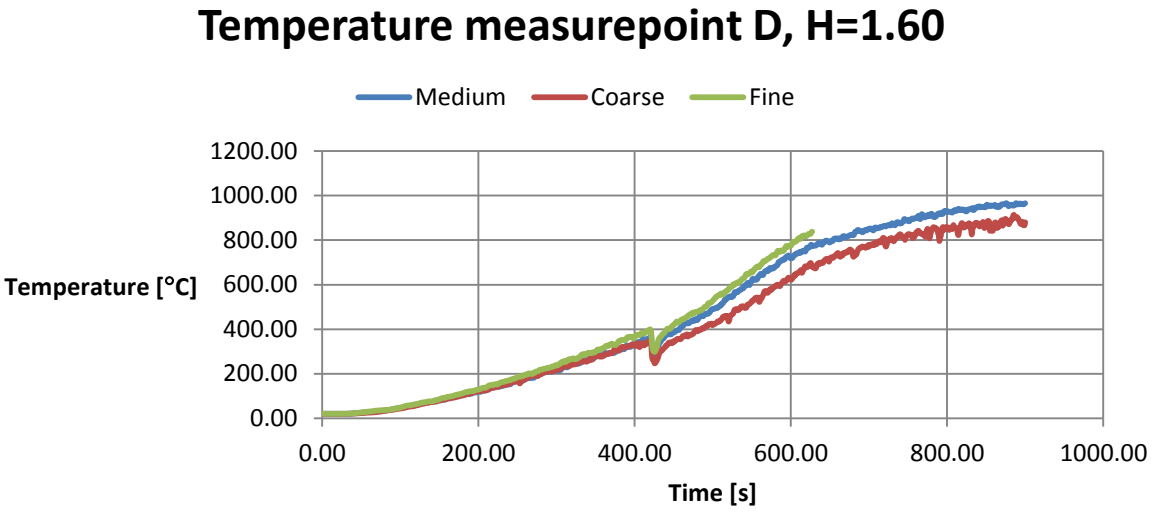

Figure F.9. Temperature in measurepoint D, H=1.60 m.

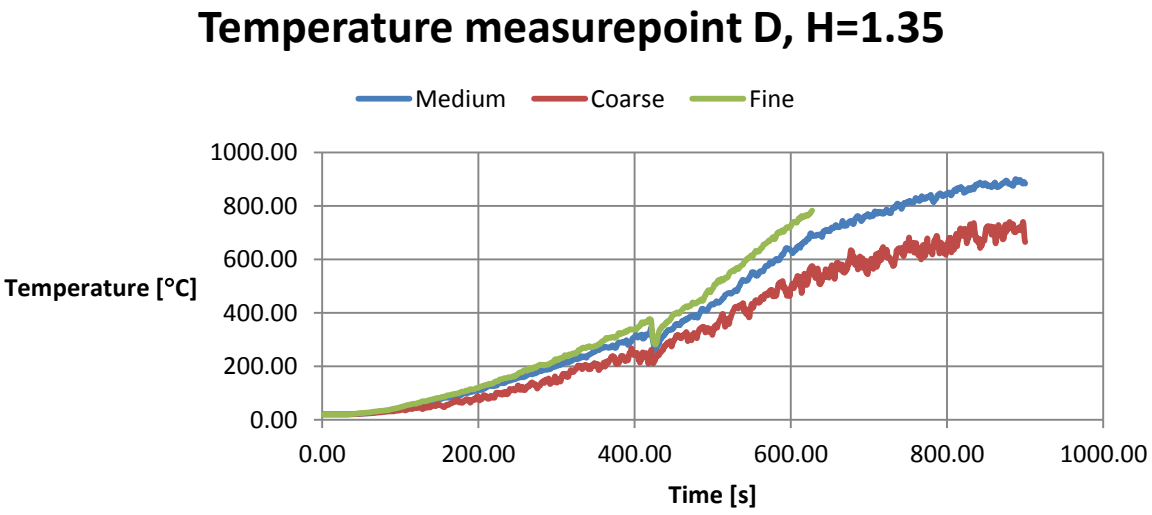

Figure F.10. Temperature in measurepoint D, H=1.35 m.

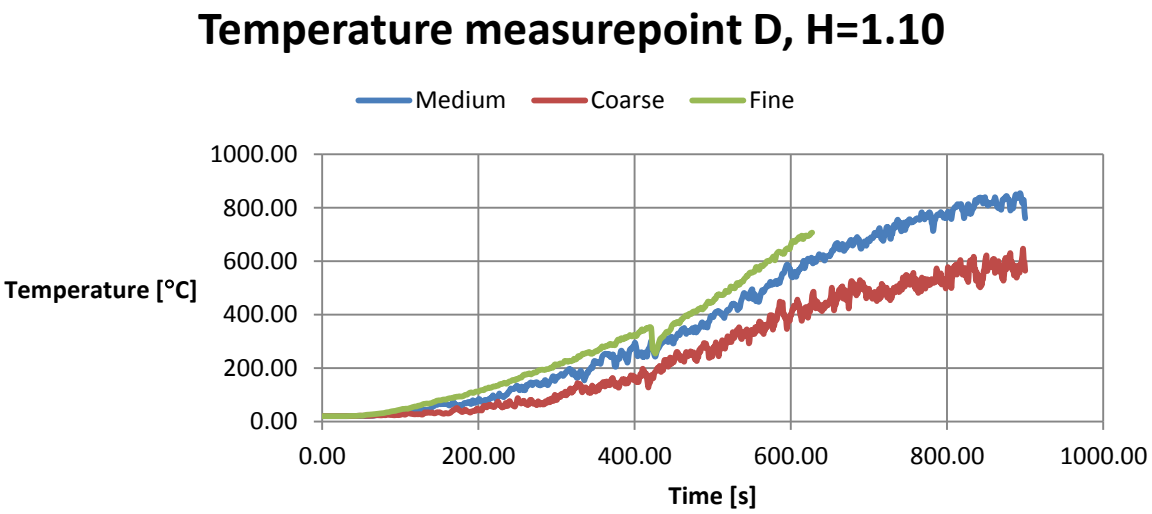

Figure F.11. Temperature in measurepoint D, H=1.10 m.

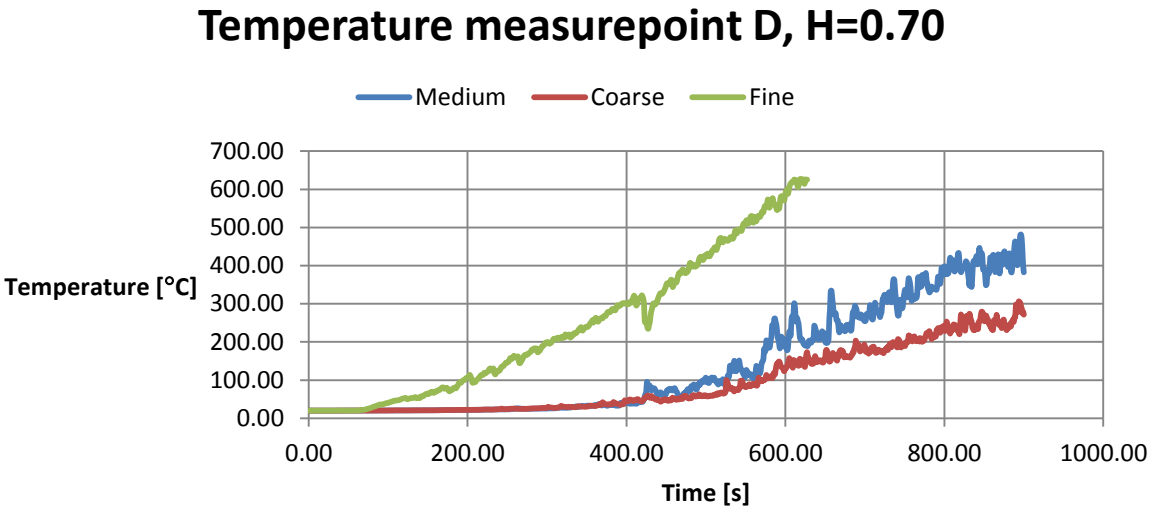

Figure F.12. Temperature in measurepoint D, H=0.70 m.

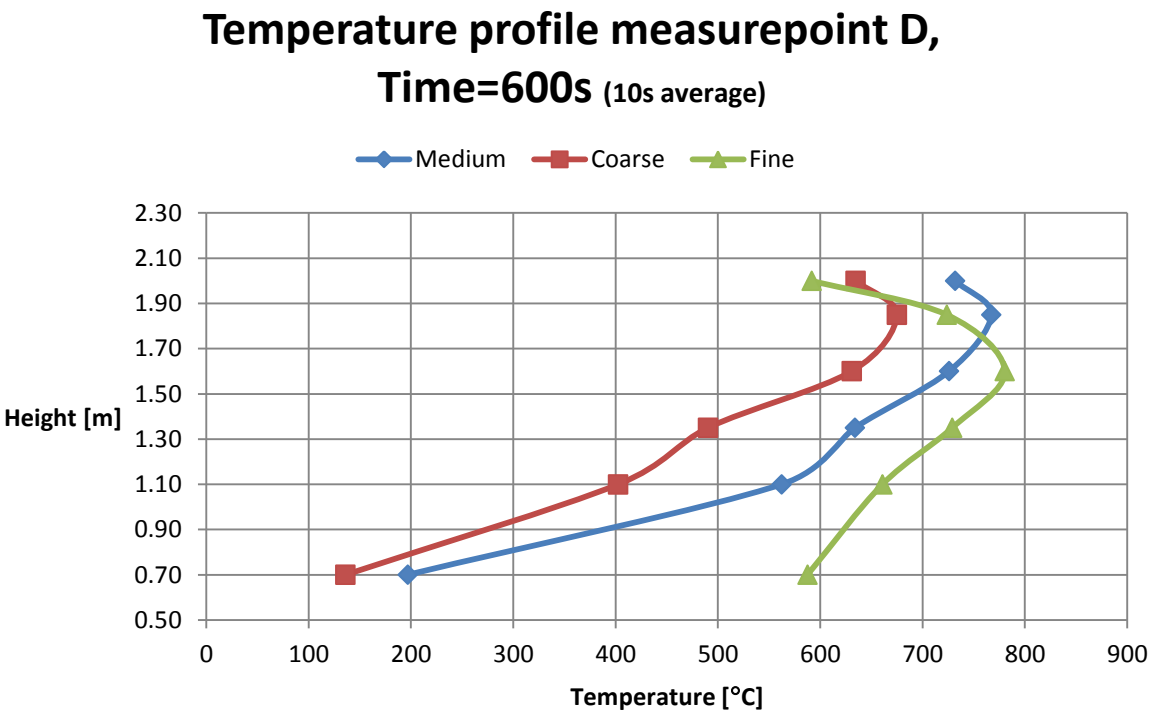

Figure F.13. Temperature profile at 600 s, measurepoint D.

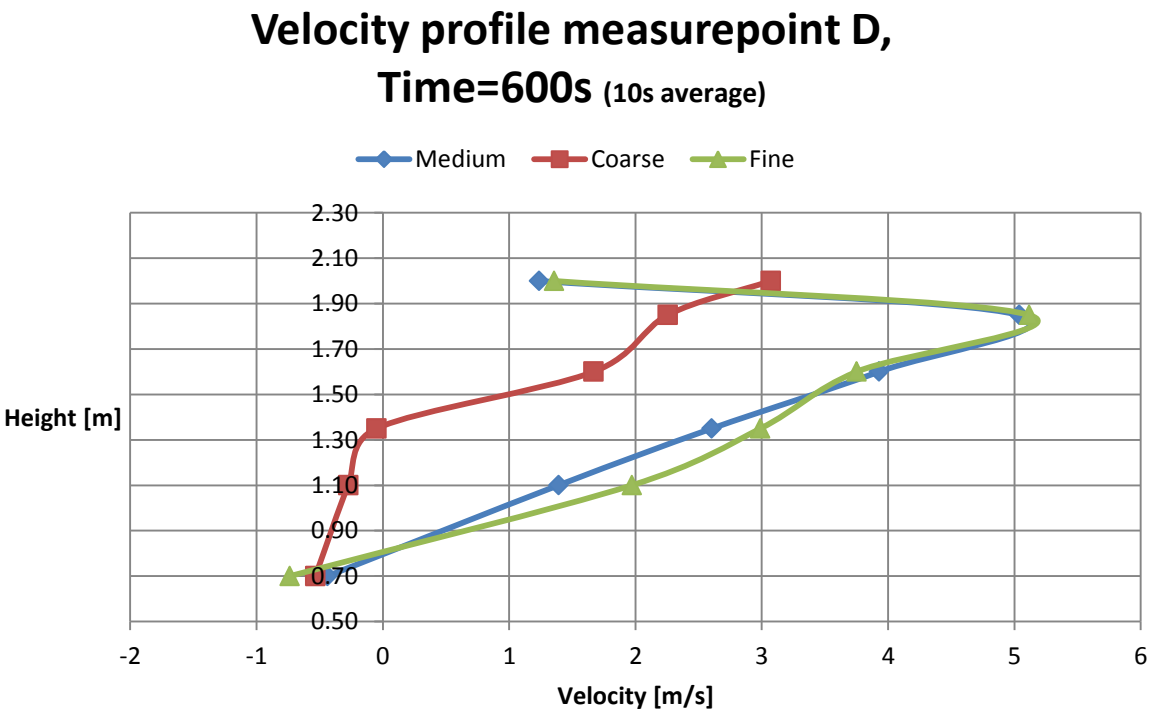

Figure F.14. Velocity profile at 600 s, measurepoint D.

Velocity probe tree in point A

The lines for the fine and medium cases have similar shapes and the magnitudes are similar except for the lowest height point (0.7 m), and the two highest points. The coarse differentiates more in both shape and magnitude for all heights, except the two highest points. See graphs in Figure F.15 - Figure F.20.

Thermocouple tree in point A

The medium and fine cases have similar shapes and magnitudes on all heights. The only exception is on height 1.10 m where the difference in magnitude is 50°C. See graphs in Figure F.21 - Figure F.26.

Profiles point A

The temperature and velocity profiles for trees point A can be seen in Figure F.27 and Figure F.28. Not much can be concluded by looking at the velocity profile. Both medium and coarse cases are in total equally deviating from the fine case. However, the temperature profiles shows that medium has both better fit to the fine case regarding shape and magnitude compared to the coarse case. The highest differences to the fine case lies around 30°C for the fine, whilst coarse differences lies around 50°C

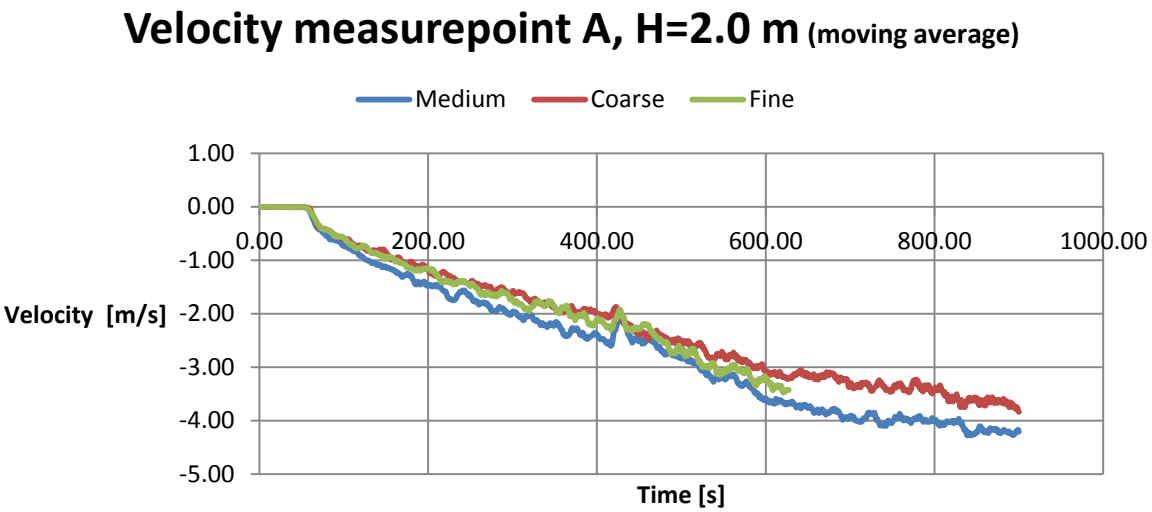

Figure F.15. Velocity in measurepoint A, H=2.00 m.

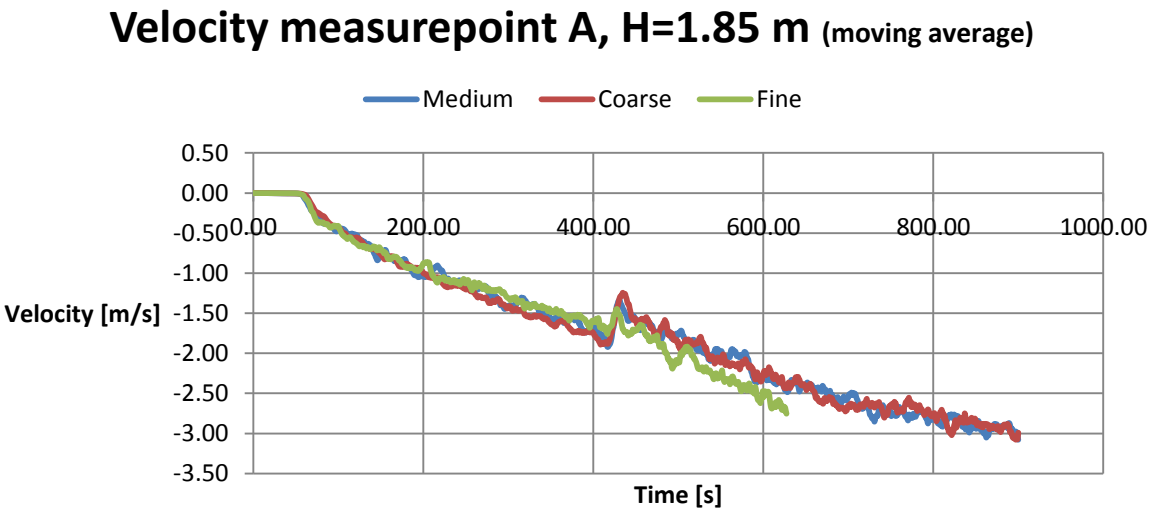

Figure F.16. Velocity in measurepoint A, H=1.85 m.

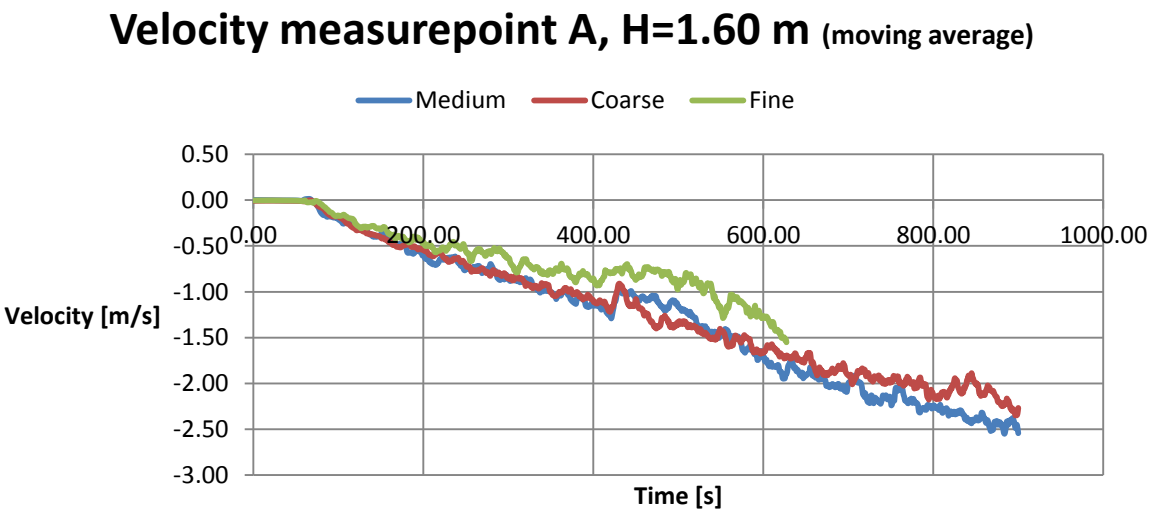

Figure F.17. Velocity in measurepoint A, H=1.60 m.

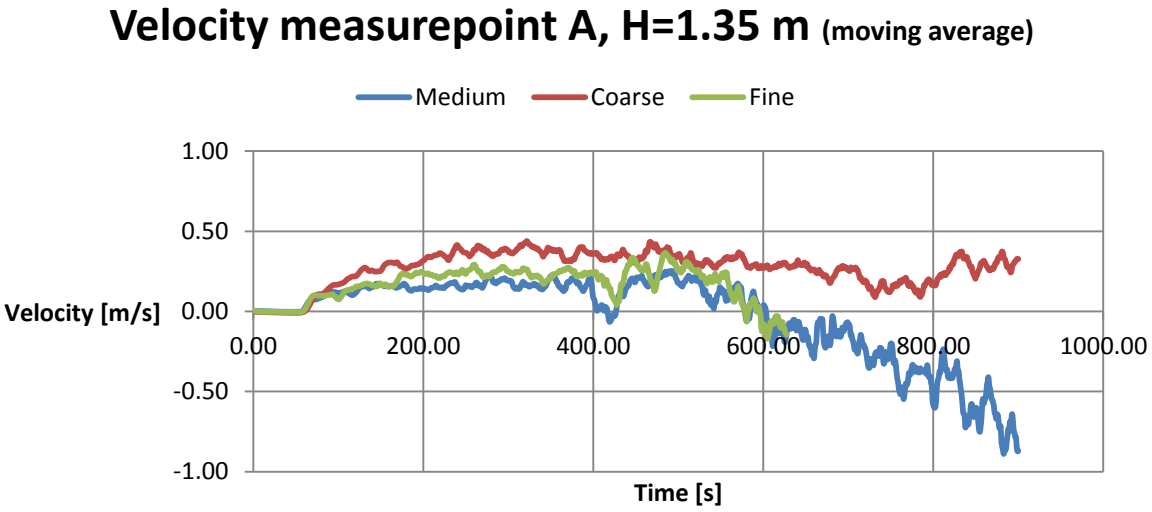

Figure F.18. Velocity in measurepoint A, H=1.35 m.

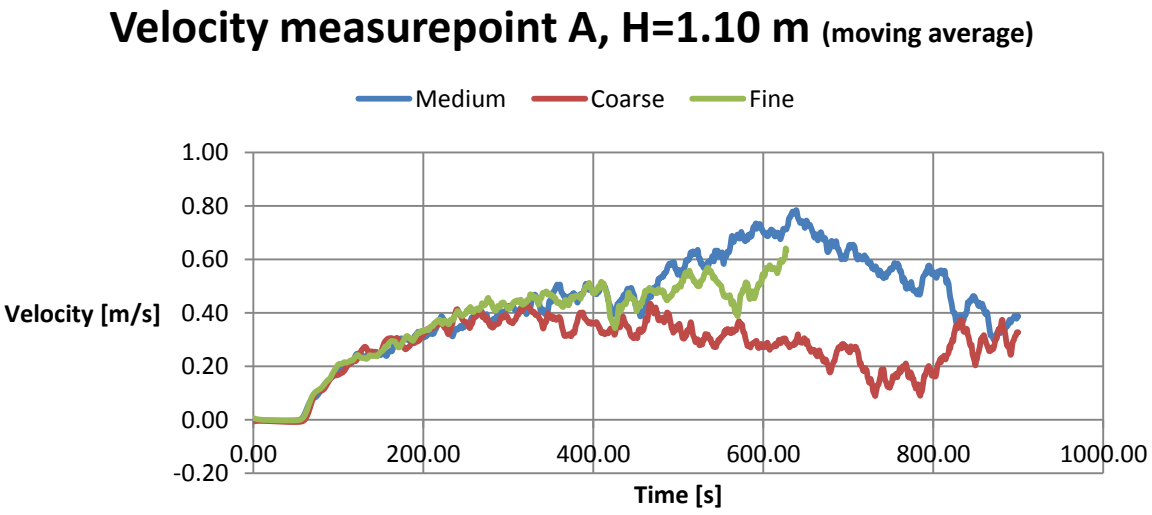

Figure F.19. Velocity in measurepoint A, H=1.10 m.

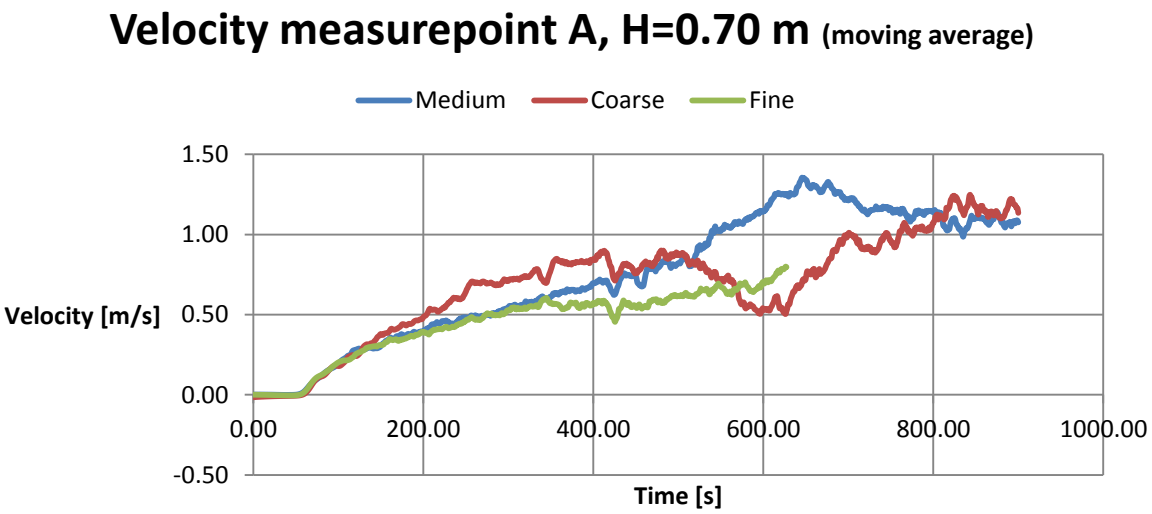

Figure F.20. Velocity in measurepoint A, H=0.70 m.

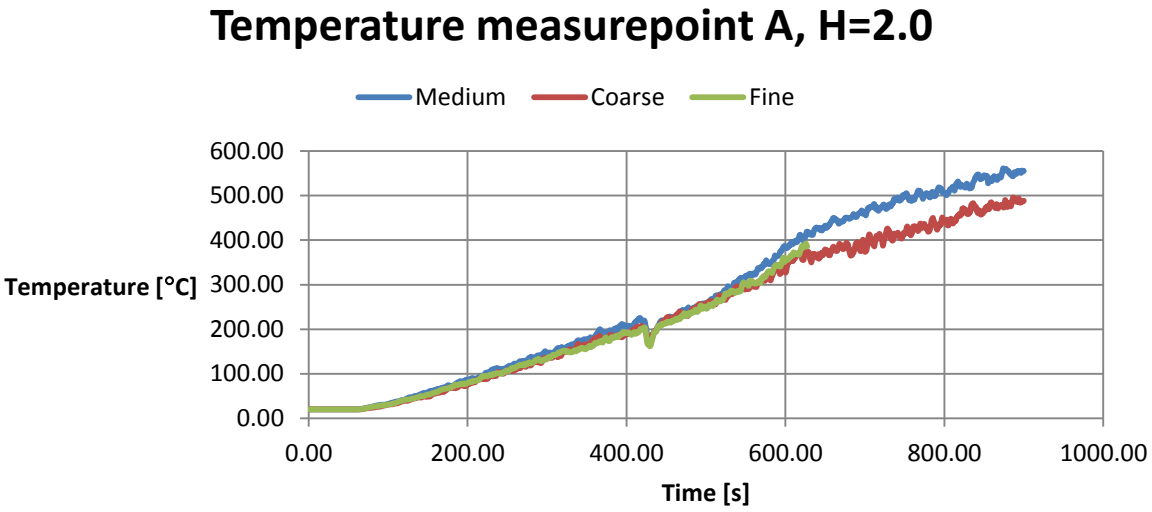

Figure F.21. Temperature in measurepoint A, H=2.00 m.

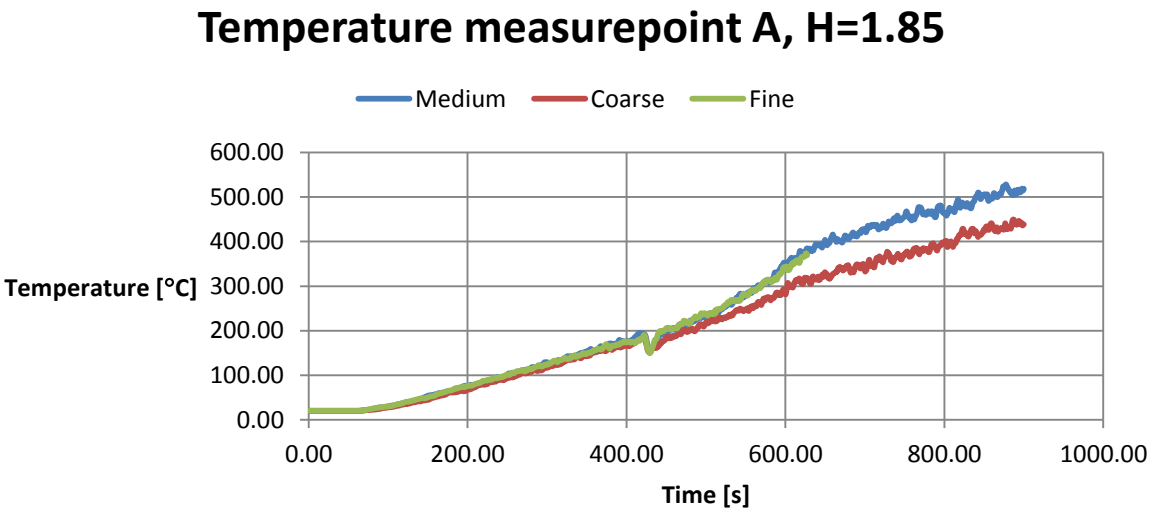

Figure F.22. Temperature in measurepoint A, H=1.85 m.

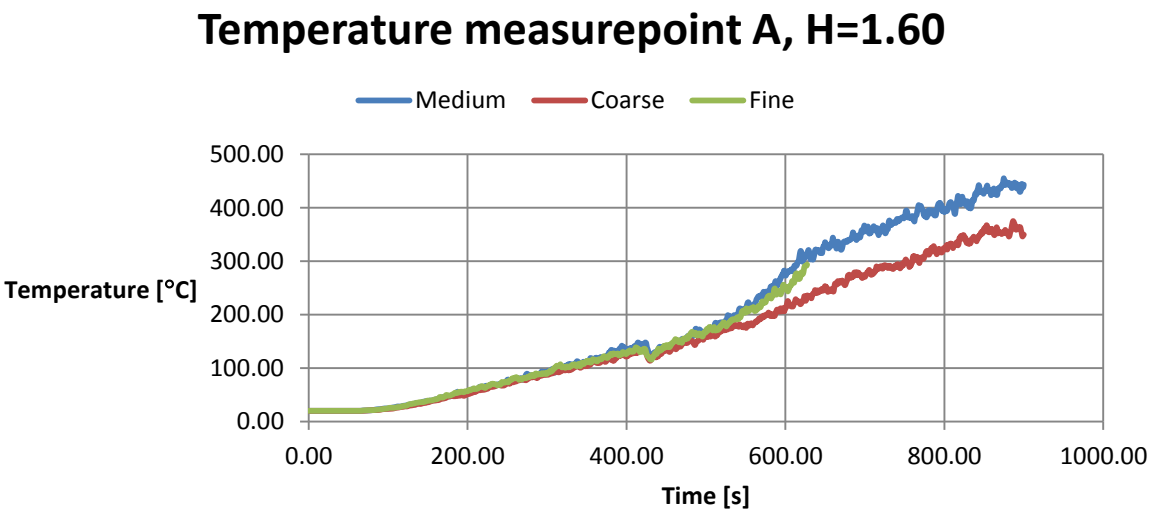

Figure F.23. Temperature in measurepoint A, H=1.60 m.

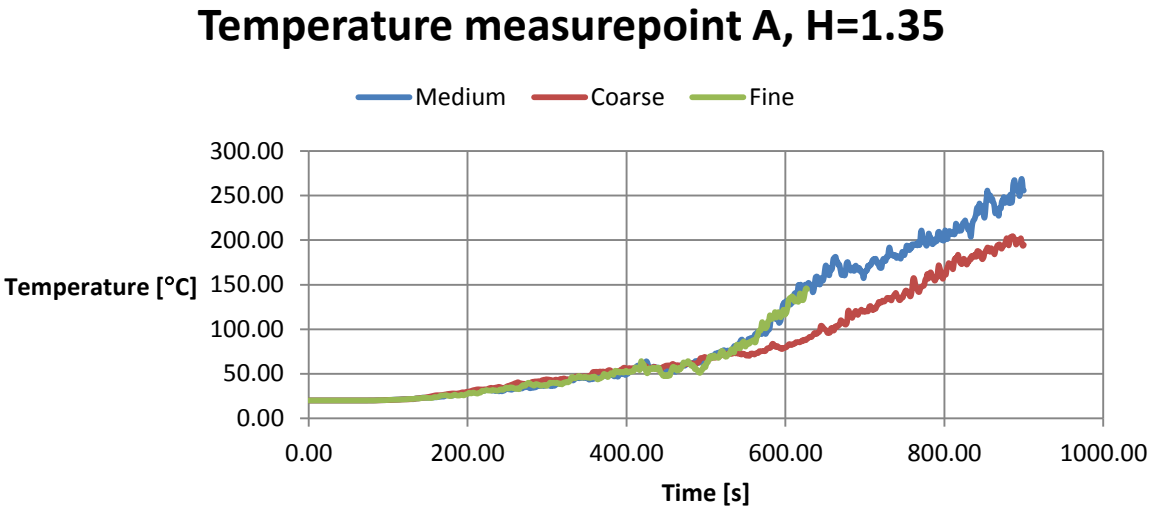

Figure F.24. Temperature in measurepoint A, H=1.35 m.

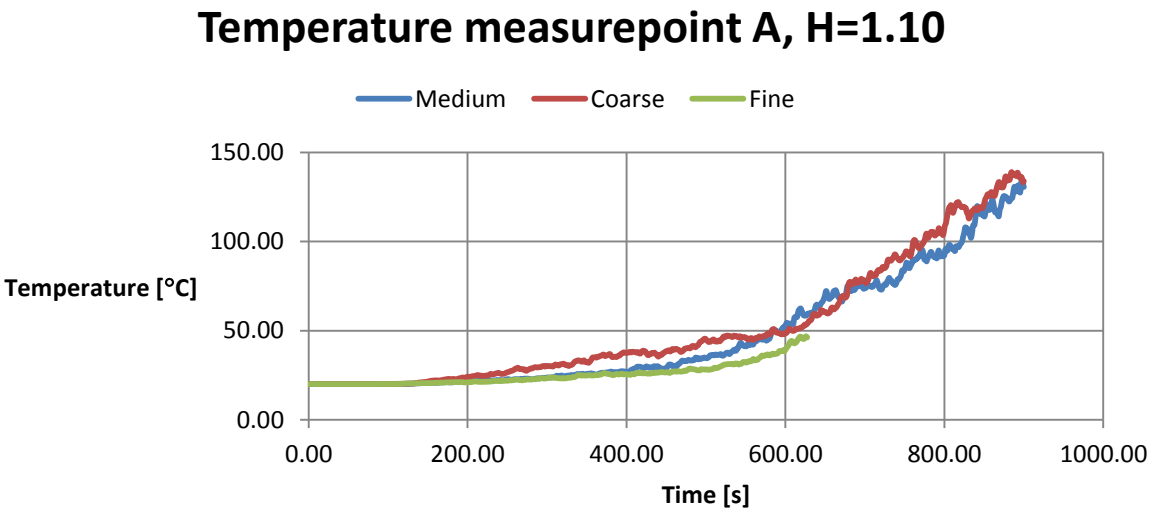

Figure F.25. Temperature in measurepoint A, H=1.10 m.

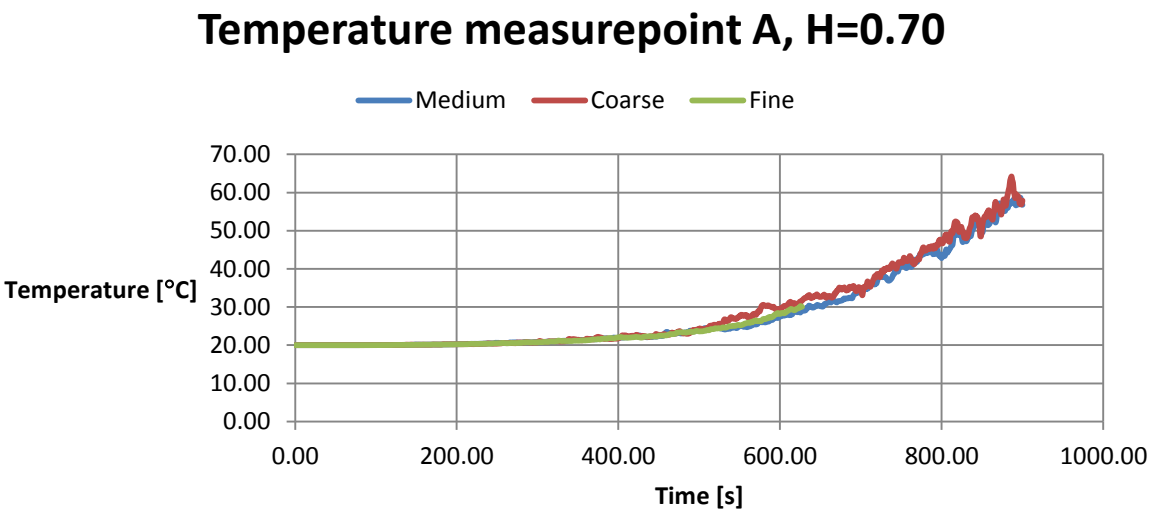

Figure F.26. Temperature in measurepoint A, H=0.70 m.

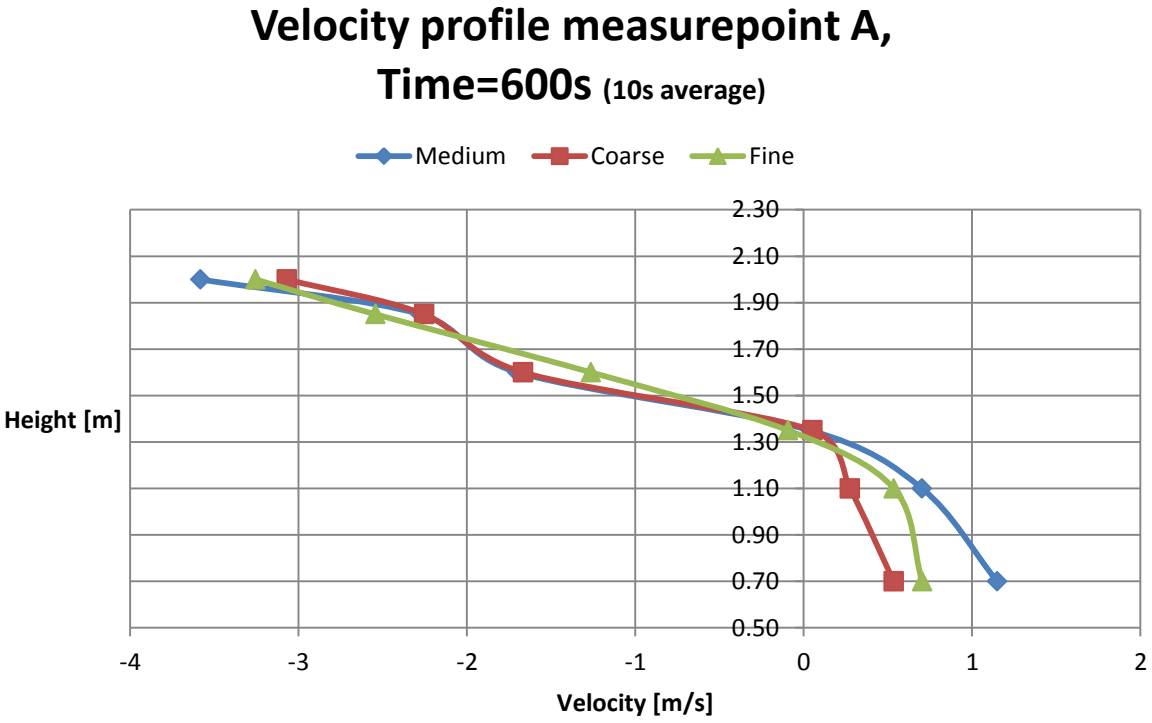

Figure F.27. Velocity profile at 600 s, measurepoint A.

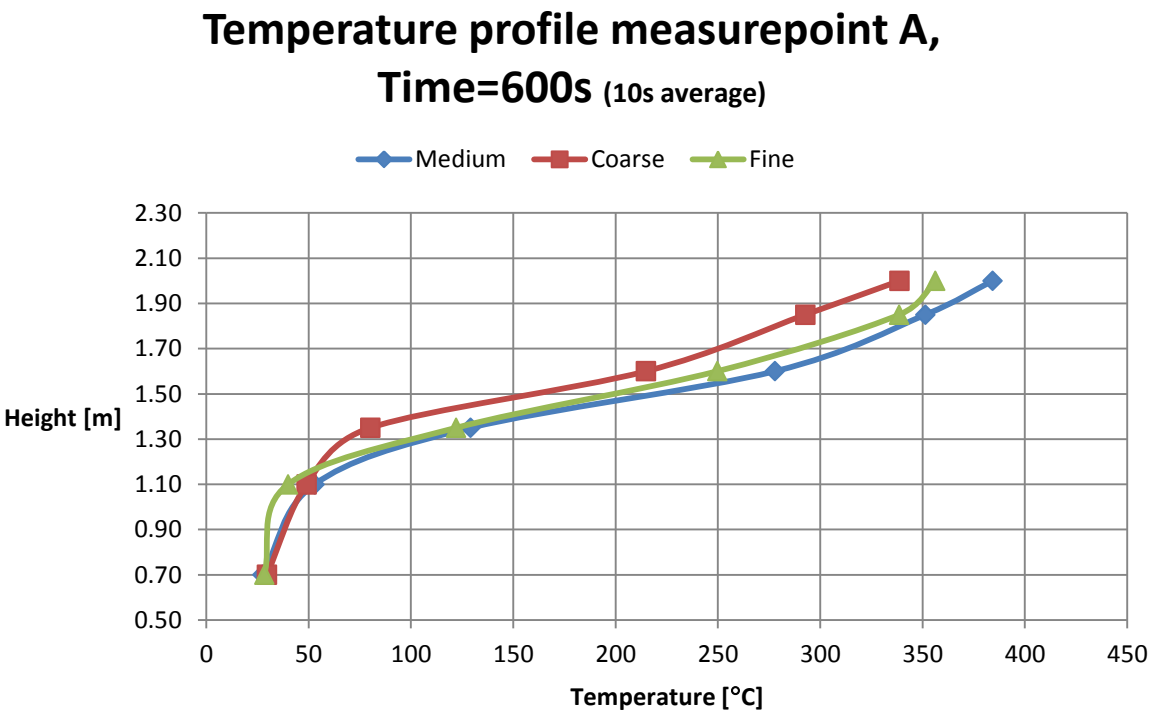

Figure F.28. Temperature profile at 600 s, measurepoint A.

Fire

Instantaneous pictures of the slice files in the fire enclosure are rendered for times 50-, 150- and 600 seconds for each of the cases medium, coarse and fine.

Looking at Figure F.29 - Figure F.37 it is possible to distinguish a better resolution of the temperatures in the flow field as the grid size decreases. In the fine case there is a high resolution and the turbulence is accentuated in the fire room. In the medium case there is a smoothening of this resolution, while in the coarse case the temperatures are more uniform within the fire enclosure due to the large size of the cells which results in low deviations in temperature.

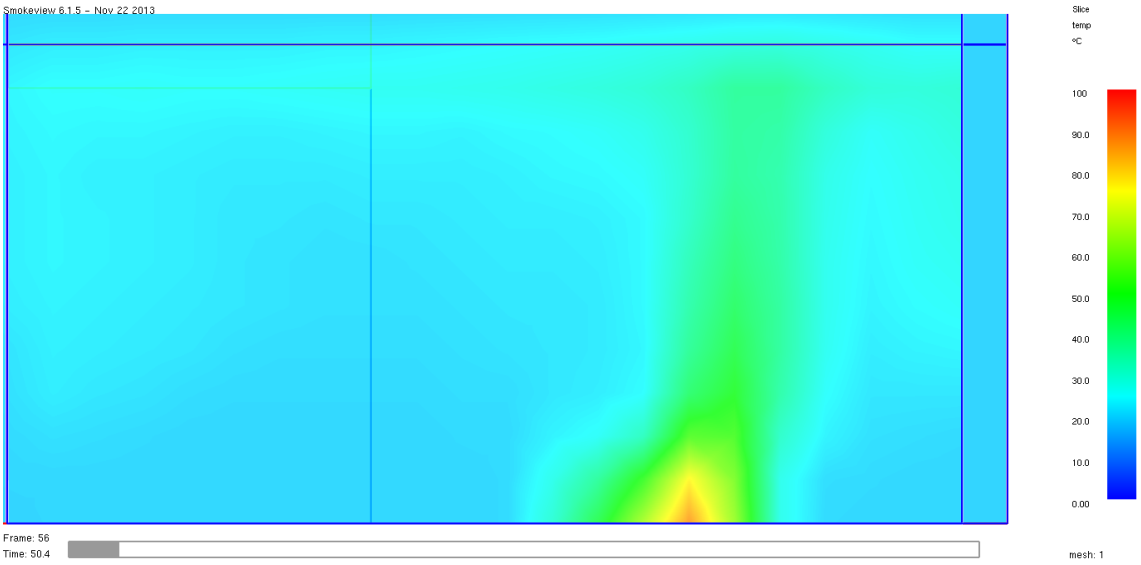

Figure F.29. The coarse fire temperatures after 50s.

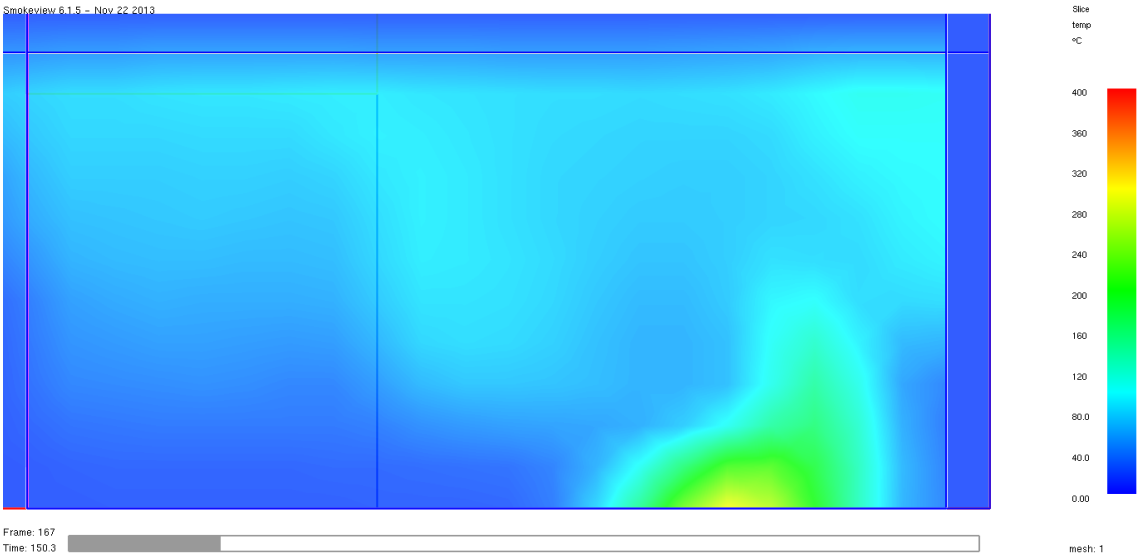

Figure F.30. The coarse fire temperatures after 150s.

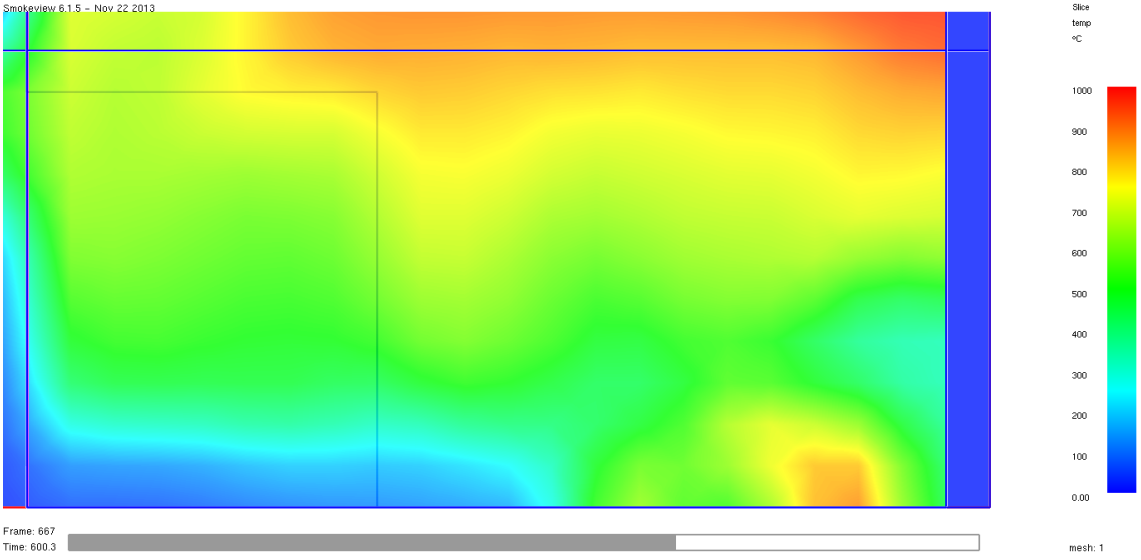

Figure F.31. The coarse fire temperatures after 600s.

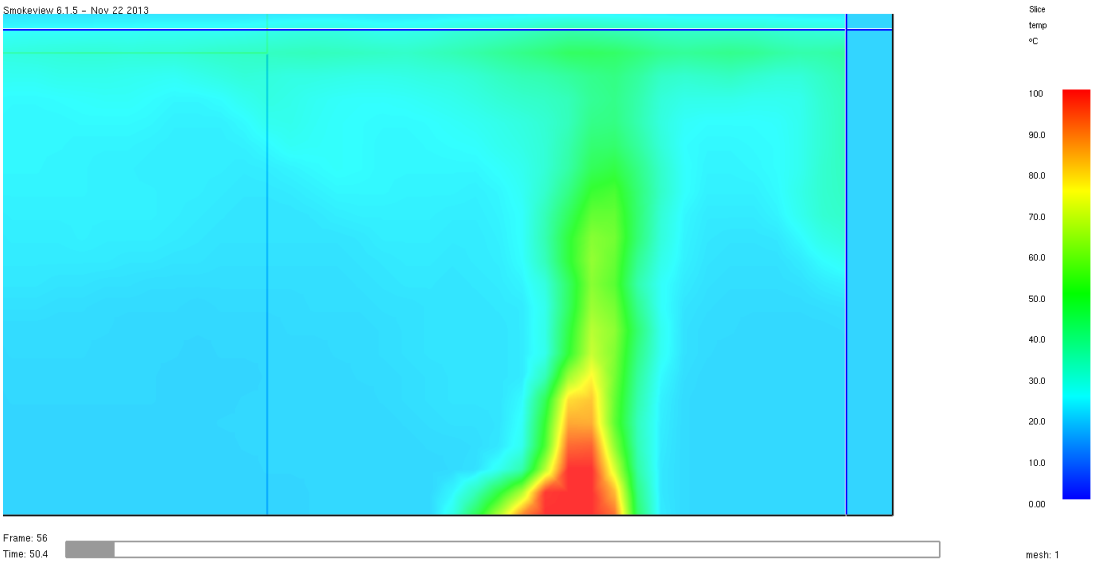

Figure F.32. The medium fire temperatures after 50s.

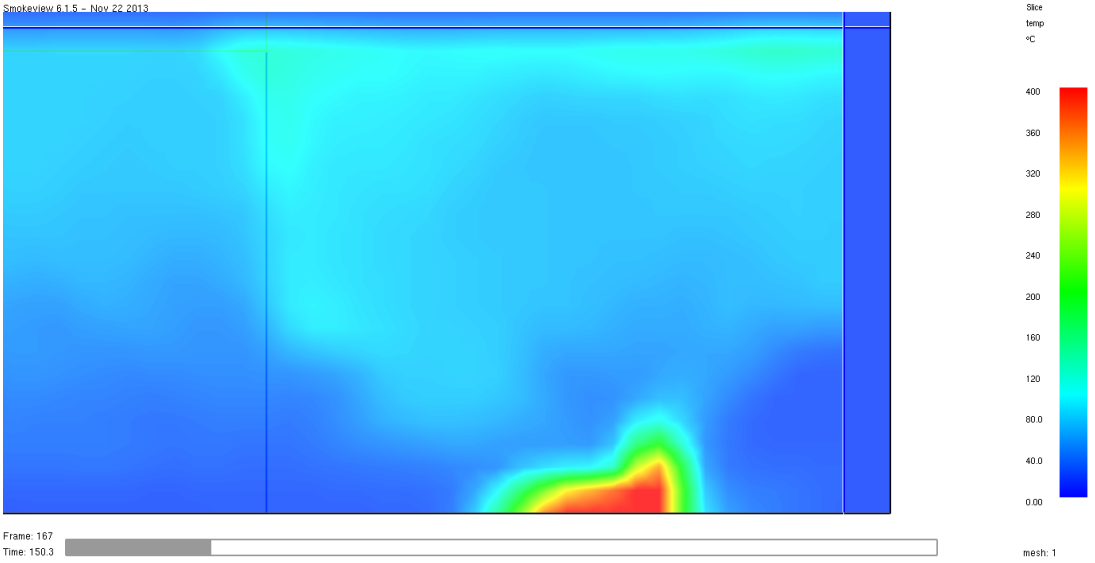

Figure F.33. The medium fire temperatures after 150s.

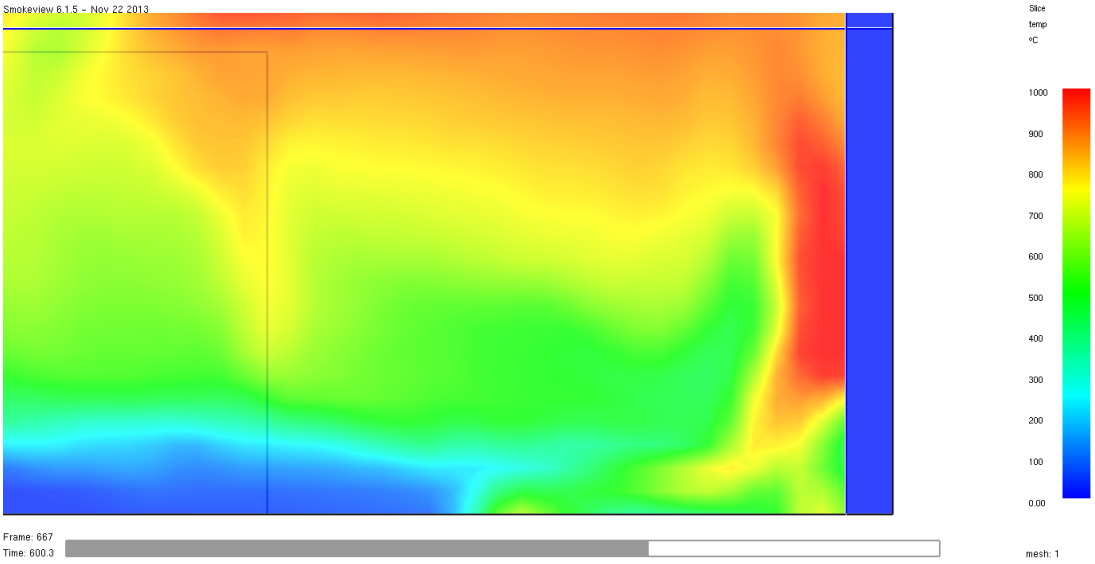

Figure F.34. The medium fire temperatures after 600s.

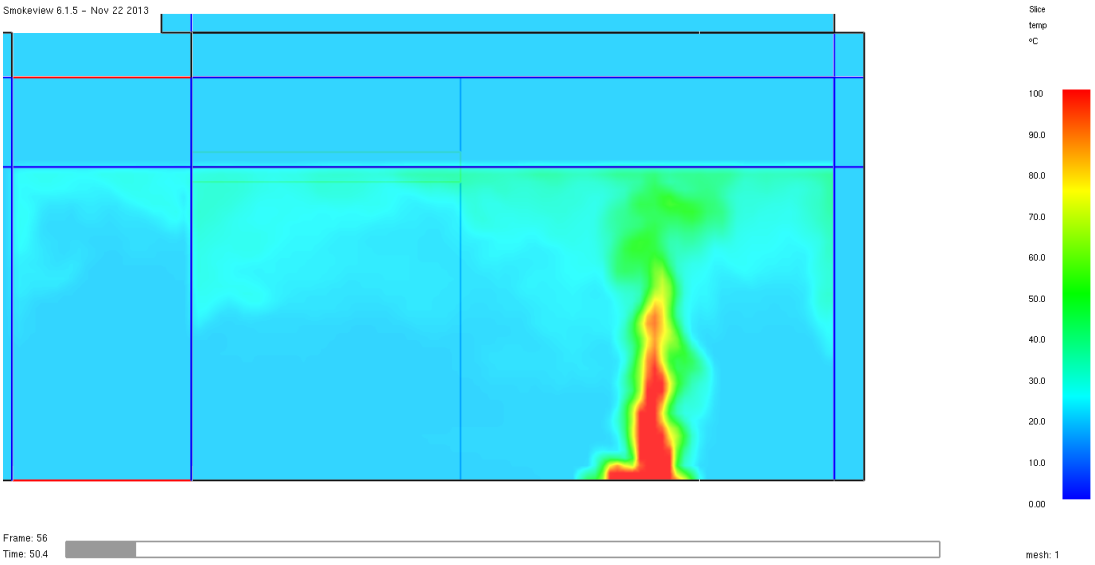

Figure F.35. The fine fire temperatures after 50s.

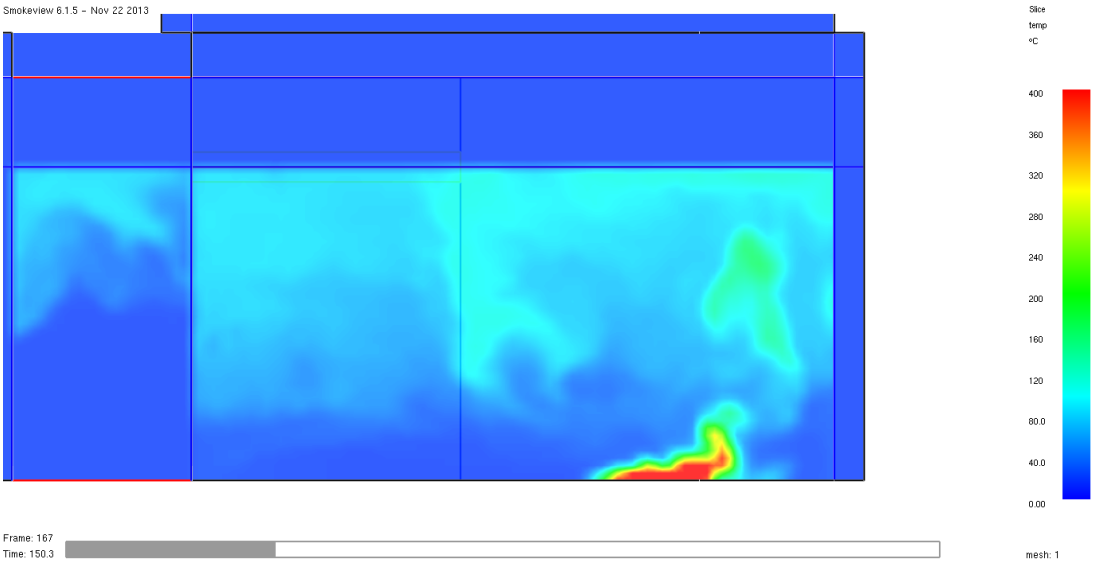

Figure F.36. The fine fire temperatures after 150s.

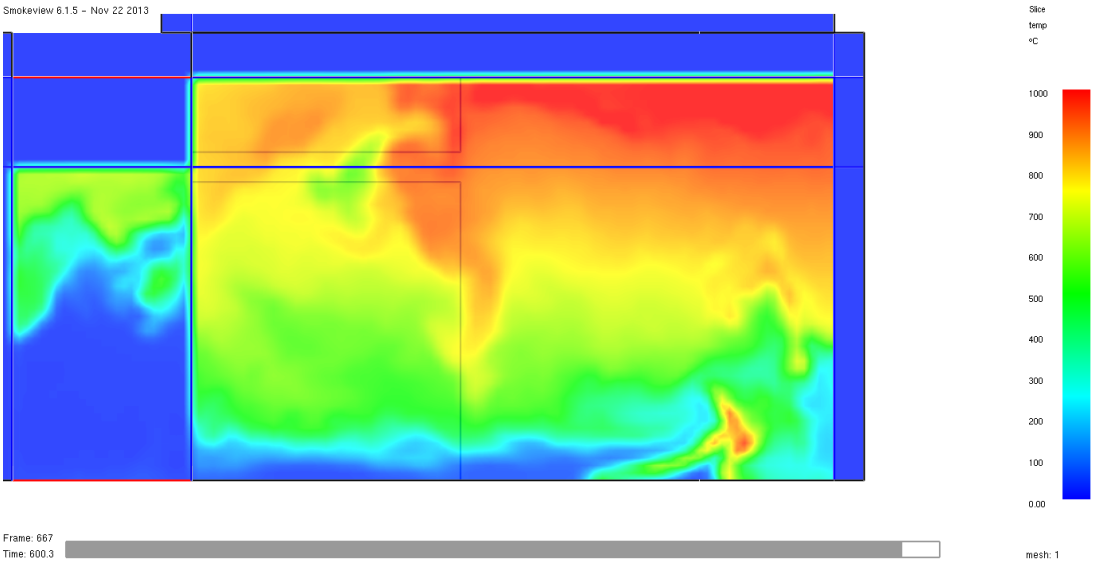

Figure F.37. The fine fire temperatures after 600s.